Degree Project in Heat and Power Technology

Second Cycle, 30 credits

TECHNO-ECONOMIC MODELLING OF A CARBON CAPTURE AND UTILIZATION VALUE CHAIN:

A CASE STUDY FOR CEMENT AND PULP & PAPER INDUSTRIES

JAVIER VENDRELL GRANERO

Master of Science Thesis

Department of Energy Technology

KTH 2024

TECHNO-ECONOMIC MODELLING OF A CARBON CAPTURE AND UTILIZATION VALUE CHAIN: A CASE STUDY FOR CEMENT AND PULP & PAPER INDUSTRIES

Javier Vendrell Granero

Approved	Examiner	Supervisor
22/8/2024	Andrew Martin	Jagruti Thakur, Ahmed Elberry
TRITA: ITM-EX 2024:511	Industrial Supervisor Carlos Alcobia	Contact person Jagruti Thakur

Abstract

In the context of global efforts to reduce carbon emissions, renewable fuels of non-biological origin (RFNBO) are poised to help decarbonize industrial emitters as well as the maritime transportation and chemical sectors. eMethanol (eMeOH) could function as a carbon-neutral fuel and chemical. This work models a techno-economic carbon capture and utilization (CCU) value chain, connecting ten industrial CO_2 emitters from the Iberian Peninsula to an eMeOH plant located in Sines, Portugal, using CO_2 tanker and truck transportation. The study models the various components of the CCU chain, including CO_2 capture, liquefaction, intermediate storage, transportation, and the eMeOH plant, to evaluate the levelized cost of eMeOH (LCOeM) and the levelized cost of CO_2 ($LCOCO_2$) across the ten different scenarios. A detailed examination of industrial emitters across Spanish and Portuguese geography was conducted to identify the most cost-effective biogenic and geogenic CO_2 sources for the eMeOH plant. By comparing truck and tanker transport options, the study identifies the cost implications associated with each method under varying conditions. The analysis reveals that transport costs are highly variable, influenced by the distance for truck transport and, for tankers, both the distance and the mismatch between tanker capacity and emitter CO_2 output. Maritime transport stands out as a more cost-effective option for routes connecting Spanish emitters, with costs ranging from €17 to €30 per ton of CO_2 transported, compared to truck transport, which ranges from €35 to €75 per ton of CO_2.

As the eMeOH plant accounts for more than 80% of the costs of the value chain, the comparison of extra costs for transport selection remains secondary. The production capacity of eMeOH, limited by CO_2 availability, emerges as the major driver to lower both LCOeM and $LCOCO_2$, leveraging economies of scale. This is evident in the case of the Portuguese cement factory CIMPOR in Alhandra, which achieves the lowest LCOeM of €1,072 per ton of eMeOH among all the scenarios modelled. The findings contribute to a broader understanding of the technical and cost implications of the different blocks of a CCU value chain. The definition and analysis of the ten different scenarios support comprehending how to target viable cases, which help decarbonize not only the cement and pulp and paper industries but also the maritime transportation and chemical sectors, as eMeOH could function as a carbon-neutral fuel and chemical.

Key words: eMethanol, biogenic, geogenic, carbon dioxide, hard-to-abate sectors, carbon capture and utilization, logistics, transport, tanker and truck

Sammanfattning

I samband med de globala insatserna för att minska koldioxidutsläppen kan förnybara bränslen av icke-biologiskt ursprung (RFNBO) bidra till att minska koldioxidutsläppen från industriella utsläppskällor samt sjötransport- och kemikaliesektorerna. eMetanol (eMeOH) kan fungera som ett koldioxidneutralt bränsle och kemikalie. I det här arbetet modelleras en teknisk-ekonomisk värdekedja för koldioxidavskiljning och -användning (CCU) som förbinder tio industriella koldioxidutsläpp från Iberiska halvön till en eMeOH-fabrik i Sines, Portugal, med hjälp av koldioxidtankfartyg och lastbilstransporter. Studien modellerar de olika komponenterna i CCU-kedjan, inklusive CO_2-fångst, kondensering, mellanlagring, transport och eMeOH-anläggningen, för att utvärdera den utjämnade kostnaden för eMeOH (LCOeM) och den utjämnade kostnaden för CO_2 ($LCOCO_2$) i de tio olika scenarierna. En detaljerad undersökning av industriella utsläppskällor i Spanien och Portugal genomfördes för att identifiera de mest kostnadseffektiva biogena och geogena CO_2-källorna för eMeOH-anläggningen. Genom att jämföra transportalternativen med lastbil och tankbil identifierar studien de kostnadskonsekvenser som är förknippade med varje metod under varierande förhållanden. Analysen visar att transportkostnaderna är mycket varierande och påverkas av avståndet för lastbilstransporter och, för tankfartyg, både avståndet och missmatchningen mellan tankfartygets kapacitet och utsläppskällans CO_2-produktion. Sjötransporter framstår som ett mer kostnadseffektivt alternativ för rutter som förbinder spanska utsläppsländer, med kostnader på mellan 17 och 30 € per ton CO_2 som transporteras, jämfört med lastbilstransporter, som kostar mellan 35 och 75 € per ton CO_2.

Eftersom eMeOH-anläggningen står för mer än 80 % av kostnaderna i värdekedjan är jämförelsen av extra kostnader för transportval sekundär. Produktionskapaciteten för eMeOH, som begränsas av tillgången på CO_2, framstår som den viktigaste drivkraften för att sänka både LCOeM och $LCOCO_2$ genom att utnyttja stordriftsfördelar. Detta är tydligt i fallet med den portugisiska cementfabriken CIMPOR i Alhandra, som uppnår den lägsta LCOeM på 1,072 € per ton eMeOH bland alla scenarier som modellerats. Resultaten bidrar till en bredare förståelse för de tekniska och kostnadsmässiga konsekvenserna av de olika blocken i en CCU-värdekedja. Definitionen och analysen av de tio olika scenarierna bidrar till att förstå hur man kan rikta in sig på lönsamma fall, som bidrar till att minska koldioxidutsläppen inte bara inom cement- och massa- och pappersindustrin utan även inom sjötransport- och kemikaliesektorerna, eftersom eMeOH kan fungera som ett koldioxidneutralt bränsle och en koldioxidneutral kemikalie.

Nyckelord: eMetanol, biogen, geogen, koldioxid, sektorer där koldioxidutsläpp är svåra att minska, avskiljning och användning av koldioxid, logistik, transport, tankfartyg och lastbilar

List of Figures

List of Tables

List of Abbreviations and Acronyms

ASU – Air Separation Unit

BECCS – Bioenergy with Carbon Capture and Storage

BEIS – Business, Energy & Industrial Strategy

CAPEX – Capital Expenditure

CBAM – Carbon Border Adjustment Mechanism

CC – Carbon Capture

CCS – Carbon Capture and Storage

CCU – Carbon Capture and Utilisation

CCUS – Carbon Capture, Utilisation and Storage

CDR – Carbon Dioxide Removal

CH_4 – Methane

CO – Carbon Monoxide

CO_2 – Carbon Dioxide

CODN – Cost of Doing Nothing

DAC – Direct Air Capture

DEVEX – Development Expenditure

EC – European Commission

EII – Energy Intensive Industries

eMeOH – eMethanol

ETS – Emissions Trading System

EU – European Union

EUA – EU Allowance

FEED – Front-End Engineering Design

FID – Final Investment Decision

GHG – Greenhouse Gases

H_2 – Hydrogen

IPCC – Intergovernmental Panel on Climate Change

LCOCO2 – Levelized Cost of CO_2

LCOE – Levelized Cost of Energy

LCOeM – Levelized Cost of eMethanol

LCOH – Levelized Cost of Hydrogen

LNG – Liquid Natural Gas

LPG – Liquid Petroleum Gas

MEA – Monoethanolamine

MeOH – Methanol

MI – Methanol Institute

N_2 – Nitrogen

NPV – Net Present Value

NO_x – Nitrogen Oxides

NH_3 – Ammonia

O_2 – Oxygen

OPEX – Operational Expenditure

PPA – Power Purchase Agreements

PLC – Project Lifecycle Cost

PtL – Power-to-Liquid

PV – Photovoltaic

SAF – Sustainable Aviation Fuel

SMR – Steam Methane Reforming

TRL – Technology Readiness Level

WtE – Waste-to-Energy

Table of Contents

1 Introduction

The accelerating pace of climate change has become one of the most pressing global challenges, with carbon dioxide (CO_2) emissions being a major contributor. Over the past century, atmospheric CO_2 concentrations have risen significantly compared to pre-industrial levels, largely due to human activities such as the burning of fossil fuels for energy, deforestation, and various industrial processes. These emissions are driving global temperatures higher, leading to more frequent and severe weather events, rising sea levels, and widespread disruptions to ecosystems and human societies [1].

Industries such as steel manufacturing, chemicals, transport and cement production are among the largest CO_2 emitters, collectively accounting for a significant portion of global greenhouse gas (GHG) emissions. These sectors are particularly challenging to decarbonize due to their physical, technological, or market-specific circumstances, often referred to as "hard-to-abate" sectors. For instance, the steel industry alone is responsible for approximately 7% of global CO_2 emissions, while the chemical sector contributes around 4%, with the majority of emissions stemming from the production of key chemicals like ammonia (NH_3), methanol (MeOH) , and steam cracking products. The transport sector, encompassing heavy-duty trucking, shipping, and aviation, adds another 10% to global carbon emissions, further complicating efforts to reduce GHG emissions [2]. These sectors are considered hard-to-abate due to their physical, technological, or market-specific challenges, making decarbonization particularly difficult. However, carbon capture (CC) technologies are of global importance because they offer a viable solution for reducing emissions in these sectors. Capturing CO_2 at the source and utilizing it for industrial processes like MeOH production not only mitigates environmental impact but also plays a crucial role in achieving net-zero emissions, paving the way for a decarbonized economy [2], [3].

MeOH and CO_2 are pivotal compounds in the quest for sustainable energy solutions and industrial processes. The interplay between these two centric molecules forms the core of this work, which investigates innovative pathways to capture industrial CO_2 emissions and convert them into eMethanol (eMeOH). Industrial emissions, particularly CO_2, significantly impact the environment and climate. This work explores how capturing CO_2 from industrial sources and utilizing it to produce eMeOH can provide a dual benefit: reducing GHG emissions and producing a valuable chemical. By integrating these processes, the research aims to highlight effective strategies for mitigating industrial CO_2 emissions while advancing sustainable eMeOH production.

1.1 eMethanol

MeOH is a clear, colourless, and highly flammable liquid at ambient temperature and pressure. As the simplest alcohol, it consists of a methyl group (CH_3) bonded to a hydroxy group (OH), forming a molecule with one carbon atom and four hydrogen (H_2) atoms. Widely used as both a chemical feedstock and fuel, methanol plays a crucial role in various industrial applications and energy solutions [4].

MeOH production currently hovers around 100 Mt annually, predominantly derived from fossil fuels like natural gas (NG) or coal [5]. The primary consumer of this versatile liquid fuel is the chemical industry, employing it in the synthesis of formaldehyde, acetic acid, and plastics, as shown in Figure 1 [5]. The graph below illustrates the usage distribution of fossil-based MeOH across various product categories and production capacity.

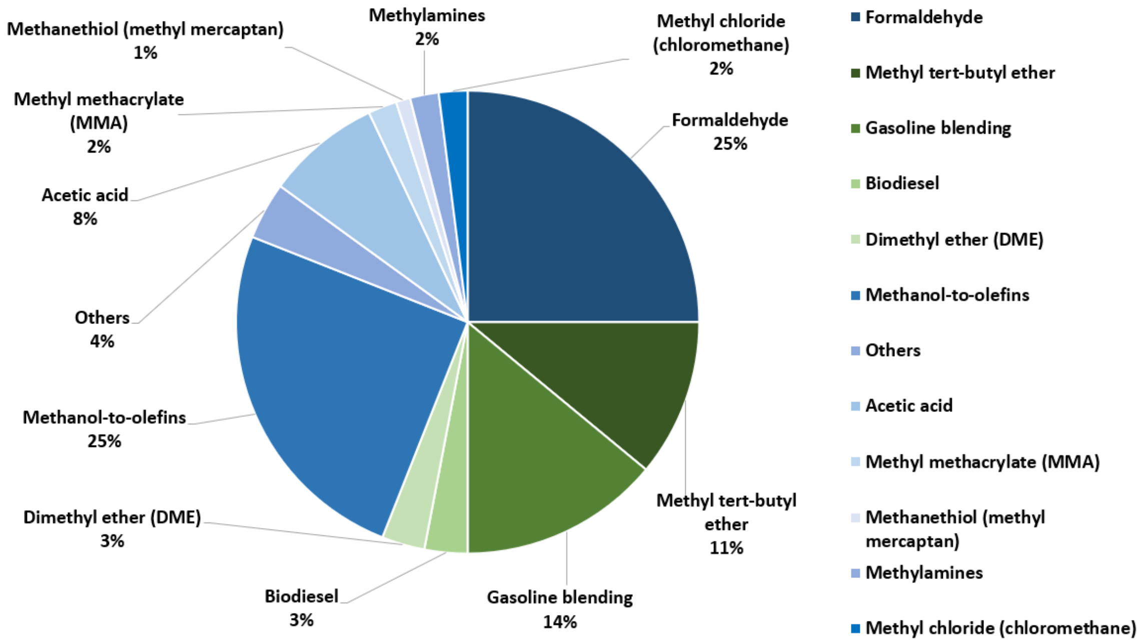

Figure 1: Global MeOH demand in 2019 [5]

In the past two decades, global demand has doubled, with China leading this upward trend [5]. The escalating demand for this fossil fuel-derived chemical commodity poses a significant threat to exacerbating climate change. Consequently, this issue cannot be ignored, prompting the European Commission (EC) to take the lead in initiatives aimed at reducing its impact.

This is precisely where renewable MeOH emerges with its carbon-neutral attributes. Classified within the Renewable Fuels from Non-Biological Origin (RFNBOs) category by Article 2.36 of Directive (EU) 2018/2001, it denotes "liquid or gaseous fuels used in the transport sector, excluding biofuels or biogas, with energy content sourced from renewables other than biomass [6]. Presently, without distinction whether the end-use sector is transport or any other. In practice, green eMeOH holds the potential to serve as feedstock for the chemical industry, as current major off-taker, and as fuel for both road and maritime transport, substantially mitigating CO_2 emissions. It is crucial to emphasize that, since green eMeOH is synthesized using green H_2 together with CO_2 captured from renewable sources, such as Bioenergy with Carbon Capture and Storage (BECCS), Direct Air Capture (DAC), the carbon footprint of this chemical commodity's production is markedly reduced. Furthermore, when MeOH is derived from biomass feedstocks, it earns the designation of bio-MeOH, sharing the carbon-neutral status attributed to eMeOH. Regarding the feedstock to produce eMeOH in Power-to-Liquid (PtL) plants, green H_2 and CO_2 are required. However, the CO_2 cannot originate from fossil fuel emitters but must instead come from either biogenic or geogenic sources. It is important to note that the use of geogenic CO_2 emissions for producing this carbon-recycled fuel is limited to the year 2041. After this point, only biogenic sources will be utilized. This information is derived from the Commission Delegated

Regulation (EU) 2023/1185 and the Directive 2003/87/EC of the European Parliament and of The Council [7], [8].

Moreover, as presented by Intergovernmental Panel on Climate Change (IPCC) 6th Assessment Report, alternative energy carriers, on applications where electrification finds adoption difficulties, must be widely deployed in between other mitigation options to secure sustained reduction of emissions [9]. MeOH is among the alternative energy carriers identified as having significant potential to reduce CO_2 emissions across various modes of transport, including heavy-duty land transport, shipping, and aviation. However, as for today, they necessitate to improve its production processes and decrease its production cost.

Maritime transportation and chemical industries are expected to be the primary off-takers of eMeOH in the mid-term. This is evidenced by significant players and organizations in both sectors making commitments to incorporate this organic chemical compound into their operations.

On one side, leaders in maritime transport, such as the Danish container logistics company A.P. Moller – Maersk, have made significant investments in dual-fuel MeOH-enabled vessels. In the early 2020s, Robert Maersk Uggla, CEO of A.P. Moller Holding, expressed Maersk's commitment to resolving the chicken-or-egg dilemma regarding MeOH-powered ships and placed a groundbreaking order for eight 16,000 TEUs dual fuel containerships from Hyundai Heavy Industries [10]. As of today, two of these initial containership orders have been launched, marking the beginning of the MeOH-enabled vessel fleet that Maersk will operate in the coming years [11]. Similarly, in their segment, China Merchants Energy Shipping (CMES) and China Ocean Shipping Company (COSCO) have followed the Danish giant by placing orders for their first dual fuel crude oil tankers [12].

Furthermore, A.P. Moller – Maersk entered into an off-take agreement with the Chinese developer GoldWind for 500 ktpa and with the energy company Ørsted for 300 ktpa of eMeOH [13]. Additionally, to ensure that A.P. Moller – Maersk's fleet can be fuelled, A.P. Moller Holding acquired the majority of shares of the project developer C2X, with a minority stake acquired by A.P. Moller – Maersk. C2X plans to construct a 300 ktpa eMeOH plant in the port of Huelva, southern Spain [14].

On the other side of the off-take, chemical industries have also committed to adopting eMeOH. Last year, the world's largest toy company, LEGO Group, along with the pharmaceutical company Novo Nordisk, agreed to procure eMeOH for plastic production, demonstrating their commitment to sustainability [15]. Additionally, the energy and chemicals firm Mabanaft GmbH has committed to purchasing eMeOH from the project developer Highly Innovative Fuels (HIF) to ensure a stable supply of e-fuel to their customers [16]. Moreover, Egypt has garnered attention through purchasing and selling agreements between Methanex and Suez Methanol Derivatives (SMD). SMD has also entered parallel agreements with other chemical firms such as ECHEM, MOPCO, and Abu Qir [17].

These pioneering initiatives and agreements are catalysing a wave of new projects that, if successfully realized, will improve eMeOH production processes. This improvement will drive down costs, making eMeOH increasingly competitive with fossil-based MeOH. As the demand for sustainable energy carriers grows, the role of eMeOH in reducing CO_2 emissions becomes more prominent, especially given its potential to serve as a carbon-neutral alternative in various sectors such as transportation and chemicals.

1.2 Carbon dioxide

The production of eMeOH is closely tied to the availability and utilization of CO_2, which serves as a key feedstock in its synthesis. CO_2 is an odourless, colourless, and non-flammable gas at ambient pressure and temperature. Constituting about 0.038% of the Earth's atmosphere by volume [18], it is the fourth most abundant gas present. CO_2 molecules are composed of one carbon atom and two oxygen (O_2) atoms [19]. Its averaged global concentration has steadily increased more than 50 % since pre-industrial levels till 420 ppm in 2023 at a rate of more or equal than 2 ppm per year, according to the records from National Oceanic and Atmospheric Administration (NOAA) [20].

As already highlighted in the IPCC's 5th Assessment Report, the accumulation of anthropogenic GHG emissions in the atmosphere has unequivocally heightened global average land and ocean surface temperatures since pre-industrial times. This unprecedented temperature rise is primarily attributed to the expansion of the world's economies and its population, directly linked to accumulation of emissions in the atmosphere produced from the combustion of fossil fuels [21]. This accumulation of GHGs in the atmosphere is dictated by the equilibrium among human-induced emissions, human-induced removals, and the physical-biogeochemical interactions of sources and sinks on both terrestrial and marine ecosystems. Among the most impactful GHGs are CO_2, CH_4 and NO_x and fluorinated gases (F-gases). As highlighted by the IPCC in its Climate Change 2014: Synthesis Report, there has been a persistent upward trend over the last 50 years, with a notable acceleration from 2000 to 2010 [21]. This spike is primarily attributed to the heightened CO_2 emissions resulting from the combustion of fossil fuels and industrial activities. This serves no other purpose than to reinforce the evidence that the increase in global surface temperature is caused by the rising concentrations of anthropogenic GHG, as conclusively determined by the IPCC [21].

However, carbon can be generated from sources other than the combustion of fossil fuels. These sources can be classified into biogenic and non-biogenic categories, with the latter encompassing geogenic carbon along with carbon derived from fossil fuels [21]. This distinction is crucial when assessing its impact on the climate change experienced in the Earth system.

To comprehend this distinction, attention must be given to the concept of the carbon cycle defined by the IPCC in its 2013 Climate Change report: 'The Physical Science Basis' as a contribution from Group I to the 5th Assessment Report [1]. With that understanding, it can grasp how human activity has perturbed this carbon cycle state.

The carbon cycle is considered a set of interconnected carbon reservoirs within the Earth System, linked by fluxes of carbon exchange between them. From this perspective, two distinct domains can be identified: the fast and the slow domain. The fast domain is characterized by significant carbon exchange fluxes and fast reservoir turnover times, ranging from a few years at the atmospheric level to decades or millennia at the levels of land vegetation, soils, and oceans. In contrast, the slow domain corresponds to large carbon reservoirs, mainly geological, found in sediments and rocks. These reservoirs interact with the fast domain through volcanic emissions of CO_2, chemical weathering, erosion, and sediment formation on the sea floor, resulting in renewal times of more than a decade to millennia.

This naturally occurring carbon cycle has been disrupted by the extensive extraction and combustion of fossil fuels from human activities. This disruption leads to a transference of carbon from the slow domain to the fast domain, which the Earth System cannot autonomously process, as demonstrated. In simpler terms, this translates to substantial inflows of carbon relocating from geological stores, primarily towards the atmosphere – a process that the Earth System cannot cope with as swiftly as it occurs [1].

From the above, it can be said that while the combustion of fossil fuel and geogenic sources significantly accelerates the transference from slow to fast domain, the combustion of biogenic sources runs within the fast domain. The transition must be driven to the promotion of biogenic carbon and the reduction of non-biogenic carbon.

1.3 European emissions policies and regulations for industrial emitters

In 2005, the European Union (EU) Emissions Trading System (ETS) was introduced to curb emissions using a cap-and-trade mechanism. Under this system, companies must obtain emissions allowances (EUAs), each representing one tonne of CO_2, to offset their carbon emissions. Since the ETS's inception, a significant portion of these allowances has been allocated for free, while the rest are bought through auctions. Some firms successfully lower their emissions to stay within their free allowance cap, but others struggle to meet both their free cap and the overall cap. Consequently, a market for allowances emerges. Companies with excess free allowances can sell them to those needing more due to their higher emissions. Firms that exceed their total allocated cap face penalties for each tonne of CO_2 emitted beyond the limit [22].

The ETS initially targeted power generation plants and Energy Intensive Industries (EIIs) across the EU, gradually expanding to include sectors like aviation and maritime transport. Over various phases, the program has steadily reduced the total number of allowances, including those distributed for free, to these sectors [23].

Due to emissions taxation and increased production costs, some industries have relocated to countries with less strict or non-existent emissions regulations, such as China, India, or Africa, a phenomenon known as carbon leakage. This shift risks increasing global GHG emissions and weakening European industrial competitiveness. To address this, the EC launched the transitional phase of the Carbon Border Adjustment Mechanism (CBAM) in 2023. This phase aims to collect essential data on the embedded emissions of imported goods in preparation for the final taxation methodology set to take effect in 2026. Importers in sectors at risk of carbon leakage must submit CBAM certificates for their products' embedded emissions unless the exporting region has a similar carbon pricing system. The CBAM implementation will be gradual, in line with the phase-out of ETS free EUAs until 2034. This mechanism aims to harmonize the carbon pricing of imports with domestic production, promoting cleaner industrial practices in non-EU countries while supporting the EU's climate objectives [23].

Also, in 2023 the EC published the EU's definition of green H_2 in the Official Journal, completing the legislative process for the Delegated Acts. These Delegated Acts, now established as European law, define RFNBOs, including eMeOH [24].

These taxation policies, alongside other European regulations and incentives, are designed to guide industries in reducing, sequestering, or valorising their emissions. eMethanol plays a role in valorisation, enabling the development of CCU value chains, such as the one explored in this work.

In recent years, literature has increasingly focused on evaluating the economic, technological, and environmental implications of producing RFNBO compliant eMeOH compared to the currently less expensive fossil-based MeOH [25].

Studies on eMeOH production often emphasize sensitivity analyses on how the cost of H_2 impacts the final eMeOH cost, as well as reviewing the impact of the levelized cost of energy (LCOE) in H_2 production, which in turn affects eMeOH production expenditure [26], [27], [28].

Acknowledging that the cost of eMeOH production is primarily driven by the cost of H_2 feedstock and electricity pricing, this Master Thesis shifts the focus to another essential feedstock for eMeOH production: CO_2. Sourced from industrial processes, CO_2 is captured using various CC technologies that are tailored to the specific characteristics of each emitting source, as extensively reviewed in recent literature [3], [29], [30], [31]. However, CO_2 sources are often not located near MeOH consuming hubs, necessitating from a robust CO_2 logistics infrastructure. This logistics network is essential to connect CO_2 emitters with eMeOH plants, thereby forming a comprehensive CCU value chain. This connection ensures that CO_2 can be efficiently transported and utilized, which is critical for the feasibility and success of the entire process

2 Research objective and questions

In the context of global efforts to reduce CO_2 emissions, there is limited literature on the development of novel CCU value chains. This work aims to address this research gap by examining the CO_2 logistics infrastructure and process plants that are integral to these value chains. It also evaluates the costs associated with establishing and operating these assets, including CO_2 capture and liquefaction plants, CO_2 transportation by tanker and truck, and intermediate storage sites.

2.1 Research questions

The study aims to address the following research questions:

- What are the scales and primary cost drivers of the different stages that form a CCU value chain for various eMeOH production capacities?
- Which industrial CO_2 emitters present the best potential for CC to serve as feedstock in the study cases considered?
- Is it more cost-effective to transport CO_2 using tankers or truck fleets, and what variables significantly impact the decision between these options?

2.2 Scope and limitations

In this work, it is recognized that eMeOH and electrolysis plants, operate under a wide range of influencing factors, including fluctuating renewable energy availability, potential interruptions in the delivery chain, and varying demand. However, their primary objective remains the maximization of benefits while ensuring the fulfilment of product demand. Considering all the various ramifications that fall under these factors remains outside the scope of this Master Thesis, which instead seeks to provide an estimation of techno-economic figures for establishing a project which aims to commercialize eMeOH. Therefore, the direct optimization of different segments of this CCU value chain to maximize profitability is not conducted. Instead, the modelling process aids in comprehending the economic prerequisites for developing the value chain, which are grounded in the technical requirements. The insights gleaned from these figures allow for the simulation of various scenarios, reflecting the context encountered during the deployment of a CCU value chain.

Also, it is important to note that CO_2 emitters, as well as MeOH and H_2 production plants, typically operate at variable rates depending on several factors, resulting in outputs that are generally far from constant. Recognizing the fluctuating nature of these processes, this Master Thesis adopts a simplified modelling approach. It assumes that the CC plant receives a constant exhaust stream throughout the year and that the eMeOH production continuously converts the H_2 and CO_2 feed into the reactor at a steady rate. This approach simplifies the interdependent CO_2 logistics, which involve multiple steps of intermediate storage between the capture plant and the eMeOH plant, including transitions between different transport modalities.

In the economic modelling area, Development Expenditure (DEVEX) and decommissioning or site restoration expenditure are considered outside the scope of this academic work. This model focuses solely on calculating Capital Expenditure (CAPEX) and Operational Expenditure (OPEX).

3 Background

To produce eMeOH, it is essential to use green H_2 and CO_2 from biogenic or geogenic sources. This work focuses on the value chain that must be developed to ensure a continuous supply of CO_2 to the eMeOH plant, assuming that H_2 is produced on-site, thereby eliminating the need for upstream logistics. Understanding how CO_2 reaches the eMeOH plant from the industrial emitter involves recognizing that the carbon logistics chain can be divided into five stages: capture, liquefaction, transportation, storage, and utilization. This chapter will introduce the essential insights required for each of these five stages to generate a comprehensive understanding of the CCU value chain model simulated in this work.

3.1 Carbon capture plants

The critical urgency to combat climate change has emphasized the reduction of GHG emissions, with CO_2 being a major contributor. Between 1970 and 2010, CO_2 emissions from industrial activities and fossil fuel use made up about 78% of total GHG emissions [32]. This has prompted international initiatives like the Kyoto Protocol and the Paris Agreement, which aim to curb global temperature increases and achieve carbon neutrality by 2050. Among various decarbonization methods, such as energy-efficient technologies, clean fuels, and renewable energy deployment, CC has gained substantial attention as one of the most effective methods for cutting CO_2 emissions from existing industrial infrastructure [33].

Among the available CC methodologies, three primary categories stand out as the most cost-effective: post-combustion, pre-combustion, and oxy-combustion. Each of these approaches offers distinct advantages and disadvantages in terms of implementation and efficiency [34]. Notably, DAC is excluded from this discussion due to its significantly higher energy requirements compared to other CC technologies, driven by the low concentration of CO_2 in the atmosphere, rendering it less favourable for widespread adoption [35].

Pre-combustion CC entails decarbonizing the fuel prior to combustion by reacting fossil fuels with air or O_2, with or without steam, to generate syngas, predominantly composed of H_2 and CO. This syngas then passes through a water-gas shift reactor, where carbon monoxide (CO) reacts with water to produce CO_2 and H_2. The CO_2 is subsequently captured using methods such as adsorption, absorption, or membrane techniques. Given that the fuel has been pretreated prior to its combustion, this method presents elevated efficiencies in the capture process due to the higher concentration of CO_2 in the flue gas compared to other technologies. Additionally, the higher pressure and concentration of CO_2 result in reduced equipment size and increased energy efficiency, as the capture process operates at elevated pressures, minimizing the energy required for further CO_2 transportation [33], [34]. However, while the pre-combustion route can significantly reduce the required expenditure compared with post-combustion and oxy-combustion methods, it requires additional investment for setting up process units like gasifiers and water-gas shift reactors, which can hinder its widespread adoption [3].

In contrast, post-combustion CC entails capturing CO_2 from flue gas after combustion. This method is widely implemented in existing power plants because it can be retrofitted with minimal changes to current infrastructure. Flue gas, typically containing low CO_2 concentrations, passes through a capture system where solvents like aqueous amine solutions absorb the CO_2. Its advantages include its retrofit capability in existing industrial plants with minimal disruption, commercial viability, and operational flexibility [33]. Various pathways can be considered in the post-combustion method, such as membrane separation, chemical absorption, chemical looping, and physical adsorption [3].

Oxy-fuel combustion, on the other hand, involves burning fuel with pure O_2 instead of air. This generates flue gas mainly composed of CO_2 and water vapor, easily separated through condensation. An air separation unit (ASU) provides the necessary O_2. Oxy-fuel combustion offers high-purity CO_2, simplifying separation, substantially reducing nitrogen oxide (NOx) emissions due to the absence of N_2 in combustion, and enabling efficient capture with smaller equipment [33].

In summary, each CC technology offers diverse advantages tailored to specific applications. Post-combustion capture stands out as a mature technology that can be seamlessly integrated into existing industrial plants, making it versatile and cost-effective for retrofitting. Conversely, pre-combustion methods demonstrate superior sorption efficiency but come with higher initial and operational costs due to their complex setup. On the other hand, oxy-fuel combustion, an emerging technology, delivers high-purity CO_2 with reduced emissions and operational flexibility, albeit at the expense of higher energy consumption due to the ASU integration. Each method addresses different operational needs and scenarios, from enhancing efficiency in existing facilities to achieving high-purity CO_2 for various industrial applications.

As it will be later justified in Section 4.2.3, the selected technology for this study is the post-combustion amine-based CC. The process for this technology involves a series of absorption, cooling, and regeneration steps to transform flue gas into a CO_2-rich amine solution, from which pure CO_2 is ultimately extracted.

Initially, the flue gas, which has been quenched and saturated in a water pre-scrubber, enters the absorber column. This step ensures that the gas is cooled, and any large particulates are removed before further processing. Within the absorber, a counter-current flow of lean amine solution comes into intimate contact with the CO_2 in the flue gas. The amine solution absorbs the CO_2, leading to the formation of a CO_2-rich amine solution. The treated flue gas, now depleted of CO_2, exits the absorber column and is released into the atmosphere or fed into another treatment process. Midway through the absorber column, partially loaded amine is extracted, cooled in an intercooler, and then reintroduced into the column. This cooling step improves the efficiency of CO_2 absorption by maintaining optimal temperature conditions within the absorber.

The CO_2-rich amine solution is pumped from the absorber column to a lean-rich amine heat exchanger. This heat exchanger preheats the CO_2-rich amine solution before it enters the regeneration column. In the regeneration column, the solution is further heated to the boiling point using low-pressure saturated steam from a reboiler. This heating process strips the CO_2 from the amine solution. The now lean amine solution is then pumped back to the absorber column to be reused in capturing more CO_2 from the incoming flue gas. Energy recovery mechanisms, such as mechanical vapor recompression or condensate flash systems, are employed to reclaim energy from the process. This reduces the overall energy demand required for the reboiler to regenerate the amine solution, making the process more efficient.

The CO_2 that has been stripped from the amine solution is collected as a pure, water-saturated product at the top of the regeneration column. This needs to be dried before being liquefied.

The product rises to the condenser, where it is partially condensed. The condensed liquid, which is primarily water, is collected in the reflux accumulator. The reflux accumulator helps maintain the balance of liquid and vapor in the stripper column, ensuring efficient CO_2 separation. Reflux pumps then return a portion of this condensed liquid back to the top of the stripper column as reflux, while the remaining liquid is removed from the process [36], [37], [38]. After these steps, the dried CO_2 is ready to pass to the liquefaction process, which will be explained in the following section.

3.2 Carbon liquefaction plants

CO_2 liquefaction is essential for preparing the captured CO_2 for intermediate storage and subsequent transportation. In its liquid form, CO_2 has a density of approximately 1,100 kg/m^3, compared to less than 2 kg/m^3 at room temperature and atmospheric pressure. This significant increase in density makes liquid CO_2 much more cost-efficient for storage and transport

Initially, the CO_2 provided by the CC plant typically arrives at atmospheric pressure. The first liquefaction step involves its compression. There are two primary methods for cooling the CO_2 in the liquefaction process: the internal cooling loop and the external cooling loop. In the internal cooling loop method, the compressed CO_2 is further pressurized to approximately 70 bar and then expanded to the desired transport pressure. However, not all the CO_2 is liquefied during this process; some remains in a gaseous state, known as flash gas, which requires recompression. Water removal is a critical component of this stage, achieved through condensation and adsorption columns to meet specific water content specifications [39]. Alternatively, the external cooling loop method involves compressing the CO_2 to the desired transport pressure and cooling it using an external refrigeration system. This approach typically cools the CO_2 to temperatures as low as -28 °C and pressures of 15 bar, making it suitable for storage in tanks. Depending on the initial state of the CO_2 and transport requirements, a combination of internal and external cooling methods may also be employed [39].

The equipment involved in the liquefaction process includes compressors, cooling systems (internal or external), condensers, and adsorption columns. Internal cooling loop systems are simpler but typically less efficient than external cooling loop systems.

3.3 Carbon transport

CO_2 can exist in different physical states depending on the temperature and pressure. At low temperatures, CO_2 exists as a solid. When pressure drops below 5 bars (0.5 MPa), it sublimates into a vapor state. Within the temperature range spanning from its triple point to its critical point (-56.5 °C to 31.1 °C, respectively), gradual pressurization and heat removal facilitate the transition of gaseous CO_2 to a liquid phase [40].

CO_2 can be transported in gaseous, liquid, or, rarely, solid phase. Current CO_2 transportation methods adhere to specific end-use and transport specifications. Modular transport employs tanks conveyed by truck, train, or ship to deliver refrigerated liquid CO_2 to diverse industrial sectors, including food and beverage. The source of CO_2 is typically an ethanol plant because its exhaust concentration requires only purification, not CC. Product specifications ensure purity ranging from 99.5% to 99.9995%. Conversely, CO_2 pipeline transport, primarily for enhanced oil recovery (EOR) and geological storage, maintains less stringent quality standards. It predominantly occurs in North America, with CO_2 typically in a gaseous state [41]. To manage the large volume CO_2 occupies at atmospheric pressure, it is either pressurized or liquefied. Pressurized CO_2 is prevalent in pipeline transportation, while liquefaction is common in modular transport. Trucks are frequently utilized due to their flexibility, especially for destinations inaccessible by railways or located far from the coast [42].

Typically, CO_2 transportation in modular settings operates within a pressure range of 8 to 19 bar (0.8-1.9 MPa) and temperatures ranging from -55 °C to -20 °C. These conditions are conducive to maintaining CO_2 in its liquid state, ensuring efficient and safe transport. In the context of pipeline transportation, liquid-phase CO_2 at temperatures below 0 °C is usually not feasible unless the CO_2 emitter is located near the consumption point. This is due to the need for continuous refrigeration under negative temperature operating conditions.

Supercritical CO_2 pipeline transport involves pressures exceeding the critical pressure and temperatures higher than the critical temperature, around 74 bars (7.4 MPa) and 31 °C. In this state, CO_2 does not exhibit distinct gaseous and liquid phases, possessing a density akin to liquid CO_2 while maintaining a viscosity similar to its gaseous state. Dense-phase transport, achieved by lowering the temperature below 31 °C and increasing pressure above the critical pressure, increases density, enabling more efficient CO_2 transportation per unit volume. Supercritical and dense-phase CO_2 transport methods are considered the most cost-effective for long-distance pipelines and high-throughput scenarios. Conversely, transporting CO_2 in a pressurized gas state at pressures below 48 bar, while offering higher operational security, is typically more expensive. It is best suited for short distances or when the CO_2 source is in gaseous form, as it minimizes the need for additional compression or cooling equipment [43].

Additionally, careful consideration of CO_2 composition is essential to mitigate potential issues during its transport such as corrosion or the release of toxic chemicals, particularly when CO_2 is not in a pure state [42].

3.3.1 Carbon transport by tanker

Examining the maritime sector more closely, although CO_2 transport by tanker is a well-established technology, its current implementation is limited to small-scale carriers with capacities of up to 1,500 m^3 [39]. However, maritime transport is anticipated to play a pivotal role in the advancement of commercial-scale Carbon Capture, Utilization, and Storage (CCUS) value chains. This is primarily due to its flexibility, cost-effectiveness, and expedited deployment compared to pipeline infrastructure. The maritime sector's advantages include its ability to adapt to varying scales of operation and its relatively lower capital investment requirements. Major shipping companies have highlighted that deploying CO_2 transport by sea faces fewer obstacles compared to the challenges associated with pipeline systems, which often involve complex permitting and construction processes. In fact, leading shipping companies have noted that there are no significant barriers to maritime CO_2 transport when compared to the current practices of bunkering and shipping other gases [44]. This potential is underscored by significant financial commitments already made towards CCUS infrastructure, as evidenced by the Northern Lights CCS project. This pioneering project has seen substantial investment, including the commissioning of the first three liquefied CO_2 carriers by Dalian Shipbuilding Offshore (DSOC). Of these, the initial two vessels have already been floated out in Chinese waters, marking a significant milestone in the project's logistics [45]. Moreover, the growing interest in maritime CO_2 transport is reflected in recent orders for liquefied CO_2 carriers. Notably, in the latter half of 2023, Capital Maritime, under the direction of Evangelos Marinakis, placed an order for two 22,000 m^3 capacity vessels with HD Hyundai Mipo Dockyard (HMD) [46]. Concurrently, Bernhard Schulte has ordered a 7,500 m^3 capacity vessel from DSOC, which will join the fleet as the fourth sister vessel for the Northern Lights project [47]. These developments highlight the increasing confidence and investment in maritime CO_2 transport as a viable and scalable solution for CCUS application.

Even though capacities reaching the 74,000 m^3 or 40,000 m^3 were presented by HMD and classified by American Bureau of Shipping and Lloyd's Register in late 2022, the reality is that only smaller size carriers have been ordered. These vessels could serve different routes of CO_2 supply and consumption. However, long-term contracts between consortia will be required to de-risk investments for such vessels sizes and those agreements are unlikely to occur in the short-term. In contrast, the current design of the vessels ordered is smaller in size, which entails a lower investment risk and is adapted to the specificity of the projects for which they are sized.

3.3.2 Carbon transport by truck

Truck transportation offers a flexible solution for CO_2 logistics, particularly when CO_2 sourcing sites are not accessible by ship or rail. Additionally, when pipeline deployment is hindered by environmental concerns or technical constraints, trucks can effectively transport CO_2 since all industrial plants are connected by road infrastructure. Additionally, the swift deployment capability of truck fleets makes them an optimal initial transport solution while more permanent transportation infrastructure is being developed. However, given the large volumes of CO_2 that need to be handled in the CCU value chain, trucks are unlikely to be a cost-effective long-term option.

In the context of liquid CO_2 transportation, tanks can either be integrated with the truck's chassis or designed as containerized units within a standardized frame. In the former case, the liquid cargo is loaded and unloaded directly on the truck, as depicted in Figure 2.

Figure 2: Loading of truck carrying liquid CO_2 [48]

In the latter case, illustrated in Figure 3 and Figure 4, the entire tank container can be transferred to another transport mode, such as a train or ship.

Figure 3: 40-foot tank container carried by a truck [49]

Figure 4: 20-foot container for liquefied CO_2 transportation [50]

This method is particularly beneficial when multiple transport modalities are involved, as it minimizes transfer losses by keeping the CO_2 within the same container throughout the transport process. Tank containers are commonly used for transporting liquid cargoes such as Liquid Natural Gas (LNG), Liquid Petroleum Gas (LPG), ethane, ethylene, and liquid nitrogen (N_2). These containers are designed within a frame-type structure with corner castings to meet various container standards, typically available in sizes of 10, 20, and 40 feet [49]. The dimensions of these containers allow them to carry approximately 12 m^3, 25 m^3, and 48 m^3 of liquid cargo, respectively.

Regarding transport pressures, literature indicates a range of values from low pressures of 6 barg to middle pressures of 19 barg or even exceeding 20 barg [51], [52], [53]. These pressures influence the tonnage each truck can carry for a given tank volume. For instance, tonnages can vary from 10 to 26 tons, with volumes ranging from 6 to 48 m^3, depending on the pressure [49],

[52], [53], [54], [55]. While 10- and 20-foot container tanks can handle pressures exceeding 20 barg in some cases, larger 40-foot tanks typically operate at low pressures rather than middle pressures. For example, in Figure 3, a truck is shown carrying a low-pressure 40-foot tank container suitable for LNG transport. Figure 4 illustrates a 20-foot tank container designed for transporting liquid CO_2 under middle pressure [50].

3.4 Intermediate carbon storage

In any batch-wise logistics chain, the introduction of multimodal transportation necessitates the inclusion of intermediate storage facilities both before and after the transportation link. These storage options encompass various configurations, such as horizontal or vertical cylindrical tanks, as well as spherical tanks. Among these options, cylindrical tanks are the most frequently utilized due to their simpler manufacturing process compared to spherical tanks. Additionally, cylindrical tanks can be organized into rectangular structures on-site, between other utilities, and transported in these structures to the operational location for installation. Conversely, spherical tanks offer reduced heat transfer to the environment for the same capacity. However, given the spatial constraints typically associated with intermediate storage sites, vertical tanks are often preferred due to their efficient utilization of space compared to spherical and horizontal cylindrical tanks [39]. Concerning the storage conditions for CO_2, it is typically stored in liquid form at medium pressures ranging from 15 to 23 bar, with less frequent storage occurring at lower pressures of 8 bar.

Regarding tank capacity, various safety margins for operational flexibility are explored in the literature, with sizing typically quantified as multiples of the ship's carrying capacity in tons. Reported minimum capacities range from 100% to maximum arrangements of 150% of the ship's capacity. However, the majority of capacities fall around 120% of the ship's carrying capacity which has to be sufficient in case of delays [44], [56]. These tanks not only decouple CO_2 production from the batched loading into transportation but also reduce loading times, as they enable a faster flow rate than typically provided by the CO_2 source.

To transfer CO_2 between the tank farm and the corresponding transport medium and vice versa, supplementary equipment such as loading arms, pipelines, pumps, heaters, coolers, compressors, and valves are required. For example, during the offloading process from the tanker to the storage tanks, an internal ship pump powered from onshore conveys the CO_2 into the storage tanks through the loading arms and insulated pipelines. This process generates a pressure drop in the tanker while pressure increases in the onshore tanks due to gas compression. An equilibrium vent line between the onshore tank farm and the tanker ensures that gas is returned to the tanker tanks with the help of compressors, facilitating a balanced and efficient transfer process. Similarly, when CO_2 is being loaded into the tanker, the CO_2 is conveyed through the insulated pipelines designed for the specified pressure and temperature from the storage area to the loading arm and tanker, utilizing pumps situated near the tank facility. A secondary line, aided by compressors, returns boil-off gas from the tanker's tanks back to the onshore storage tanks, maintaining system pressure balance [56], [57]. This set of supplementary equipment, which transfers CO_2 between storage tanks and tankers, is identified as the loading and unloading systems.

3.5 eMethanol production plants

The production process of eMeOH involves multiple steps and specific equipment to transform raw materials, H_2 and CO_2, into eMeOH with concentrations exceeding 99% [58], [59], [60].

This section aims to present the general configuration of eMeOH production plants, which generally consists of two main stages: the synthesis loop followed by the distillation phase. Across the plants reviewed, it has been recognized various liquid-gas separation assemblies to increase eMeOH concentrations. Similarly, diverse heating and cooling integration arrangements are utilized to for example, make use of the heat from the exothermic reaction in the reactor, addressing part of the plant's thermal needs. Given the numerous and diverse settings for liquid-gas separations and thermal integrations, which vary from plant to plant, this section provides an overview of their typical configurations rather than delving into specific details.

Initially, the eMeOH production plant receives H_2 and CO_2, which are first compressed independently and then combined, or just combined, reaching pressures between 50 and 100 bar, determined by the operational requirements of the MeOH reactor [60], [61]. Before entering the reactor, the mixture is blended with the unconverted gases recycled from the reactor's output, to reach the targeted high feedstock conversion. The mixture is then preheated to temperatures typically ranging from 200 to 300 °C [60], depending on the reactor specifications. These temperatures are achieved by recovering thermal energy from the reactor’s outlet stream, attributable to the exothermic nature of the overall reactions occurring within. The main reactions occurring are listed here:

$$CO_2 + 3H_2 \leftrightarrow CH_3OH + H_2O \tag{1}$$

$$CO_2 + H_2 \leftrightarrow CO + H_2O \tag{2}$$

$$CO + 2H_2 \leftrightarrow CH_3OH \tag{3}$$

CO_2 hydrogenation (1), reverse water-gas shift (2), and CO hydrogenation (3), reactions occur under the aforementioned conditions with the contribution of typically used Cu/Zn/Al-based catalyst [26], [27], [61], [62].

The heat proceeding from the outlet reactor stream is also utilized in some instances for other heat requirements, such as those in the reboiler for the distillation phase [61]. In order to separate the product, the stream is cooled and thereby it undergoes partial condensation. Subsequently, a gas-liquid separator is employed to segregate the gas stream, characterized by a higher concentration of reactants than of eMeOH, from the liquid stream, which mainly consists in MeOH and H_2O. The gas stream gets recycled back to the reactor, while the liquid stream, (raw eMeOH) proceeds to the distillation phase. Another gas-liquid separation process is typically applied to the liquid stream at atmospheric pressure after passing through a valve, thereby increasing the eMeOH concentration at each stage [26], [60], [61]. At the conclusion of the liquid-gas separation process, a compressor is utilized to restore the circuit pressure of the recirculated stream, which is in a gaseous state, to the level required by the reactor.

Within the synthesis loop, a purge is conducted to avoid the accumulation of inert gases. In conventional MeOH plants, this purge is typically combusted to produce thermal energy for heat requirements [26], [58], [61]. This practice is adopted because the purged gas contains heat content from CO, H_2, MeOH, and CH_4. Additionally, the purge is incinerated due to the toxicity and hazardous nature of its components, which cannot be freely released into the atmosphere.

In the second phase, the product from the synthesis loop is fed into the distillation train, where the purification of MeOH from H_2O and other impurities is achieved, owing to its lighter nature. The liquid stream enters the centre of the distillation column and descends due to gravity. Meanwhile, it interacts with a vapor flow ascending in the column, also propelled by its buoyancy. These counterflowing streams pass through stacked trays within the distillation column, maximizing the surface area for liquid-vapor contact and thus enhancing evaporation efficiency. The ascending vapor flow is generated by the reboiler, located at the bottom of the column. Due to the higher volatility of MeOH compared to H_2O and other impurities, its concentration is higher at the top of the column. The vapor-rich stream at the column's uppermost section condenses into liquid form in the condenser, located downstream from the top of the column. After condensation, a liquid-gas separation takes place. A portion of the liquid output from this separation, known as distillate, proceeds to the next distillation column, while the rest is recirculated back to the top of the distillation column as reflux. Depending on the desired MeOH concentration, one or more distillations are performed.

In summary, this chapter has detailed the key stages of the CO_2 logistics chain—capture, liquefaction, transportation, storage, and utilization—essential for understanding how CO_2 is managed from its source to the eMeOH plant. This background sets the stage for the methodology discussed in Chapter 4, which will build on this foundational knowledge to further analyse the CCU value chain proposed scenarios.

4 Methodology

This chapter outlines the methodology employed to conduct the techno-economic analysis of the CCU value chain. It begins with an introduction to the LCOeM, followed by the technical sizing of each stage of the CCU value chain. Finally, the economic assessment is coupled with the technical analysis to provide comprehensive insights.

4.1 Levelized Cost of eMethanol

The LCOE represents the unit cost of energy produced throughout the economic life of a project [63]. Two predominant methods can be distinguished for calculating levelized costs: the "annuitizing" method, followed by the US National Renewable Energy Laboratory (NREL), and the "discounting" method, favoured by the UK Government Department for Business, Energy & Industrial Strategy (BEIS). The BEIS method has been selected for this study due to its comprehensive approach that provides a straightforward application for the capital and fuel costs (which is more suitable for this study's objectives) [64].

This Master Thesis adopts the LCOE metric and focuses on the levelized cost of eMeOH (LCOeM), which can be calculated as follows:

$$LCOeM = \frac{PLC}{eMeOH\ LP} = \frac{€}{kton\ eMeOH} \tag{4}$$

While the numerator computes the project lifecycle cost (PLC) in euros (€), the denominator calculates the eMeOH lifetime production in kilotons of eMeOH. When discussing the PLC or the expenditures required to bring a project to fruition, they are typically categorized into four main types: DEVEX, CAPEX, OPEX and decommissioning or site restoration expenditure.

DEVEX primarily involves costs associated with the early stages of project development, from initial planning to the Final Investment Decision (FID). These costs often include feasibility studies, environmental impact assessments, pre-FEED (Front-End Engineering Design) and FEED studies, detailed project design and planning, engineering and consultancy fees, project management costs during development, regulatory and permitting costs, and sometimes land acquisition if it occurs early in the process.

CAPEX typically covers the costs necessary to create and set up an operational asset. This includes construction costs, machinery and equipment purchases, installation costs, initial project design and engineering, licenses and permits, and the initial infrastructure setup. Once the asset is operational, OPEX comes into play. OPEX includes recurring costs required to keep the asset running smoothly. These expenses cover raw materials, labour, maintenance, utilities, and other ongoing operational costs.

At the end of the asset's lifecycle, decommissioning or site restoration expenditure becomes relevant. This includes costs for dismantling and removing plant and equipment, site cleanup and remediation, waste disposal and management, restoration of the site to its original state or repurposing it for other uses and ensuring regulatory compliance and environmental impact mitigation.

In this work, while CAPEX and OPEX are central to levelized cost calculations, DEVEX and decommissioning expenditures have not been considered. This approach helps avoid the complexities related to preliminary and end-of-life financial considerations. Additionally, within the OPEX category, variable costs have been treated as constant throughout the project lifetime to streamline the cost analysis. This deliberate focus allows for a simplified analysis of the direct costs associated with establishing and operating the asset, consistent with the available literature reviewed.

As presented in equation (5), both costs and production volumes are evaluated in Net Present Value (NPV) terms, ensuring that future expenditures and outputs are appropriately discounted to their present value for accurate comparison with current costs and outputs [65].

$$LCOeM = \frac{NPV_{Cost}}{NPV_{eMeOH}} = \sum_{t=1}^{N} \frac{CAPEX_t + OPEX_t}{(1+d)^t} \Big/ \sum_{t=1}^{N} \frac{eMeOH\ capacity_t}{(1+d)^t} \tag{5}$$

Here, N denotes the number of years the plant will operate, t signifies the specific year, and d represents the real discount rate. The literature typically uses 8% as the nominal discount rate. [26], [27], [66]. The average inflation rate i over the last 20 years is calculated to be 2.21% [67], and applying equation (6) is to calculate the real discount rate results in 5.66%.

$$d = \frac{1 + d_n}{1 + i} - 1 \tag{6}$$

If careful attention is paid to the denominator of the formula in equation (5), representing the production of eMeOH throughout the lifetime of the project, it can be noticed that the production is discounted. In this work, it is posited that the discount factor in the denominator of the LCOeM formula represents the depreciation of assets, including the eMeOH, CC and CO_2 liquefaction plants, as well as the transport and storage infrastructure. This suggests that by discounting the production of eMeOH, the revenue associated with future production is actually being discounted. This understanding stems from academic discussions surrounding the discounted energy production in the original LCOE [68]. However, BEIS has not explicitly clarified the grounds for this reduction in annual electricity production in their approach.

If the project's Internal Rate of Return (IRR) equals d, then the costs incurred by the project are equivalent to the revenues extracted from it. This relationship allows for the derivation of LCOeM, as specified in equation (8):

$$NPV_{project} = NPV_{revenues} - NPV_{costs} = 0 \tag{7}$$

$$LCOeM = \frac{NPV_{revenues}}{NPV_{eMeOH\ capacity}}$$

(8)

For the purpose of this work, the LCOeM considered can be segmented into different stages as outlined below:

$$LCOeM = LCOCO_{2\ Capture} + LCOCO_{2\ Liquefaction} + LCOCO_{2\ Loading\ intermediate\ storage} + LCOeM_{CO_2\ Transport} + LCOCO_{2\ Unloading\ intermediate\ storage} + LCOeMeOH_{Production}$$

(9)

The different summands of this equation represent, in order of appearance, the LCOeM for:

- *$LCOCO_2$ Capture*: the cost of capturing the CO_2 from the source,
- *$LCOCO_2$ Liquefaction*: the cost of liquefying the CO_2 throughput from the CC plant,
- *$LCOCO_2$ Intermediate Storage*: the cost associated with storing the liquid CO_2 in the origin and receiving intermediate storage sites,
- *$LCOCO_2$ Transport*: the cost of transporting the liquid CO_2 from the loading to the unloading intermediate storage
- *LCOeMeOH Production*: the cost of producing eMeOH, also including expenses associated with acquiring feedstocks such as H_2 and CO_2 acquisition.

Lastly, it is important to mention that when calculating the levelized cost of the various assets within the project's value chain, it is assumed for simplicity that CAPEX is incurred in a single year, specifically the year prior to the start of operations. This simplification is made despite the fact that the acquisition timelines for different assets may vary, potentially requiring more than one year or, in some cases, less.

4.2 Technical assessment

In conducting a techno-economic analysis of a CCU value chain, which includes the eMeOH production process and its associated CO_2 logistics and capture, a logical sequence typically starts with CO_2 capture and ends with the production of eMeOH, as illustrated in Figure 5 from left to right.

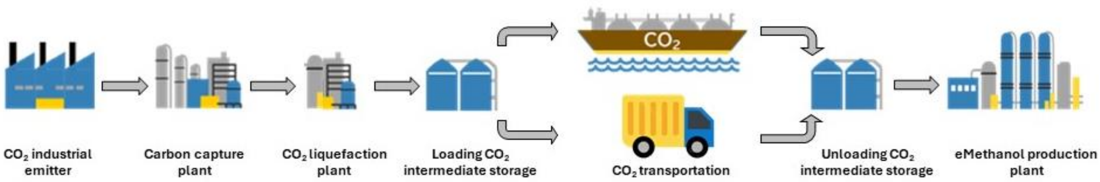

Figure 5: Schematic of the CCU value chain modelled

However, for practical reasons, this Master Thesis does not follow this sequential order when sizing each stage of the value chain. Instead, it assesses the technical and economic requirements of each stage in the following order:

- eMeOH plant
- Unloading CO_2 intermediate storage
- Tanker and truck CO_2 transportation

- Loading CO_2 intermediate storage
- CO_2 liquefaction
- CC plant
- Industrial CO_2 emitters

The work began with the sizing of the eMeOH plant to determine the CO_2 feedstock requirements accurately. This step was crucial for establishing the precise CO_2 demand which will vary depending on the desired eMeOH capacity. Following this, the receiving intermediate storage site was assessed and sized to ensure adequate CO_2 storage prior to its consumption at the eMeOH plant. Next, the logistics design of the truck and tanker transport fleet was evaluated, to meet the CO_2 feedstock requirements of the eMeOH plant. After optimizing the transport logistics, the study then addressed the origin intermediate storage site, ensuring it could effectively load the trucks and tankers. Subsequently, the needs of the liquefaction plant were analysed, considering the requirements for liquefying the captured CO_2. Afterwards, the design and operational requirements of the CC plant were assessed to complete the process chain.

Finally, potential industrial sources of CO_2 feedstock for the eMeOH plant were identified. By following this order, it is ensured that each stage of the value chain was optimally designed to meet the specific needs of the preceding stages, thereby enhancing the overall efficiency and feasibility of the eMeOH production system. However, this chapter will present the technical and economic sizing from the industrial emitter to the eMeOH plant, as illustrated in Figure 5. This aims to enhance the reader's understanding of the CCU value chain modelled, with a narrative that begins upstream at the CO_2 emitter and concludes downstream at the CO_2 consumer, the eMeOH plant.

Furthermore, it is crucial to understand that each plant and logistics infrastructure modelled is interconnected and operates in harmony with both upstream and downstream stages to ensure CO_2 demand is consistently met. However, these interconnections and the varying unavailability periods throughout the year from each of the plants and logistics infrastructure mean that they must have higher capacities to cover non-operational hours.

For instance, to ensure the CO_2 demand at the eMeOH plant is met, the transport option will require a higher number of trips per year since the fleet is not operating the full 8,760 hours in a given year. Consequently, more trips are necessary, implying that the upstream intermediate storage must have a higher capacity to ensure sufficient CO_2 availability for transport. This necessitates oversizing these logistics infrastructures to account for both the intermediate storage's non-operational hours and the transport option's ones. Similarly, the liquefaction and CC plants must have a higher throughput to compensate for their downtime and the non-operational hours of the storage. It is worth noting that the storage sizing already accounts for sufficient design overcapacity to balance the downtimes at both the origin and receiving intermediate storage sites. However, for other process plants and transport options, the total operational hours per year must be carefully considered. The modelling has accounted for these overcapacity requirements and performed the calculations accordingly.

The upcoming sections will detail the technical and economic sizing of each stage within the value chain depicted in Figure 5. These sections utilize metrics most representative of their respective value chain stages. Specifically, the sections on CC, CO_2 liquefaction, transport, and storage are calculated based on the CO_2 capacity, measured in ktons of CO_2. Conversely, for the eMeOH plant, the metric used is the production capacity of eMeOH, measured in ktons of eMeOH. This approach facilitates the integration of the different stages within the CCU value chain. By adjusting the desired eMeOH production capacity, the corresponding upstream process plants and CO_2 logistics infrastructure are recalculated accordingly, ensuring coherence and scalability throughout the entire value chain.

Lastly, it is essential to note that, for the sake of simplicity, the inclusion of pipelines connecting various plants as means of transporting CO_2 has been excluded in this study. This decision means that practical infrastructure, such as the pipeline required for transporting CO_2 from the eMeOH plant to the receiving intermediate storage site, is not accounted for in this work. Similarly, this exclusion applies to interconnections between the CC plant and the liquefaction plant, as well as between the liquefaction plant and the origin intermediate storage site.

4.2.1 Carbon emissions characterisation

This section discusses the diverse sources of carbon emissions that can serve as feedstock to produce renewable fuels like eMeOH.

Biogenic CO_2 is poised to play a significant role in achieving climate action objectives by serving as a feedstock for e-fuels production. These e-fuels have immense potential to replace traditional fossil fuels. Consequently, it is anticipated that biogenic CO_2 will emerge as a valuable commodity, given its crucial role in advancing a sustainable closed-loop carbon economy. This presents an opportunity for various biogenic sources, including ethanol plants, biomass power plants, Waste-to-Energy (WtE) plants, cement industries, pulp and paper industries, alcohol and sugar production plants, and biogas plants, to market their CO_2 to produce sustainable fuels.

Regarding the utilization of CO_2 for the production of eMeOH, as described in Section 1, CO_2 can be originated from both geogenic and biogenic sources until 2041, after which it is expected to be exclusively biogenically sourced. The listed production plants and industries emit biogenic emissions exclusively or a combination of geogenic and biogenic emissions while in operation.

Geogenic CO_2 emissions primarily come from industrial processes, particularly in the cement sector, where they are generated during the calcination of limestone. This process takes place in the lime kiln at elevated temperatures, resulting in the production of quicklime, which is then used to produce clinker. These geogenic emissions account for two-thirds of total CO_2 emissions in the cement industry. CO_2 concentrations in the flue gases from calcination range from 15% to 30% [69], [70], [71]. The remaining emissions are linked to the combustion of biomass and fossil fuel, as detailed later.

Similarly, in the pulp and paper industry, limestone is calcined in a lime kiln to produce quicklime, which is essential in the re-causticizing unit. The emissions from this calcination process follow a closed loop within the unit. Quicklime generated from limestone calcination is used in the re-causticizing unit to convert green liquor into white liquor. During this process, quicklime reacts with sodium carbonate (Na_2CO_3) in the green liquor to produce sodium hydroxide (NaOH) and lime mud, primarily composed of calcium carbonate ($CaCO_3$). Lime mud is recycled by returning it to the lime kiln where it is calcined to recover quicklime. This closed-loop system ensures that CO_2 released during calcination is captured and reused within the lime kiln, hence, no geogenic emissions are released [72], [73]. During these reactions, CO_2 originating from the green liquor is released, representing a significant biogenic CO_2 source within the pulp and paper plant. Yet, the primary source of biogenic CO_2 in pulp and paper plants arises from the combustion of black liquor or biomass in the recovery boiler, followed by the multi-fuel boiler, which is fed with all the bark from the wood handling plant and typically with the bio-sludge from the wastewater treatment plant. These sources account for approximately three-quarters of the total CO_2 emissions [73]. However, depending on the proportion of biomass versus fossil fuels combusted in the multi-fuel boiler for steam production and in the lime kiln for calcination, biogenic CO_2 emissions can reach up to 100% if no fossil fuels are used. This scenario is uncommon, as the use of non-fossil fuels to produce the required heat might be limited to ensure the production of high-quality lime and reduce the amount of non-performing elements (NPEs) into the system [73]. Based on literature, biogenic sources generally contribute around 80% of emissions, with the remaining 20% originating from fossil fuels, though specific proportions may vary by plant [69], [73]. The situation is similar in cement production, where the proportion of biomass versus fossil fuels used to achieve the elevated temperatures for the calcination process determines the amount of biogenic CO_2 emissions. According to literature, biogenic sources contribute approximately 6% of total emissions, in addition to two-thirds of geogenic emissions, resulting in a combined 72.7% of the cement plant's total CO_2 emissions [69].

Regarding biogenic CO_2 emissions in other industries, process emissions from plants that use fermentation to produce ethanol exhibit the highest CO_2 concentration among all plant types. The natural biological processes converting plant-based material into ethanol yield highly pure CO_2 off-gas streams with a concentration of 99 vol% [74]. Another source of process emissions with elevated CO_2 concentration is from biogas plants, which rely on the fermentation of food waste and other biomass-based resources to produce CH_4 [71], [75]. Additionally, other plants involved in fermentation processes, such as food-grade alcohol and sugar production plants, also yield elevated concentrations of CO_2, reaching 80-90% [70].

More typically, biogenic CO_2 emissions at the described plants originate from the combustion of biomass-based fuels to achieve the high temperatures necessary for industrial-scale reactions. The underlying combustion process can be simplified as follows:

$$Fuel\ (C, H, O, N)\ +\ Air\ (O_2, N_2)\ \rightarrow\ CO_2\ +\ H_2O\ +\ N_2 \tag{10}$$

The reaction output yields CO_2 concentrations ranging 5-15%, with the remainder primarily composed of N_2 and O_2 due to the use of air along with H_2O and other marginal gas concentrations [70], [76]. Alternatively, fossil fuels can be used to support combustion. The ratio between fossil fuel and biomass-based fuel utilization determines the proportion of fossil fuel or biogenic emissions related to combustion. Biomass plants contribute the largest share of biogenic CO_2 emissions, approaching 100% due to the nature of their fuel origin. They are followed by WtE plants, which incinerate municipal waste with a high biological origin [70]. Other plants typically combust a mixture of fossil fuel and biomass-based fuels to achieve the elevated temperatures required for their processes. Consequently, the amount of biogenic CO_2 emissions heavily depends on biomass availability, fossil fuel prices, and the application of fossil restrictive policies in each industry.

It is worth mentioning that the concentrations of CO_2 in combustion gases are mainly influenced by the quality of the fuel burned, along with variables such as combustion efficiency and combustion regime. However, the aforementioned values serve as a reference for selecting plants for which CC introduction will be assessed in the next sections.

4.2.2 Scenario selection

To select the scenarios for simulation, it is critical to establish industrial cases that can be realistically implemented. Therefore, an initial analysis of biogenic and geogenic CO_2 must be conducted to ensure a sufficient feedstock supply for the production of RFNBO-compliant eMeOH and this analysis is detailed in this section.

Firstly, it is important to emphasize that the project envisioned in this work consists of a CCU value chain, which includes two different transport mediums. Consequently, given that maritime transport is one of the selected mediums, the scenarios for simulation include the construction of an eMeOH plant within port premises. Upstream in the value chain, it is considered that the existing CO_2 emitting industries are located no further than 15 km from a port equipped with liquid cargo infrastructure. This consideration eliminates the need to simulate the CO_2 transportation step between the CO_2 source and the nearby harbour. Although it is acknowledged that when CO_2 emitters are not in the vicinity of a harbour, this transport is required.

Once the placement criteria for the CO_2 consumption and CO_2 production plants are introduced, the remaining plants and corresponding logistics infrastructure can be explained. In regard to CC and CO_2 liquefaction plants, as well as the origin intermediate storage, they are envisioned to be placed at the emitting point. Here, the CC will capture the CO_2 from the flue gases, and the liquefaction plant will connect to the CC, liquefying the captured CO_2, which is then stored at the storage site, awaiting transportation in liquid state from the origin intermediate storage to the receiving one.

The receiving intermediate storage site is situated at the premises of the eMeOH plant, which is located in the harbour. In terms of transport mediums, both road and maritime transport connect the intermediate storage sites. This implies that in scenarios where CO_2 is transported by truck, the CO_2 origin port and the receiving port must have adequate road infrastructure to ensure a smooth connection between sites. Similarly, CO_2 transport by tanker requires harbours with liquid cargo infrastructure capabilities. To maximize the potential for exporting eMeOH, strategic positioning within the Iberian Peninsula territory must be considered for the receiving port. The largest ports in terms of cargo handling capabilities within the territory include, in alphabetical order:

- Algeciras
- Aveiro
- Barcelona
- Bilbao
- Lisbon
- Sines
- Tarragona
- Valencia

Among these ports, the Port of Sines stands out due to its unique features that match the ideal characteristics for hosting an eMeOH plant and excels in smooth connectivity both by road and sea. As the primary port on the Ibero-Atlantic front, Sines is strategically positioned to be a key hub linking the North-West USA, Rotterdam/Antwerp, Fujairah, and Singapore through a maritime green corridor. Sines boasts critical features such as an open deep-water seaport with excellent maritime access, leading the Portuguese port sector in cargo volume handled. Additionally, it possesses unique natural characteristics that enable it to accommodate any type of vessel. These attributes position Sines as the perfect location for an eMeOH plant, given its export capabilities to connect with the largest consumers of green chemicals, primarily in Central Europe. Additionally, its increasing bunkering capabilities reinforce its suitability for importing CO_2 for the eMeOH plant.

To model real CO_2 emitting industry cases suitable for implementing a carbon logistics chain for eMeOH production via both tanker and truck, a filtering or elimination method was employed. This systematic approach is widely utilized in decision-making processes to methodically narrow down the number of options based on predefined criteria. The initial sample comprised all industrial CO_2 emitting sources in Spain and Portugal. This broad dataset was then progressively filtered, applying specific criteria at each stage to exclude non-qualifying sites. The objective was to identify a unique subset of emitters that could feasibly supply CO_2 for an eMeOH RFNBO compliant plant situated in the port of Sines. This method ensures that the selected sources not only meet emission type and volume requirements but are also geographically viable.

To initiate the filtering method, the territorial scope of this model is confined to the Iberian Peninsula, encompassing Portugal and Spain. Within this defined territory, the types of emitting industries that exist were reviewed in Section 4.2.1, focusing on those emitting biogenic and geogenic CO_2 emissions as part of their total CO_2 output. The relevant industries identified include ethanol plants, biomass power plants, WtE plants, cement industries, pulp and paper industries, alcohol and sugar production plants, and biogas plants. As detailed before, only biogenic and geogenic CO_2 emissions are possible for producing eMeOH compliant with RFNBO standards until 2041, according to RED III [7]. Consequently, CO_2 emissions originating from fossil fuels were excluded from this CCU approach for eMeOH production.

The following step in the process of selecting viable CO_2 sources for large-scale eMeOH production is identifying the existing plant typologies within the Spanish and Portuguese territories. Comprehensive data revealed that all targeted plant types are present in both countries, but the scale of these plants emerged as a critical factor. Ensuring sufficient CO_2 supply for eMeOH production necessitated the exclusion of plant types typically operating on a smaller scale with lower CO_2 emissions.

To initiate this exclusion process, data from the biogenic and geogenic CO_2 potential assessment for Sustainable Aviation Fuel (SAF) production by ERM Worldwide Group Limited was utilized [77]. Additionally, relevant figures were sourced from Endrava, a company specializing in databases of large CO_2 emitters and CC projects.

The filtration criteria led to the exclusion of several plant types due to their insufficient CO_2 emissions, leaving cement and pulp and paper plants as the primary candidates. Initially, biomass plants were considered due to their CO_2 emissions originating entirely from biogenic sources. However, they were excluded because their average CO_2 output of 400 ktpa is significantly less than that of cement and pulp and paper plants. This lower output makes biomass plants less viable for large-scale eMeOH production. Ethanol plants, although among the largest of the excluded types, also fell short. Their CO_2 emissions rarely exceed 200 ktpa, and with 98% of these emissions being biogenic, they produce approximately 198 ktpa of CO_2, which is insufficient for the project's needs [70], [77].

Similarly, WtE plants, with an average CO_2 production of 285 ktpa and 60% of emissions from biogenic sources, contribute around 170 ktpa of biogenic CO_2. This figure does not meet the required threshold for our project. Alcohol and sugar production plants were also excluded because they typically produce less than 100 ktpa of biogenic CO_2 emissions, making them unsuitable for supplying the necessary CO_2 for eMeOH production [70].

After this comprehensive assessment, only cement and pulp and paper plants were found to have the high CO_2 production levels needed for effective eMeOH production, thus being selected as the ideal sources for CO_2 supply.

The next step in the filtration process involves identifying cement and pulp and paper industries located near a harbour to facilitate CO_2 shipping by tanker and truck. As previously mentioned in this section, these industries should be no further than 15 km from the port. Based on this criterion, the selected sites are displayed in Figure 6 and in **Error! Reference source not found.**. The latter details the industry typology, the company, and its location.

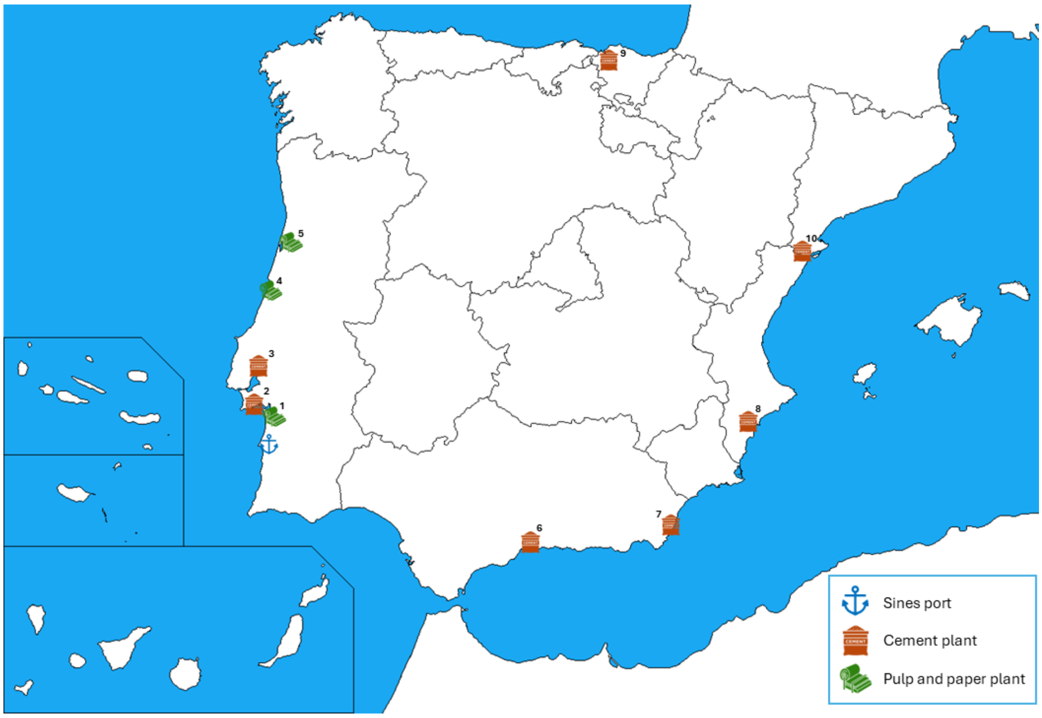

Figure 6: Locations of cement industries, pulp and paper industries and Sines port

Table 1: Details of the selected industries

	Origin	Industry	Company
Route 1	Setúbal, PT	Cement	SECIL
Route 2	Setúbal, PT	Paper and Pulp	The Navigator Company
Route 3	Alhandra, PT	Cement	CIMPOR
Route 4	Figueira da Foz, PT	Paper and Pulp	The Navigator Company
Route 5	Aveiro, PT	Paper and Pulp	The Navigator Company
Route 6	Málaga, SP	Cement	Votorantim
Route 7	Carboneras, SP	Cement	Holcim
Route 8	Alicante, SP	Cement	CEMEX
Route 9	Bilbao, SP	Cement	Cementos Lemona
Route 10	Alcanar, SP	Cement	CEMEX

The ten different routes presented in Table 1, aim to represent ten distinct scenarios in which emitting industries are connected to Sines Port by tanker or truck. In this work, the terms "route" and "scenario" will be used interchangeably to refer to these ten cases, each combining the eMeOH plant at Sines Port with one of the ten emitting industries simulated.

From the available literature, it has been established that both cement and pulp and paper industries across Europe have annual total CO_2 emissions capacities ranging from 600 to 740 ktons [70], [77]. However, as reviewed in Section 4.2.1, there are differences regarding the share of RFNBO-compliant CO_2, which includes geogenic and biogenic emissions. In cement production, geogenic process emissions account for two-thirds (66.7%) of total emissions, with biogenic emissions contributing approximately 6%, totalling 72.7% of RFNBO-compliant CO_2 emissions. In pulp and paper production, emissions from both processes and biomass combustion are considered biogenic, collectively contributing 80% of the plant's total CO_2 emissions [69], [70], [73], [77].

Additionally, the total CO_2 emissions factor for cement is found to be 0.595 tons of CO_2 per ton of final product [77], [78], while for pulp and paper, it is 0.667 [79]. Under these assumptions and from publicly available information on final product site capacities [80], [81], [82], [83], [84], the following table calculates the capacity of RFNBO-compliant CO_2 available for eMeOH production.

Table 2: RFNBO compliant CO_2 availability calculation per industrial emitter

	Origin	Industry	Company	Final product total capacity (Mtpa)	Emissions factor	Total CO_2 capacity (ktpa)	RFNBO compliant CO_2 (ktpa)
Scenario 1	Setúbal	Cement	SECIL	2000	0,595	1190	865
Scenario 2	Setúbal	Paper and pulp	The Navigator Company	1345	0,667	897	718
Scenario 3	Alhandra	Cement	CIMPOR	5200	0,595	3094	2248
Scenario 4	Figueira da Foz	Paper and pulp	The Navigator Company	1370	0,667	914	731
Scenario 5	Aveiro	Paper and pulp	The Navigator Company	320	0,667	213	171
Scenario 6	Málaga	Cement	Votorantim	1600	0,595	952	692
Scenario 7	Carboneras	Cement	Holcim	2600	0,595	1547	1124
Scenario 8	Alicante	Cement	CEMEX	2851	0,595	1696	1233
Scenario 9	Bilbao	Cement	Cementos Lemona	1890	0,595	1125	817
Scenario 10	Alcanar	Cement	CEMEX	3985	0,595	2371	1723

From this table, it can be extracted that the average production capacity for RFNBO-compliant CO_2 in the Iberian Peninsula's cement and pulp and paper industries is 1,032 ktpa, with the CIMPOR cement site in Alhandra having the highest capacity at 2,248 ktpa of geogenic and biogenic CO_2. This value is significantly higher than the initially assumed average production capacity of 600 ktons for these types of industries in Europe [70]. It indicates that nearly all the selected industries have production capacities greater than the average for European cement and pulp and paper facilities. To capture the emissions at these sites, post-combustion amine-based technology will be employed, and the concentration of

CO_2 will be considered to refine the available CO_2 capacity. This will be explained in detail in the following section to ensure a consistent storyline throughout this work.

4.2.3 Carbon capture plant

The suitability of CC technology differs for the diverse emitting industries. The concentrations of CO_2, its pressure levels and feeding flows across the emitting sources widely varies case by case. This is because each industry is characterised by different process off-gases and flue gases inherent to their activity which leads to the need of developing CC solutions tailored for each carbon-emitting source.

The analysis in Sections 4.2.1 and 4.2.2 is essential for providing context to the CC technology used to extract CO_2 from the diverse plants' exhaust gases. This section defines and justifies the most suitable technology with regard to the CO_2 emissions characteristics of these plants.

Pre-combustion is unsuitable for cement production because most emissions originate from calcination, and this technology cannot capture CO_2 during this step. Additional modifications are required when burning clinker, along with other investments before combustion [85]. This technology is best suited for fertilizer manufacturing and grey H_2 production via Steam Methane Reforming (SMR), which are characterized by very clean gas mixtures or few impurities. These conditions make them ideal for pre-combustion as they perform better with physical absorption solvents, which have higher performance at elevated partial pressures, such as in these plants and Integrated Gasification Combined Cycle (IGCC) plants. However, a significant disadvantage is the high energy requirement to regenerate the sorbent, leading to increased operational costs [86].

Oxy-combustion is utilized to enhance the CO_2 concentration in flue gases, making CC more efficient. Although pilot-scale tests are being conducted for cement plants, the high capital and operational costs associated with the ASU required to produce the necessary O_2, along with the substantial investments needed to retrofit kilns and boilers, diminish the feasibility of this technology for the selected industries. Consequently, oxy-combustion has been deemed unsuitable and has been excluded from consideration for the targeted sectors [87].

Amine-based post-combustion CC is considered appropriate for both the cement and pulp and paper industries because it operates efficiently with exhaust gases that have lower CO_2 concentrations, as found in these industries. Furthermore, a significant advantage of this technology is that it can be integrated without necessitating major modifications to the existing plants. Additionally, amine-based absorption technology is the most mature post-combustion method, with the most readily available chemical absorption system being amine scrubbing with Monoethanolamine (MEA). This group of amines also includes diethanolamine, diglycolamine, diisopropanolamine, and triethanolamine. This CC method is capable of capturing CO_2 from streams with low partial pressure. However, it is characterized by a significant requirement for steam during solvent regeneration, which proves disadvantageous in terms of OPEX [86].

Given that in Section 4.2.2, biogenic and geogenic CO_2 capacities for the different plants in this model have been categorized under the broader category of RFNBO compliant CO_2, the specific concentrations of the different sources can be disregarded when calculating CO_2 availability per industrial emitter. The critical factor becomes the efficiency of the CC technology in defining the actual CO_2 capacity available to be liquefied, stored, and transported. Assuming a CC efficiency of 90%, the capacities of CO_2 available throughout the year from the different emitters are presented in this table.

Table 3: Calculation of annual available RFNBO compliant CO_2 from the different emitting industries

	Industry	Company and location	RFNBO compliant CO_2 (ktpa)	Available CO_2 (ktpa)
Scenario 1	Cement	SECIL - Setúbal, PT	865	778
Scenario 2	Paper and pulp	TNC - Setúbal, PT *(1)*	718	646
Scenario 3	Cement	CIMPOR - Alhandra, PT	2248	2023
Scenario 4	Paper and pulp	TNC - Figueira, PT *(1)*	731	658
Scenario 5	Paper and pulp	TNC - Aveiro, PT *(1)*	171	154
Scenario 6	Cement	Votorantim - Málaga, SP	692	623
Scenario 7	Cement	Holcim - Carboneras, SP	1124	1012
Scenario 8	Cement	CEMEX - Alicante, SP	1233	1110
Scenario 9	Cement	Lemona - Bilbao, SP	817	735
Scenario 10	Cement	CEMEX - Alcanar, SP	1723	1551

(1) TNC is The Navigator Company

Based on the report on CCS technologies from the Global CCS Institute, licensors such as Air Liquide, Honeywell, Linde, and Novozymes have achieved capture rates of more than 90% of the flue gas CO_2 across a variety of plants, with most values ranging between 98% and 99% [31], [87]. Therefore, assuming a 90% capture rate for cement and pulp and paper plants is considered conservative, given that the capabilities of the available technologies highlighted in this Global CCS Institute report surpass 95%. Furthermore, it is noteworthy that the CO_2 output stream purity generally ranges from 96% to 99.9% [87]. Note that, the CC plant is envisioned to be connected to the flue gases from the boilers and lime kilns at the corresponding cement and pulp and paper plants, as these are the RFNBO-compliant CO_2 sources described in Section 4.2.1.

To technically size the CC plant, a simplified balance-of-plant approach is adopted, concentrating on sizing the primary electricity-consuming equipment within the facility and determining the associated mass requirements.

From the post-combustion amine-based CC plant described in Section 3.1, it is evident that the primary energy consumption stems from the steam required for the regeneration column in the reboiler, as well as the auxiliary pumps and compressors, which are grouped under the category of auxiliary electric systems. To meet all energy needs sustainably, the reboiler will be electrically powered, ensuring that the plant operates entirely on green electricity. The required thermal energy is thus converted into electrical energy consumption, with a conservative conversion efficiency assumption of 98% from electrical to thermal energy. This assumption is based on an assessment of currently available electric industrial boilers in the market, as evidenced in [88], [89], [90], [91]. Additionally, interviews with process plant experts indicate that 5% of the overall steam energy is lost as thermal losses, and this has been included in the calculations [92].

The following table summarizes the energy and mass ratios corresponding to a unit of kton of CO_2 captured per year.

Table 4: Mass and electric energy requirements for a kton of CO_2 captured in a year

Resource	Annual consumption	Unit
Amine - MEA make-up	0,003	ktons/year
H_2O for cooling	0,022	ktons/year
Aux. electric systems	75	MWh/year
Electric reboiler	888	MWh/year

For amines, MEA is the most readily available chemical absorption system and is selected for this work [86]. Limited literature presents information on the required amines in the CC process. Antzaras et al. modelled CC plants with different capturing technologies for a cement plant and found that MEA degrades over time due to the presence of acidic gases and high desorption temperatures. A portion of the regenerated stream should be purged and replaced by fresh MEA to ensure efficient CO_2 separation. The variability in MEA degradation for different operating conditions presents make-up flow needs from 0.5 to 3.1 tons MEA/kton of CO_2 captured [30]. In the work of Antzaras et al. it is assumed conservatively tons of MEA per kton of CO_2 captured, which is also assumed in this work to represent absorption and desorption amine requirements while operating the plant.

Furthermore, to calculate the energy cooling requirements with water, the works of Gervasi et al. and Nazmul Hassan, which simulated amine-based CC technologies applied to the cement sector, were reviewed. By adapting values in GJ/ton of CO_2 from their simulated CC plants and considering a water specific heat capacity of 4184 J/kgK and a temperature difference of 10 °C, it results in 22 tons of cooling water required for each kton of CO_2 captured in a year [29], [37].

In terms of electrical energy requirements for the steam produced in the reboiler for the regeneration column, literature simulating CC amine-based plants for both cement and pulp paper indicates an average value of 888 MWh of electricity for each kton of CO_2 captured annually. This is adapted from the typical industry metric expressed in GJ/ton of CO_2, which ranged from 2.33 to 3.68 GJ/ton of CO_2 [38], [86]. In regard to the auxiliary electric systems introduced previously in this section, it has been observed that they typically correspond to 8%, on average, of the electrical energy required for the reboiler, which translates to 75 MWh per kton of CO_2 per year [93], [94].

Additionally, according to figures reported by Linde, their pilot post-combustion CC plant in Niederaussem, Germany, achieved above-average availability rates of more than 97%. This translates to 8,497 operational hours per year, which is assumed for the technical sizing of this plant [95]. Regarding the operational hours of the industrial emitters, it is assumed for simplicity that they run continuously throughout the year and are coupled with both the CC and CO_2 liquefaction plants during these 8,497 operational hours, ensuring a continuous liquid CO_2 input for the intermediate storage. However, it is known that cement and pulp and paper plants do not operate continuously throughout the year.

4.2.4 Liquefaction

In this Master Thesis, the scope does not include the detailed sizing of each individual component within the storage and liquefaction plants. Instead, the technical sizing, which informs the economic analysis, is conducted at the plant level. This approach avoids a detailed analysis of each component, focusing instead on the overall plant requirements.

The liquefaction plant designed in this Master Thesis is inspired by the CO_2 storage hub modelled by Fraga et al., which operates at a pressure of 15 bar. In this scenario, a CCS setup is designed that includes a liquefaction plant situated between the CC plants and the intermediate storage for further tanker transportation and permanent storage. This study sizes the different stages of the CCS chain to handle a maximum capacity of 2,000 ktons of CO_2 per year under different pressures [39]. Furthermore, the energy consumption for this liquefaction process is calculated to be 83.1 MWh per kton of CO_2.

Lastly, since liquefaction plants are to be coupled with the selected amine-based post-combustion CC plants, it is assumed that they share the same yearly operational hours. Data from Linde's existing pilot plants indicate availability rates of 97%, corresponding to 8,497 operational hours per year. This figure is adopted for the technical sizing in this Thesis [95].

4.2.5 Carbon transport

Effective CO_2 transport is a crucial component in the CCU value chain, impacting both operational efficiency and cost-effectiveness. This section delves into the technical and logistical considerations for transporting CO_2 using tankers and trucks.

4.2.5.1 Carbon transport by tanker

Due to the novelty of CCU value chain deployment, literature on CO_2 transportation is primarily limited to small-scale cases, such as those involving its use in the beverage or food industries. This Master Thesis aims to outline the logistics requirements for an eMeOH plant producing between 90 and 1,200 ktons annually. This production scale ranges from 150 to 2,050 ktons of CO_2 per year, representing a small to large-scale scenario. The Northern Lights project, which aims to handle more than 1,200 ktons of CO_2 per year, aligns well with the targeted scale of the eMeOH plant. The Northern Lights project entails the establishment of a CCS value chain, with an initial phase capacity projected at 1,500 ktons per year [96]. This CO_2 originates from the Yara NH_3 production plant in Sluiskil, Netherlands, and the Ørsted biomass power stations in Avedøre and Asnæs, Denmark. Northern Lights has signed commercial agreements for the permanent storage of 800 ktons per annum from Yara and 430 ktons per annum from Ørsted.

CO_2 capture occurs at the emitting plants and is subsequently transported by ship to a receiving terminal in Øygarden, Norway. The proximity of the emitting plants to the shore facilitates CO_2 transportation between terminals. Subsequently, the CO_2 is injected into an underwater reservoir in the North Sea, situated 2,600 meters beneath the seabed and located 100 km offshore from the receiving terminal.

The receiving terminal is equipped with intermediate storage tanks to buffer between CO_2 vessel unloading and reservoir injection [96]. Northern Lights anticipates being ready to receive CO_2 from industrial emitters by 2024, with plans to inject 37.5 million tons of CO_2 over the first phase spanning 25 years [97].

Differing from the Northern Lights project, this Master Thesis concentrates on harnessing CO_2 for eMeOH production instead of opting for permanent storage. However, the CO_2 ship transportation and intermediate storage stages retain relevance for the CCU case, with insights drawn from the open-access reports of the Northern Lights project informing the CO_2 ship transportation study.

To stimulate the emergence of a new CO_2 market, it is envisioned that the ships tasked with transporting this commodity will need to resemble those used for LPG. Additionally, adherence to shipping industry standards is vital to ensure compatibility with most harbours worldwide, facilitating competitive shipyard offerings without the need of detailed engineering for each different contract. Deviating from established ship design standards could necessitate modifications to existing infrastructure, increasing the overall cost of the value chain and requiring a premium payment. Following discussions with shipyards and classification societies, Northern Lights opted for a multi-gas tanker capable of handling both LPG and liquid CO_2. This decision helps to mitigate risks during the project's start-up phase, as it minimizes modification costs for existing LPG carriers and ensures alignment with shipyard standards and harbour capabilities [57]. The two recently inaugurated vessels, each measuring 130 meters in length with a draught of 8 meters, have the capacity to carry 7,500 m^3 of liquid CO_2 in their two high tensile steel C-Type tanks, each with a capacity of 3,750 m^3. Designed to withstand a pressure of 19 barg and a temperature of -35 °C, they ensure that CO_2 remains in a liquid state with a density of approximately 1,100 kg/m^3. However, for operational safety, the chosen pressure is 15 barg and a temperature of -26 °C, strategically positioned above the CO_2 triple point. As capacities scale up, lower pressures will likely be required. Additionally, Equinor's logistics study has determined that a design speed of 14 knots (26 km/h), with a 15% sea margin, strikes a balance between LNG fuel consumption and scheduling flexibility for a Wärtsilä 10V31DF engine system with rated power of 5,500 kW and a guide cost of 404 €/kW [57]. Ultimately, Northern Lights accomplishes with this pioneering approach to minimize entry costs for new CO_2 suppliers and expedite the deployment of future vessels, facilitating earlier commercial volumes in the market and advancing the creation of the CCS value chains.

The chosen modelling approach for CO_2 transportation via tanker is based on the research conducted by Fraga et al. [39]. The paper outlines the design of a multi-user CO_2 intermediate storage facility, simulating the Northern Lights CCS hub across various conditions and CO_2 shipping pressures.

The selected tanker, presented in Figure 7, is designed to carry 7,500 m^3 of liquid CO_2 at a pressure of 15 barg, mirroring the specifications of Northern Lights tankers.

Figure 7: Liquified CO_2 carrier tanker [57]

For the chosen volume and pressure, the tanker can transport 8,233 tons of liquid CO_2 per trip at a temperature of -35 °C, with a corresponding density of 1,098 kg/m^3. The temperatures and densities for other potential transport pressures are calibrated to maintain CO_2 in a liquid state, following the recommendations from DNV GL's evaluation of innovative type C containment tanks for liquefied CO_2, as illustrated in Table 5 [98].

Table 5: Calculation of densities under different liquid CO_2 transport conditions (author's calculations)

Pressure (barg)	Temperature (°C)	Density (kg/m^3)
7	-50	1143
15	-35	1098
18	-31	1082
19	-30	1078

In its liquid state, CO_2 increases in density as temperatures decrease at a fixed pressure and as pressures increase at a constant temperature. Interestingly, the selected conditions show a decrease in density with an increase in pressure due to variable temperature settings needed to ensure the liquid state. For simplicity, this Master Thesis assumes that the CO_2 handled throughout the value chain is 100% pure. However, it is well known that purification is required to safely liquefy, store, transport, and utilize CO_2 as a feedstock.

The selected tankers are assumed to have an adapted fuel consumption rate of 256 MWh/day or 11 MWh/hour [39]. The vessel is loaded and unloaded at a maximum cargo discharge rate of 800 m^3/hour (roughly 850 tons/hour), which would take over 9.5 hours. For the base case scenario of this Thesis, it is conservatively assumed that loading and unloading 7,500 m^3 of CO_2 at a pressure of 15 barg will each take 11 hours. This pressure is within the range of 13-15 barg and temperatures between -30.5 °C and -26.5 °C, which are the conditions at which Northern Lights claims that CO_2 cargo shall be conditioned, stored, and loaded by the shore terminal onto the CO_2 ship, always ensuring a density below 1,100 kg/m^3 [99].

Additionally, delving into the logistics modelling the time required for approach and departure, quay, and mooring operations from beyond the harbour to the berths generally takes 1 to 2 hours. Conservatively it will be assumed that a loading will take 11 while manoeuvre time is 2 hours. Consequently, considering loading and unloading processes to be equal as well as the berthing while approaching and departing the respective ports, the complete loop will total 26 hours of port operations plus the corresponding travel times. This conservative timeframe accounts for minor delays that the tankers might encounter during berthing, unberthing, loading, and unloading. Significant delays are not anticipated because this Master Thesis models a terminal specifically designed to ensure the uninterrupted supply of CO_2 for eMeOH production. Therefore, no other cargo operations will take place at either the loading or unloading terminals, similar to the dedicated purpose of the Northern Lights Øygarden terminal for CCS. Additionally, although the maximum limit for cargo tank filling is specified to be 97-98%, for simplicity, it will be considered that the tanks are fully loaded [100]. In regard to the lifespan of tankers, historically they have had an economic lifespan of 25 years, but this has recently decreased to closer to 20 years due to industry changes. Tanker companies apply various asset depreciation policies, usually between 18 to 25 years. Thus, using a conservative estimate of a 20-year lifespan for tankers is well-founded and consistent with current industry standards and matches with the assumed plant years of operation for the eMeOH plant [101], [102].

Tankers must adhere to a strict regulatory schedule to ensure safety and compliance. This includes annual surveys every 12 months, intermediate surveys every 30 months, and special surveys every 60 months. Each survey typically takes around two weeks (336 hours) to complete [101]. Over a 20-year lifespan, these surveys accumulate significant downtime. The total downtime due to surveys is 10,416 hours, resulting from the increasing survey frequency as the tanker ages. Initially, surveys are required every five years, but after 15 years, intermediate surveys occur every 30 months, further increasing the downtime. This results in an average annual downtime of approximately 521 hours (5.95%), calculated by dividing the total downtime (10,416 hours) by the total operational hours in 20 years (175,200 hours). Consequently, a downtime of 6% has been assumed, resulting in approximately 8,234 operational hours per year, which aligns with values reported in studies such as those by Fraga et al. [39].

Drawing upon the earlier assumptions and data, a fleet of tankers has been meticulously designed to fulfil the constant annual CO_2 demand for the eMeOH plant. To ascertain the requisite number of tankers, it is crucial that the time required for berthing, unberthing, and loading operations remains consistently lower than the frequency of tanker unloading. A margin of 3 hours in the total loop time has been incorporated to accommodate unexpected delays along the route and during tanker operations in the harbour. Notably, careful analysis reveals that no overlaps occur under any circumstances for the different routes and capacities.

The model considers an overlap when the frequency of tanker offloading in the harbour is less than 15 hours, which is the time required for a tanker to be berthed, unloaded, and unberthed before returning to the loading facility. The optimized value chain, modelled after the Northern Lights project and validated in this Master Thesis, effectively accommodates various annual CO_2 capacities and route distances. This optimization is facilitated by selecting a tanker with a capacity of 7,500 m^3 of CO_2.

4.2.5.2 Carbon transport by truck

For this work, a container tank has been selected for transporting CO_2 by truck. This choice eliminates the need for an intermediate storage facility when both trains and trucks are used for transporting CO_2 from the production plant to the eMeOH plant. The selected pressure has been set at 15 barg, consistent with the tanker conditions. At this pressure, the chosen 20-foot container tank with a volume of 24 m^3 can carry 26.3 tons of liquid CO_2. These trucks load CO_2 at the loading storage site, transport it to the unloading site, unload it there, and then return to the initial loading site. This forms a complete loop that is continually repeated throughout the year, connecting the CO_2 production of industrial emitters with the CO_2 demand of the eMeOH plant.

In regard to the logistics modelling of the truck fleet, several limitations have been set according to Spanish regulations on driving hours, which are similar to those in Portugal. The Regulation (CE) No. 561/2006 establishes comprehensive guidelines for driving times and required breaks for truck drivers within the EU. According to this regulation, drivers must take an uninterrupted break of at least 45 minutes after a continuous driving period of four and a half hours, unless they opt for a rest period. This break can alternatively be split into a 15-minute break followed by a 30-minute break, interspersed within the four and a half hours of driving. Additionally, the maximum driving time per day is limited to 9 hours, but it can be extended to 10 hours twice a week. For weekly driving time, drivers are restricted to a maximum of 56 hours within a single week. Over a biweekly period, the total driving time must not exceed 90 hours [103]. This regulation ensures that drivers maintain a balance between driving and rest periods, aiming to enhance road safety and driver well-being.

These limitations apply to the different routes in different manner, and all have been introduced in the model. As shown in Table 6, the breaks every 4.5 hours are not applicable for routes 1 to 4, which take less than 4.5 hours. For these shorter routes, driver break times are compensated while the truck is being loaded and unloaded, a process that takes 1.5 hours. For all other routes, stops of 45 minutes or the corresponding "15+30" minutes are required along the route.

For routes such as 7, 8, 9, and 10, which take more than 9 hours, a 15-hour rest stop is mandated midway before reaching the destination. For routes exceeding 10 hours, a 14-hour rest pause is required.

Table 6: Distances and timings for single-trips, complete loops, breaks and rest pauses for the different considered routes

	Industry location	Company	Distance (km)	Time single-trip (hours)	Loop time (hours)	Break or rest pause time (hours)
Route 1	Setúbal, PT	SECIL	138	1,7	6,4	0
Route 2	Setúbal, PT	TNC *(1)*	139	1,7	6,5	0
Route 3	Alhandra, PT	CIMPOR	181	2,3	7,5	0
Route 4	Figueira, PT	TNC *(1)*	321	4,0	11,0	0
Route 5	Aveiro, PT	TNC *(1)*	400	5,0	14,5	0,75
Route 6	Málaga, SP	Votorantim	623	7,8	20,1	0,75
Route 7	Carboneras, SP	Holcim	878	11,0	52,9	14
Route 8	Alicante, SP	CEMEX	994	12,4	55,9	14
Route 9	Bilbao, SP	Cementos Lemona	1029	12,9	56,7	14
Route 10	Alcanar, SP	CEMEX	1203	15,0	61,1	14

(1) TNC is The Navigator Company

To maximize the operational hours of each truck, it is assumed that once a driver completes their 9 to 10 maximum daily driving hours, the truck is immediately handed over to the next driver. In some instances, three drivers may rotate to keep the truck running continuously.

To illustrate this, a complete round trip or loop involves three drivers assigned to the same truck. The first driver transports the loaded truck from the loading site to the unloading site. After the CO_2 is unloaded, the second driver drives the truck back to the loading site. The third driver repeats the trip of the first driver. By the time the third driver completes their trip, the first driver will have rested sufficiently and can drive again. This setup ensures that trucks are operational for the maximum possible hours annually, aside from loading and unloading times. This three-driver model is intended for routes 5 to 10. Route 4, despite requiring three drivers to ensure each driver gets the necessary 14 hours of rest, involves a single trip of less than 5 hours. This allows for a return trip within the permitted daily driving hours, enabling the driver to rest at the starting point. Similarly, route 3 needs three drivers to meet daily rest requirements but allows for two full loops in one day. Routes 1 and 2 can be managed by two drivers using the same approach as the three-driver setup. For these routes, two full loops can be completed in one day, with the maximum daily limit permitting up to five single trips or 2.5 complete loops. However, with five single trips, drivers will end their day at opposite storage sites. Hence, only 2 complete loops are assumed to be done within the same working day.

The average speed of trucks typically ranges from 80 to 90 km/h [104]. For this Master Thesis, a conservative average speed of 80 km/h has been assumed. Potential route deviations have been accounted for within the conservative assumptions of this chapter. This includes not only speed but also the calculated distances that trucks cover, which have been oversized by 105%. Regarding truck consumption, truck drivers have reported values ranging from 0.32 €/km when loaded to 0.22 €/km when empty. Consequently, an average of 0.27 €/km has been assumed to simulate the diesel consumption for the round trip.

Additionally, it is assumed that trucks will have a downtime of 5% out of the total 8,760 hours per year to account for refuelling and preventive maintenance. This downtime includes approximately 3% for refuelling and 2% for maintenance activities [105].

Based on the assumptions and data mentioned earlier, a fleet of trucks has been designed to meet the constant annual CO_2 demand for the eMeOH plant. To determine the required number of trucks, an additional 30-minute buffer is added to the time it takes for a truck to complete a full operational cycle or loop. For clarity, consider Table 6: if, for instance, a truck is projected to complete loading, transportation, unloading, and return within 52.9 hours on route 7, it is conservatively approximated to 53.4 hours for prudence. The resulting Table 7 specifies the required number of trucks for each designated route.

Table 7: Number of trucks required for the different routes for a 600 ktpa eMeOH plant capacity

	Route distance (km)	Loop time (hours)	Fleet size
Route 1	138	6,4	68
Route 2	139	6,5	68
Route 3	181	7,5	78
Route 4	321	11,0	113
Route 5	400	14,5	146
Route 6	623	20,1	200
Route 7	878	52,9	520
Route 8	994	55,9	548
Route 9	1029	56,7	557
Route 10	1203	61,1	599

Industry experts claim that trucks generally have a lifespan of 1,000,000 km [92]. This means the lifetime of the fleet will vary for each selected route in this Master Thesis, depending on the different distances covered and the number of trucks used per route. Table 8 displays the annual km driven per truck for different routes and the number of trucks per route.

Table 8: Distances covered by a truck per year and corresponding lifetimes

	Route distance (km)	Number of trucks	Yearly distance covered (km)	Lifetime
Route 1	138	68	155569	6,4
Route 2	139	68	156757	6,4
Route 3	181	78	178072	5,6
Route 4	321	113	218805	4,6
Route 5	400	146	210826	4,7
Route 6	623	200	239720	4,2
Route 7	878	520	129914	7,7
Route 8	994	548	140203	7,1
Route 9	1029	557	142002	7,0
Route 10	1203	599	155226	6,4
Average	**591**	**290**	**172709**	**6,0**

This data indicates an average truck lifespan of 6 years, which has been conservatively rounded down to 5 years. Consequently, the transport provider will need to acquire new trucks every 5 years. In contrast, according to industry experts, the tank containers have a lifespan exceeding 20 years [92]. Therefore, no additional acquisitions are included for the tank containers in the calculations, given the project's lifespan. Lastly, loading and unloading times for trucks are each assumed to be 1.5 hours [53].

Due to the number of trucks needing to load and unload simultaneously at intermediate storage sites, multiple loading and unloading arms are necessary to prevent bottlenecks. These arms are considered to share the same characteristics, as indicated by the study conducted by the UK BEIS department on shipping CO_2 cost estimation and are designed identically despite their placement at different sites [56]. They are integral parts of the broader loading and unloading systems, which include components such as pipelines, pumps, heaters, coolers, compressors, and valves required for these operations.

These loading and unloading systems at the intermediate storage sites facilitate the transfer of yearly CO_2 capacity from the tank farm to the respective transportation mediums. However, due to simultaneous operations of multiple trucks at each site, the system's capacity must be divided into different subsystems.

Assuming a conservative average delay of 30 minutes per truck for all trips throughout the year, whether during transit or while operating at the intermediate storage sites, allows for the calculation of the required number of loading and unloading subsystems to avoid overlaps.

These subsystems must evenly distribute the annual CO_2 capacity to ensure a smooth and continuous flow of trucks loading and unloading, thereby minimizing delays and inefficiencies. Subsequently, the frequency at which trucks should unload CO_2 at the receiving intermediate storage site can be determined to meet the CO_2 feedstock requirements for the eMeOH plant.

4.2.6 Intermediate carbon storage

The tanks selected for this Master Thesis are designed according to the specific attributes of the intermediate storage tanks at the Øygarden terminal in the Northern Lights project. These tanks are vertically oriented and pressurized storage tanks, measuring 6.1 meters in diameter and 35 meters in height, with a design pressure of 21.8 barg and a temperature range of -46 to 50 °C. However, for this study, the selected operating conditions will be within the range of 13 to 18 barg and temperatures ranging from -30.8 to 20.8 °C, aligning with the operational parameters of the value chain [100]. The storage capacity at the Øygarden terminal is 9,150 m^3, with a total operational capacity of 8,250 m^3. This represents a 22% margin relative to the 7,500 m^3 ship size, which not only allows for operational flexibility but also mitigates potential issues in the delivery chain. The storage facility consists of 12 tanks, each capable of accommodating approximately 760 m^3 of CO_2. Of this unitary tank capacity, 625 m^3 corresponds to the 7,500 m^3 unloaded from the ship, leaving a surplus of 22%, which serves as the overcapacity margin [100]. However, the model uses the amount of CO_2 transported in mass units. Consequently, the mass of CO_2 delivered to the receiving terminal will vary based on the pressure at which it is transported. This applies to tankers, trains, or trucks, each utilizing their respective fixed volumetric capacities. For instance, tankers will transport CO_2 in their 7,500 m^3 tanks, with the mass determined by the pressure conditions, according to the Air Liquide CO_2 data sheet for densities at different pressures and temperatures [106].

The number of tanks in this CCS value chain has been designed to handle 1.5 million tons of CO_2 annually by ship, with intermediate storage at Øygarden. Assuming a linear relationship between the number of tanks and the volume of CO_2 handled, each tank would accommodate approximately 125 ktpa. In the context of cost reduction, if the CC capacity is less than 1.5 million ktpa, it may seem intuitive to reduce the number of storage tanks. However, this reduction would necessitate the use of tankers with smaller capacities or partial loads, thereby diminishing the economic viability of deploying such a value chain project. This approach was not considered, given Northern Lights' extensive studies, which concluded that 7,500 m^3 tankers operating at medium pressure, as in the case 15 barg, are optimal for minimizing risks and maximizing profitability in this novel CO_2 logistics chain. Moreover, this configuration aligns with shipyard standards, facilitating the earlier introduction of commercial CO_2 volumes to the market [57]. Consequently, cost optimization through a reduction in the number of tanks in the CO_2 intermediate storage, when tankers are part of the logistics, is not pursued. The total tank capacity must be sized in increments of 7,500 m^3 to handle tanker offloading, which corresponds to 12 tanks with a total volumetric capacity of 9,150 m^3, reflecting a 22% overcapacity. The total gravimetric capacity of the site is 10,044 tons, with an operational capacity of 9,056 tons at the selected pressure of 15 barg. Furthermore, the plant is designed and engineered for a technical lifetime of 25 years [107].

Additionally, the Northern Lights CCS value chain is designed to accommodate the intermittent and batched offloading of tankers, with sufficient tank capacity while injecting CO_2 into wells. Lessons can be drawn for the development of the CCU value chain in this Master Thesis by assuming that the wells' injection pattern mirrors the consumption pattern of the eMeOH plant. For CCS, when less CO_2 is transported, injection rates can be linearly decreased. This principle applies to different scales of eMeOH production plants, as shown in Table 9.

Table 9: Calculation of CO_2 consumption rates for different eMeOH plant sizes

eMeOH production capacity (ktpa)	CO_2 required (ktpa)	CO_2 consumption rate (tons/hour)
200	306	35
500	764	87
800	1222	140
1200	1834	209

Assuming a constant CO_2 consumption rate from the eMeOH plant throughout the year, tanks can be nearly or fully emptied to accommodate CO_2 offloaded from tankers upon arrival. This is achieved by adjusting the consumption rate according to CO_2 availability. Adequate CO_2 supply is ensured by the tankers' offloading capability, with a maximum rate of 800 m^3/hour (approximately 850 tons/hour), which significantly exceeds the CO_2 consumption rates required for eMeOH production, ensuring that consumed volumes are consistently met. Additionally, the tanks have a superior design pressure of 21.8 barg, and this thesis assumes that storage will occur at 15 barg, matching the selected transport pressure. This alignment avoids the extra costs associated with increasing the pressure at the storage site.

To undertake the loading and unloading activities in the intermediate storage site loading arms, pipelines, pumps, heaters, coolers, compressors, and valves are required. This Thesis treats this loading and unloading systems as a complete system adapted to the tank farm needs to handle the selected CO_2 annual capacity. For scenarios involving tankers as the transport medium, no technical optimization is performed to reduce the investment costs of loading and unloading systems. This approach is consistent with the methodology used for the tank farm when tankers are included. Consequently, cost reductions are not achievable in this scenario, as the sizing of loading and unloading systems is integrated into the overall tank farm sizing strategy. Moreover, as reported by the Northern Lights Project Concept report, loading arms for tankers have a life expectancy of at least 25 years [57]. If the sites are connected by truck rather than tanker, they are likely to be located further from the shore. This means they will be exposed to less demanding conditions than typical equipment near a seashore environment. Consequently, the lifespan of equipment at these inland, truck-connected sites will be even longer. Therefore, considering the project's lifespan, no additional acquisitions for this asset are included in the calculations. This also applies to the pipelines, pumps, heaters, coolers, compressors and valves, which are assumed to have similar characteristics and durability for both truck and tanker-connected sites. Additionally, for both the tank farm and the loading and unloading systems, 8,716 operational hours per year are assumed, as reported by the Northern Lights FEED report by Equinor, which estimates a 0.5% unavailability for the intermediate storage site annually [100]. However, the previously established overcapacity margin is considered sufficient to buffer the hours during which the entire facility is unavailable.

Furthermore, due to the significantly different transport capacities per trip of these two transport methods, attention must be paid when designing the loading and unloading systems. The frequency of arrivals at the intermediate storage sites varies significantly between tankers and trucks. To address this, for intermediate storage sites connected by tankers, a unique loading system is required at the origin site and an offloading system at the receiving site to manage the tankers. Given the capacity of the tankers, it has been observed that no overlaps occur during loading or unloading for fleets of more than one tanker, demonstrating the optimized sizing of the Northern Lights project, which this Master Thesis references.

In contrast, sites connected by trucks are equipped with multiple smaller loading and unloading subsystems to prevent overlap and ensure continuous operations. The number of subsystems is based on the logistics fleet model described in Section 3.3.2, ensuring a seamless flow of trucks loading and unloading at the respective intermediate storage sites.

Finally, it is important to note that in this Master Thesis unloading systems are considered to share the same characteristics as loading systems. According to the UK's BEIS Department, the required infrastructure for loading and unloading operations is identical [56]. Consequently, if

CO_2 transport losses are disregarded, both systems would handle identical quantities of CO_2, ensuring consistency in the design and functionality of the infrastructure.

4.2.7 eMethanol production plant

Building on the foundational understanding of MeOH plants presented in Section 3.5 and with established mass and energy flows, the focus now shifts to plant modelling. This work employs a simplified balance-of-plant methodology for calculating the LCOeM production as done in Section 4.2.3 with the CC plant.

This approach streamlines the plant modelling process by concentrating on the primary electricity-consuming equipment within the production facility and its associated mass requirements.

Traditionally, conventional MeOH plants rely on the combustion of fossil-based or biomass-based fuels to meet the reboiler's heat requirements. However, in this study, the modelled plant will utilize an electric boiler. This approach aligns with the methodology used for the CC plant, as detailed in Section 4.2.3, ensuring consistency and supporting the transition to cleaner energy sources. This boiler has a conversion efficiency of 98% and 5% thermal losses, as computed in the model calculations.

To ensure clarity and precision in modelling, the plant's mass and electric energy requirements are categorized as follows:

Mass requirements:

- H_2 as feedstock
- CO_2 as feedstock
- Cooling H_2O

Electric energy requirements:

- Compression of H_2 and CO_2 feedstock
- Compression for recirculation, also covering the pressure drops within the process
- Electricity for the electric boiler, sourcing the thermal requirements of the distillation stage

Table 10 details the mass and electrical energy requirements for producing 1 kton of eMeOH annually at designed capacity, offering a comprehensive overview of the ratios per unit of eMeOH produced.

Table 10: Mass and electric energy requirements for a 1 kton/year MeOH plant operating at full capacity

Magnitude	Quantity	Unit
H_2	0,2	ktons/year
CO_2	1,5	ktons/year
Catalyst	0,10	tons/year
H_2O for cooling	4,8	ktons/year
Compression H_2	70	MWh/year
Compression CO_2	99	MWh/year
Compression recirculation	69	MWh/year
Electric reboiler	448	MWh/year

The values utilized in this study are derived from average data adapted from multiple academic papers that have modelled conventional and eMeOH production plants using advanced simulation software such as ASPEN Plus and CHEMCAD. These software tools enable engineers to simulate entire production chains, including the synthesis of H_2 and CO_2, their compression, and the synthesis of eMeOH, among various other process plants [25], [26], [27], [60], [61].

The plants modelled in the literature have been meticulously analysed to develop a comprehensive understanding of eMeOH production processes. This rigorous analysis enables the extraction of significant figures that effectively inform the technical model presented in this Master Thesis. This detailed information is instrumental in categorizing the various OPEX components involved in the modelled eMeOH plant. By leveraging these insights, the study not only enhances the robustness of the technical model but also ensures the reliability of the economic evaluations conducted. To illustrate the modelling approach of averaging data from multiple academic papers, catalyst consumption is used as an example. Literature on catalyst use in eMeOH production shows consumption rates ranging from 92.76 to 101.14 kg per ktpa of eMeOH [25], [61]. These values align with ranges provided by consulted process engineering experts, who indicated that catalysts typically last about 3 years [92]. Therefore, this Thesis assumes an average annual catalyst consumption of 96.95 kg per kton of eMeOH produced. Other values, as shown in Table 10, have been calculated using a similar approach of averaging data from the various sources discussed in Section 3.5.

Additionally, based on the comprehensive review of the literature and corroborated through discussions with industrial experts in MeOH plants [92], it has been determined that the plant will have an operational lifetime of 20 years with an average of 8,090 operational hours per year [26], [27], [60].

4.3 Economic assessment

Once the different components of the value chain have been technically sized and its energy and logistics needs discretized, it becomes straightforward to identify the requirements for concurrent operation. These requirements come with respective costs, necessitating careful distinction between outsourced costs and in-house expenditures. This distinction depends on the type of organization managing the project and which components of the value chain fall within its scope.

For this Master Thesis, the role of an atypical project developer is assumed. Typically, a project developer purchases CO_2 and H_2, and subsequently converts these into eMeOH for sale to various off takers. However, because eMeOH plants are unlikely to be situated near CO_2 emitters, logistics services must be outsourced to transport CO_2 to the eMeOH plant. These logistics services require intermediate storage sites at both the emitter's location and the eMeOH plant, as well as transport fleets to connect these sites. Additionally, because exhaust gases are not composed solely of CO_2, conditioning of these gases, involving a CC plant and a coupled liquefaction plant, is necessary.

However, no available literature was found detailing the profits that logistics service providers charge project developers for their services. Therefore, in this scenario, the adopted atypical project developer role involves not only owning and operating the eMeOH plant but also purchasing H_2 and CO_2 and managing the corresponding CO_2 logistics assets that are also owned. This includes acquiring and operating tanker or truck fleets, intermediate storage sites, the CC plant, and the liquefaction plant. This approach allows the Thesis to reflect the costs associated with operating and owning all the required infrastructure, providing a clearer understanding of the minimum price at which the resulting eMeOH product must be sold to off-takers to avoid losses over the expected lifespan of the project.

Lastly, all values obtained from the reviewed literature are updated to their present monetary value, as of the year 2024, based on the average annual inflation rates from the value of money converter from Statistics Finland, the National Statistical Institute of Finland [67]. Hence, the economic figures are unified for a single year, serving as a consistent basis for comparison and analysis throughout the study. For the assumed project lifetime of 20 years, an average inflation rate of 2.21% is assumed throughout the plant's operation [67]. This rate represents the historical average from 2003 to 2023 and is expected to align with the anticipated average inflation rate for the next 20 years of the project's operation.

4.3.1 Carbon capture cost

To provide a comprehensive analysis of the economic considerations for setting up a CC plant for cement and pulp and paper industries, it is essential to outline the assumptions that underpin the capital and operational cost estimations.

To calculate the CAPEX involved in setting up a CC plant for these industries, values from various sources have been considered, ranging from 104,000 to 318,000€ per kton of CO_2 captured. Based on the available data, an average of 200,850€/kton of CO_2 has been adopted, assuming a linear increase in capital cost with increasing capacity [37], [94], [108], [109].

For the calculation of the operational cost of the CC plant, the renewable electricity used to power the CC plants is priced at 40 €/MWh, as justified in Section 4.3.5 for the electrical energy consumption of eMeOH plant. This pricing reflects the cost of Portuguese renewable generation, purchased through Power Purchase Agreements (PPAs). Although half of the CC plants considered in this study are located in Spain, for simplicity, the Portuguese electricity pricing is used for both the CC plants in Portugal and Spain.

Moreover, the cost of MEA has been extracted from the literature, indicating an average price of 1.77€/kg of MEA [30], [109]. Additionally, cooling water costs have been observed to range from 0.013 to 0.078€/m^3, with an assumed average of 0.051€/m^3. This is relatively lower compared to process water, which is found to cost between 0.106 to 0.518€/m^3, with an average of 0.243€/m^3, making it approximately four times more expensive [30], [110], [111].

Finally, concerning the pricing of water for cooling purposes, values for cooling water at both CC plants in cement and pulp and paper industries have been found to range from 0.013 to 0.078 €/m^3 [94], [109], [111]. Following discussions with process engineers, it has been confirmed that an average cost of 0.051 €/m^3 is a reliable estimate for this utility [92].

4.3.2 Liquefaction cost

In this research, the CO_2 liquefaction step is analysed at the plant level. For simplicity, it is assumed that the cost of the liquefaction plant increases linearly with the annual handling capacity, as reported in [39], [56]. As a result, the required equipment, such as compressors and cooling systems, is assumed to scale proportionally with the selected capacity to ensure the efficient liquefaction of CO_2 between the CC plant and the intermediate storage. Drawing insights from the CO_2 storage hub designed by Fraga et al., the CAPEX required to liquefy CO_2 from a non-pressurized state to 15 bar is estimated to be € 21,319 per kton of CO_2.

Finally, for OPEX calculations in the energy area, a renewable electricity price of 40 €/MWh has been assumed, similar to the assumptions made for the CC plants in the previous Section 4.3.1. This price, characteristic of Portuguese renewable electricity, is applied uniformly across all the liquefaction plants modelled in this work, even though half of them are situated in Spain.

The remaining OPEX for the liquefaction process is expressed as a percentage of the CAPEX, amounting to 10% annually [39], [56].

4.3.3 Cost of carbon transport

4.3.3.1 Tanker ship

Regarding the CAPEX involved in acquiring tankers, figures from Xing et al. were adopted, which assess the technical and economic feasibility of various liquid CO_2 tanker types. They highlight the linear increase of tanker CAPEX relative to its size [112]. From their analysis, cost ratios ranging from 3,286 €/m^3 to 8,164 €/m^3 can be identified, with this Thesis conservatively assuming the highest value. The process of constructing crude oil tankers spans about 9 to 15 months from the initial keel laying to final completion. However, because critical components must be ordered and produced before construction starts, the entire timeframe from contract signing to vessel delivery is typically around two years [101], which is the value assumed in this Master Thesis. This prolonged period is essential in the tanker shipping industry, where supply and demand fluctuations significantly influence freight rates and overall market stability.

To calculate the OPEX for tanker transportation, and due to the limited information available from the Northern Lights project, this Master Thesis utilizes data from Fraga et al.'s paper. This paper models the routes for two tankers based on the design of a multi-user CO_2 intermediate storage facility, simulating various conditions and CO_2 shipping pressures at the Northern Lights CCS hub [39]. For this analysis, the primary OPEX components considered are fuel costs, crew cost, harbour fees and maintenance, as these are deemed to be the main expenses for running the tankers. If it is considered a fuel cost of 49.77 €/MWh in a European port such as Rotterdam in 2024 for the modelled 7,500 m^3 CO_2 vessel, the fuel expenses would total 12,729 €/day, as sector reference unit, or 530 €/hour of travel [39], [113]. Conversely, if the same vessel were to consume Marine Diesel Oil (MDO) priced at 46.43€/MWh, the resulting costs would be 11,875 €/day or 495 €/hour of travel [56], [114]. Regarding the crew, a team of 20 individuals has been adopted, as this number is considered independent of the ship's capacity according to Ekström et al. with an annual cost of € 772,339 for this crew [112], [115]. In regard to the harbour fees for this type of tanker, an adapted constant fee of €11,446 per berthing and unberthing operation has been adopted [39] This means that each time a tanker accesses a harbour, this fee is applied. Consequently, every complete cycle will incur a total harbour fee of €22,932, as it includes berthing and unberthing operations for loading CO_2 at the origin terminal and unloading CO_2 at the receiving terminal. Finally, it is considered a 2% of CAPEX cost for maintenance expenditure every year [115].

4.3.3.2 Truck

To evaluate the cost of transporting liquid CO_2 by truck, data from Alves' work has been considered, which provides technical and economic insights into trucks carrying this type of cargo [53]. As with ship transportation, the economic evaluation differentiates between CAPEX and OPEX.

Discussions with industry experts indicate that a diesel-fuelled truck typically costs between €100,000 and €130,000, while the container tank for high-pressure liquid cargo ranges from €115,000 to €150,000 [92]. Consequently, a conservative total cost for both the truck and the tank container is assumed to be €260,000.

OPEX for transporting liquid CO_2 include fuel costs, toll fees, vehicle taxes, CO_2 taxes, maintenance costs, and labour costs. Given that several routes span both Portuguese and Spanish roads, different fuel costs and toll fees apply. Diesel costs are considered at 1.668 €/litre, the average of 2023 diesel prices in Portugal (1.692 €/litre) and Spain (1.645 €/litre) [116]. In Spain, there are 12 tolled highway sections [117], listed here:

- Highway AP-66, Campomanes-León
- Highway AP-46, Alto de las Pedrizas - Málaga
- Highway AP-51, AP-6, connection to Ávila
- Highway AP-53, Santiago de Compostela - Alto de Santo Domingo
- Highway AP-6, Villalba - Villacastín - Adanero
- Highway AP-61, AP-6, connection to Segovia
- Highway AP-68, Bilbao - Zaragoza
- Highway AP-7, Alicante - Cartagena
- Highway AP-7, Estepona - Guadiaro
- Highway AP-7, Málaga - Estepona
- Highway AP-71, León - Astorga
- Highway AP-9, Ferrol - Portuguese border

Only the route starting at Cementos Lemona in Bilbao crosses one of these tolled highways, as can be seen in Table 11.

In Portugal, toll fees are calculated using the Via Verde toll calculator for Class 4 vehicles, as the trucks have more than three axles [118]. Table 11 details the toll fees for each route.

Table 11: One-way trip toll fee for the different selected routes

	Company and industry location	Route distance (km)	SP toll fee (€)	PT toll fee (€)	Total route fee (€)
Route 1	SECIL - Setúbal, PT	138	-	18,15	18,15
Route 2	TNC - Setúbal, PT *(1)*	139	-	18,15	18,15
Route 3	CIMPOR - Alhandra, PT	181	-	29,85	29,85
Route 4	TNC - Figueira, PT *(1)*	321	-	59,15	59,15
Route 5	TNC - Aveiro, PT *(1)*	400	-	69,25	69,25
Route 6	Votorantim - Málaga, SP	623	-	19,25	19,25
Route 7	Holcim - Carboneras, SP	878	-	19,25	19,25
Route 8	CEMEX - Alicante, SP	994	-	48,40	48,40
Route 9	Lemona - Bilbao, SP	1029	18,00	48,40	66,40
Route 10	CEMEX - Alcanar, SP	1203	-	48,40	48,40

(1) TNC is The Navigator Company

Labor costs, as discussed in Section 4.2.5.2, involve employing 2 to 3 drivers per truck to ensure continuous operation. It is assumed that drivers have a base salary of 13.8 €/hour, as presented by Alves in [53]. On top of this base salary, an additional 80% compensation is included, resulting in a total rate of 24.8 €/hour. This comprehensive rate covers all expenses incurred by transport providers, including the driver's gross salary, social security, health insurance, and bonuses.

Bonuses are provided under various conditions, such as:

- overnight stays on the route
- breaks taken far from home
- time spent at loading and unloading sites
- work on bank holidays or weekends

This compensation adjustment also considers scenarios where drivers do not meet the standard 40 working hours per week due to the operational demands of routes 7, 8, 9, and 10. On these routes, the three-driver rotation system may require drivers to wait for the arrival of the next driver and truck even after their mandatory rest period ends, resulting in part-time driving contracts. This additional rate is aligned with information gathered from consultations with truck transportation experts, ensuring it accurately reflects the practical challenges faced by drivers in this operational model [92].

Finally, the economic evaluation is translated into a more understandable metric: cost per km, as shown in Table 12. This approach ensures clarity and facilitates cost comparisons for the transportation of liquid CO_2.

Table 12: OPEX breakdown for CO_2 truck transport per km

Cost item	Cost	Unit
Diesel fuel cons.	0,4504	€/km
Vehicle taxes	0,0012	€/km
CO_2 taxes	0,0003	€/km
Maintenance	0,1378	€/km
Labour	0,3101	€/km
Toll fee	0,1320	€/km
Total OPEX	**1,0317**	**€/km**

Regarding vehicle taxes, CO_2 taxes, and maintenance costs, the values adapted from Alves and updated to 2024 figures are presented in Table 13. The updated costs include €390.08 for vehicle taxes, €100.57 for CO_2 emissions, and an average maintenance cost of €0.138 per km [53] As an example, the annual operational costs per truck for route 1 are detailed in Table 13.

Table 13: Yearly OPEX for a truck in Route 1 for an eMeOH plant of 600 ktpa capacity

Cost item	Cost	Unit
Diesel fuel cons.	144723	€/year
Vehicle taxes	390	€/year
CO_2 taxes	101	€/year
Maintenance	44277	€/year
Labour	99624	€/year
Toll fee	42398	€/year
Total OPEX	**331514**	**€/year**

It can be observed that fuel costs constitute the majority of a truck's operational expenses. This is followed by labour costs, toll fees, and maintenance costs, reflecting the comprehensive expenses involved in truck operations. This analysis highlights the significant impact of fuel and labour on the overall operational budget, emphasizing the importance of efficient route planning and cost management strategies.

4.3.4 Cost of intermediate carbon storage

To calculate the cost of CO_2 storage, this Master Thesis draws on the methodology proposed by Lauri et al., which describes a linear increase in storage costs relative to volume due to the modular nature of tank farms [119]. Given the limited availability of literature and projects handling CO_2 at medium and large scales, the values have been adapted from Svensson et al., which analyse different transport systems using steel tanks for intermediate storage. It is assumed a ratio of €2,506 per m^3 of CO_2, which is the average value of the limited literature that has been found [120], [121].

As previously explained in Section 4.2.6 the economic sizing of loading and unloading systems is coupled with the tank farm to meet the annual CO_2 handling capacity. Economic ratios for CAPEX and OPEX calculations related to loading equipment are derived from the estimation study on shipping CO_2 costs by the UK BEIS Department. This department's methodologies are also referenced for the LCOeM calculation. BEIS reports a linear dependency in between CAPEX of loading and unloading infrastructure and flow rates, on which an increase in the CO_2 flow capacity increases the capital cost of the loading and unloading equipment. Specifically, the

CAPEX ratio is estimated at £ 1.4 per ton of CO_2 handled annually. When converted to € using the average conversion rate for 2018 (1.1301), this equates to € 1.582 per ton of CO_2, which translates into € 1.977 in 2024 values.

In regards OPEX for CO_2 steel tank farms, as reported in various studies, typically range between 5% and 7% of CAPEX. For this analysis, a conservative estimate of 7% has been selected [120], [121]. For loading and unloading systems the analysis from BEIS Department presents various sources indicating that the OPEX is approximately 3% of the CAPEX [56] To ensure accurate cost assessment in this CCU value chain, it is important to note that two intermediate storage sites, each with identical characteristics, have been modelled. Consequently, when calculating the levelized cost of storage, the costs are doubled to accurately reflect the overall expense of storage across both sites.

4.3.5 eMethanol production cost

In assessing the CAPEX necessary to establish an operational eMeOH plant, this Master Thesis adopts a holistic approach. Rather than delving into the cost specifics of each technically sized piece of equipment detailed in Section 3.5, the focus is placed on estimating the entire plant expenditure relative to its production level capacity. Given the critical role of the eMeOH plant in this study and the absence of linear scaling effects in the reviewed literature, the "0.6 rule" is employed. The "0.6 rule" is a well-established principle in the field of chemical engineering, particularly for scaling up plant capacities. It helps in determining the investment cos (I_2) of a desired capacity level (C_2) based on the known cost (I_1) associated with another level of capacity (C_1) [122]. The formula is expressed as follows, with α equalling 0.6:

$$\frac{I_1}{I_2} = (\frac{C_1}{C_2})^{\alpha}$$

This power-law relationship implies that increasing returns to scale occur when the coefficient α is less than one, as is the case for this equation. This methodology offers a reliable estimate for scaling up the production capacity of chemical plants. It aids in determining an approximate cost figure for the eMeOH plant, reflecting the non-linear increase in costs with capacity expansion.

Based on available literature, it has been determined that the CAPEX for eMeOH plants generally ranges between €300,000 and €900,000 per kton of eMeOH capacity, with an average value of €554,537 per ktpa [25], [26], [28]. These values align with the typical cost range for such plants as confirmed by industry experts [92]. From these papers, the modelled plant that closely matches this average cost ratio of €554,537 per ktpa is the one presented by Pérez-Fortes et al., which is 631,738 €/ktpa. Consequently, the investment cost (I_1) and capacity level (C_1) selected to calculate the investment cost (I_2) for the target capacity level (C_2) using the "0.6 rule" are derived from this study. Specifically, I_1 is €277,965,651 and C_1 is 440 ktpa of eMeOH [25].

Regarding the OPEX for the eMeOH plant, these can be categorized into the cost of feedstock (H_2 and CO_2), electricity, water for cooling, and catalysts, which are explained here.

In the last decade, thousands of papers and reports have focused on the Levelized Cost of Hydrogen (LCOH), specifically for green H_2. This Master Thesis has concentrated on papers and reports that model electrolytic H_2 production with more than 100 MW capacity in Sines, Portugal, where both the eMeOH and electrolysis plants are envisioned to be located. To provide the most relevant and updated values for this important parameter, only works from 2022 onwards have been considered.

For projects with electrolysis capacities ranging from 300 MW to 1,500 MW, which align with the modelled eMeOH H_2 requirements and produce approximately 30 to 250 ktpa of green H_2, LCOH values range from 2.52 to 5.42 €/kg [123], [124]. These values are heavily dependent on competitive electricity prices, typically provided by a grid-assisted mode coupled with solar and onshore wind. These values are in line with IRENA's published results for the Sines area in a 2030 scenario, which range from 2.1 to 5.3 €/kg [125]. These LCOH values are significantly competitive, approaching the current costs of grey H_2 production through SMR, which range from 0.6 to 2.7 €/kg [123], [126]. Finally, this Thesis conservatively assumes 4.0 €/kg as the feedstock price for domestically produced green H_2, with the electrolyser located on the premises of the eMeOH plant to eliminate any H_2 transportation requirements.

Nowadays, the acquisition cost of CO_2 is not yet clearly defined, posing a complex challenge for industrial emitters who supply CO_2 and clients, such as eMeOH producers, who aim to purchase it for utilization. This ambiguity complicates the establishment of CO_2 acquisition agreements. Although CO_2 is expected to become a tradable commodity, a formal market has not yet been established. Currently, voluntary carbon offset markets are underdevelopment, with numerous firms engaging in the certification of CO_2 credits for companies interested in buying or selling voluntary carbon credits. However, these credits experience limited demand, lack standardization, and lack recognition from competent institutions, leaving their value undefined.

Once policies and regulations are implemented, a market for CO_2 will emerge, establishing it as a tradable commodity with prices varying according to the rules of supply and demand. Additionally, if a correlation can be established for CO_2 pricing, firms evaluating the measures they need to undertake in their energy transition are generally influenced by the fees they must pay for their emissions. For instance, when the cost of emission fees surpasses the cost of capturing CO_2, companies are more likely to invest in CC technologies, driven by the less profitable "cost of doing nothing" (CODN). Moreover, as observed in industry-related cases, the price of CO_2 is often indexed to other commodities, such as fuels produced from them like eMeOH. This pricing might be defined in bilateral agreements rather than regulated market prices, reflecting the specificities of individual business cases. To establish a meaningful CO_2 pricing value, this work calculates the CO_2 acquisition cost based on forecasts from Reuters and Bloomberg regarding reported EUAs, under the EU ETS. Additionally, the calculation considers the costs associated with connecting the industrial emitter to the eMeOH plant, including CC, liquefaction, storage, and transport. In a CCU scenario, the agreement between a CO_2 consumer and a CO_2 emitter for the acquisition of CO_2 is likely based on the costs of CC, CO_2 liquefaction, and CO_2 logistics. The CO_2 acquisition cost, when combined with these costs, represents the total cost that the eMeOH producer must account for in sourcing the CO_2 feedstock. The proposed methodology for calculating this value assumes that the total cost should be within the range of the CODN for an industrial emitter. This CODN is considered equivalent to the price of an EUA.

When developing a CCU project, it is crucial to demonstrate its profitability over its entire lifecycle. This does not necessarily mean that the project will be profitable from the start, as it is likely that its development will incur some risk of not being profitable in its first years of operation. Based on this premise, this Master Thesis aims to establish a reasonable CO_2 price that reflects this scenario.

Over the last two years, EUAs have ranged between 55 to 105 €/ton of CO_2, with current values, as of July 2024, close to 70 €/ton of CO_2 [127], [128], [129]. According to Reuters forecasts, EUAs are expected to rise to 83 and 100 €/ton in 2025 and 2026, respectively [130]. This rising trend is expected to continue as the ETS steadily reduces the total number of allowances, including those distributed for free, which will be completely phased out by 2034. According to Bloomberg NEF Global Carbon Market Outlook 2024, prices will be at 149 €/ton by 2030 [131]. This increase is expected to surpass the cost of implementing a CCU value chain, thereby enhancing the project's profitability over its lifetime.

In this work, it is assumed that the price of CO_2, combined with the aforementioned CCU project costs, has to exceed the current cost of an EUA by 40%. Consequently, the cost of CO_2 acquisition, together with the costs of CC, CO_2 liquefaction, and CO_2 logistics, should be established at 100€.

In the area of CCU costs, CC for cement is claimed to cost from 50 to 70€/ton of CO_2 captured [132]. The liquefaction of CO_2 is observed to be around 12€/ton of CO_2 [39]. For transportation, the BEIS CO_2 Shipping Report claims that maritime transport costs 13.5 €/ton of CO_2 for distances over 200km [56], while truck transport for distances under 100 km yields 4.8 €/ton of CO_2 [53]. Finally, in terms of storage, levelized costs range from 1 to 3 €/ton of CO_2, according to the BEIS report on CO_2 shipping, representing the least costly component of the CCU to be developed [56].

Averaging these values, the deployment of CC, liquefaction, and CO_2 logistics infrastructure results in a levelized cost of roughly 83 €/ton of CO_2. From the mentioned total cost of 100 €/ton, the resulting difference is 13 €/ton of CO_2. This is the value assumed to be paid to the CO_2 emitter to acquire the CO_2 feedstock for the eMeOH plant. Therefore, it is understood that under these agreement conditions, and considering the cost incurred to source the CO_2 at around 83€/ton, project developers are likely to undertake the risk of starting the operation of this value chain with the expectation of EUA prices following the described increasing trend and surpassing the established 100€ threshold.

In terms of electricity sourcing, given that the eMeOH plant will be located in Sines and in line with RFNBO criteria of geographic correlation, it is assumed that the renewable electricity must be sourced from Portuguese renewable generation assets. To ensure the lowest cost of electricity, it is assumed that additional renewable energy assets, mainly solar and onshore wind, will be developed to generate the required electricity throughout the year across Portuguese territory, fulfilling the RFNBO criteria of additionality [133].

Note that these assets are not directly connected to the eMeOH plant. Instead, the plant is connected to the grid, as are the renewable assets. PPA will be utilized to purchase electricity, aiming to ensure the lowest cost of renewable electricity.

From the literature reviewed, and with the aim of providing an order of magnitude, values are found to range from a minimum of 19.75 €/MWh for solar photovoltaic (PV) electricity to a maximum of 83.34 €/MWh for grid electricity [123], [134].

Additionally, intermediate figures of 37.05 €/MWh are found to match the described regime of a grid-connected eMeOH plant based on solar PV and onshore wind [123]. This Thesis assumes a conservative value of 40 €/MWh, which aims to mimic the described regime under which the model is built and aligns with figures discussed in interviews with industry experts [92].

Moreover, as justified in Section 4.3.1 for the CC plants, the cooling water required for the eMeOH process is priced at 0.051€/m^3 [94], [109], [111].

Finally, discussions with process engineers have validated the assumption of a catalyst cost of 35.62 €/kg [92], which is the average derived from available literature and aligns with industry standards [26], [27], [28], [60].

5 Results and discussions

This chapter aims to derive meaningful insights and observations from the developed CCU value chain model. Initially, the chapter will focus on analysing the results from the simulation of the ten modelled scenarios, drawing conclusions, and addressing the research questions proposed in Section 2.1. Secondly, the results are compared with the existing literature reviewed. Finally, the limitations of this study are discussed in order to identify opportunities for future work in this area.

To provide a clear basis on from where the conclusions drawn from this chapter are extracted, Table 14 and Table 15 are presented.

Table 14: Results of the LCOeM per transport medium and discretized per stage of the CCU value chain modelled for scenario 3

	Tanker		Truck	
LCOeM	**1072,0** €/ ton eMeOH		**1080,4** €/ ton eMeOH	
LCO eMeOH Production	935,6	87%	935,6	87%
LCO CO_2 Transport	17,6	2%	27,1	3%
LCO CO_2 Intermediate storage	6,7	1%	6,6	1%
LCO CO_2 Liquefaction	11,9	1%	11,7	1%
LCO CO_2 Capture	100,3	9%	99,3	9%

Table 15: Results of the LCOCO$_2$ per transport medium and discretized per stage of the CCU value chain modelled for scenario 3

	Tanker		Truck	
LCO CO_2	**89,3** €/ ton CO_2		**94,8** €/ ton CO_2	
LCO CO_2 Transport	11,5	13%	17,7	19%
LCO CO_2 Intermediate storage	4,4	5%	4,3	5%
LCO CO_2 Liquefaction	7,8	9%	7,7	8%
LCO CO_2 Capture	65,6	74%	65,0	69%

These tables display the Excel model results for LCOeM and LCOCO$_2$ metrics, in green. They detail, under each metric, the levelized cost breakdown for each stage of the CCU value chain and for each selected transport option. Additionally, next to each stage's levelized cost, the tables present in percentage how each stage contributes to the overall LCOeM and LCOCO$_2$.

5.1 Results discussion

This section discusses the levelized costs obtained when the model runs the selected scenarios, characterized by the distance from the emitter to the eMeOH plant, the available CO_2 capacity at the emitting industry, and its corresponding eMeOH production potential.

To better understand the specifics of each scenario, Figure 6 provided the locations of all the industrial emitters considered across the Iberian Peninsula. The Portuguese emitters are significantly closer to the eMeOH plant in Sines Port compared to the Spanish ones. While all Portuguese plants are within 450 km of the plant, the Spanish ones have larger distances to Sines, with all surpassing 550 km, as shown in Table 16. This table also includes information about the annual CO_2 available at each industrial emitter and the corresponding eMeOH production, considering the unavailability times for all stages of the CCU value chain, as explained in Section 4.2.

Table 16: Calculation of eMeOH annual production capacity from the available CO_2 from each emitting industry

	Industry	Company and location	Distance of the route with different transport mediums (km) *(1)* — Tanker	Distance of the route with different transport mediums (km) *(1)* — Truck	Available CO_2 (ktpa)	eMeOH production capacity (ktpa)
Route 1	Cement	SECIL - Setúbal, PT	66	138	778	460
Route 2	Paper and pulp	TNC - Setúbal, PT *(2)*	70	139	646	380
Route 3	Cement	CIMPOR - Alhandra, PT	142	181	2023	1200
Route 4	Paper and pulp	TNC - Figueira, PT *(2)*	360	321	658	390
Route 5	Paper and pulp	TNC - Aveiro, PT *(2)*	438	400	154	90
Route 6	Cement	Votorantim - Málaga, SP	591	623	623	365
Route 7	Cement	Holcim - Carboneras, SP	836	878	1012	600
Route 8	Cement	CEMEX - Alicante, SP	1149	994	1110	655
Route 9	Cement	Lemona - Bilbao, SP	1225	1029	735	435
Route 10	Cement	CEMEX - Alcanar, SP	1250	1203	1551	920

(1) Nautical miles from the tanker route have been converted to km to provide a comparable metric between truck and tanker transport distances. (2) TNC is The Navigator Company

The first notable outcome is the limited annual availability of RFNBO compliant CO_2, constrained by the production capacity of each emitter. This model specifically considers scenarios where a single emitter supplies all CO_2 to the eMeOH plant, restricting eMeOH production to the emitter's CO_2 production capacity.

To enhance the reader’s understanding of the specifics of each case, Table 16, which initially followed an ascending order based on the distance between the emitter and the eMeOH plant, has been reorganized in Table 17 in ascending order based on the annual quantity of CO_2 available.

Table 17: Scenarios list ordered by CO_2 available capacity

	Company and location	Available CO_2 (ktpa)	eMeOH production capacity (ktpa)
Route 5	TNC - Aveiro, PT *(1)*	154	90
Route 6	Votorantim - Málaga, SP	623	365
Route 2	TNC - Setúbal, PT *(1)*	646	380
Route 4	TNC - Figueira, PT *(1)*	658	390
Route 9	Lemona - Bilbao, SP	735	435
Route 1	SECIL - Setúbal, PT	778	460
Route 7	Holcim - Carboneras, SP	1012	600
Route 8	CEMEX - Alicante, SP	1110	655
Route 10	CEMEX - Alcanar, SP	1551	920
Route 3	CIMPOR - Alhandra, PT	2023	1200

(1) TNC is The Navigator Company

It is observed that the largest industrial emitter is the CIMPOR cement plant, which has sufficient CO_2 production to supply an eMeOH plant with more than a million tons per year. Conversely, the pulp and paper plant of The Navigator Company in Aveiro will not be able to provide sufficient CO_2 to cover a 100 ktpa eMeOH plant.

5.1.1 Levelized Cost of eMethanol analysis

To initially compare the differences between the transport options for each of the modelled scenarios, the following graph presents the LCOeM for all selected scenarios for both transport mediums: the tanker case and the truck case.

Figure 8: LCOeM for the different scenarios modelled

It can be observed that for the first five routes or scenarios, the tanker transport cost is higher than the truck transport cost. In the case of scenario 3, the difference is not significant in the graph, but it is evident in the table, where the tanker is only €2 more expensive. This is because CIMPOR, being the highest emitter, has an elevated capacity that helps dilute the difference in the LCOeM. Conversely, in scenario 5, which has the lowest capacity, the difference in LCOeM is more pronounced. For the last six scenarios, the truck transport costs tend to be higher due to the longer distances, making the tanker a more cost-efficient option.

Furthermore, Table 18, which averages the values of the different stages of the CCU value chain for all the modelled scenarios, shows that the highest cost per unit of eMeOH produced corresponds to the eMeOH production plant stage.

Table 18: Comparison of the averaged levelized costs discretized per stages of the CCU value chain for option with tanker and option with truck

	WITH TANKER TRANSPORT		WITH TRUCK TRANSPORT	
eMeOH plant	954	85%	954	84%
Transport	36	3%	56	5%
Storage	21	2%	21	2%
Liquefaction	12	1%	12	1%
Capture	100	9%	99	9%
LCOeM	**1123**	**€/ton eMeOH**	**1142**	**€/ton eMeOH**

Choosing either tanker or truck transport will not significantly impact the LCOeM for the eMeOH production plant, as it does not affect the amount of CO_2 sourced as feedstock for the plant. However, it does influence the total LCOeM.

To better analyse the significance of the costs associated with the eMeOH production plant stage, this stage is isolated from the rest, as shown in Figure 9. This helps to identify the economies of scale that apply to this area.

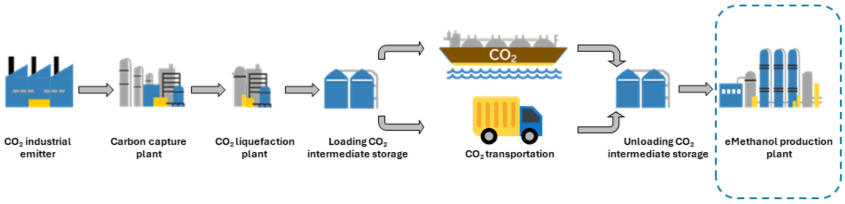

Figure 9: Schematic isolation the eMeOH production plant stage fron teh rest of the CCU value chain

Table 19: LCO eMeOH production plant corresponding to the different available capacities from CO_2 emitters

	LCO eMeOH Production (€/ton eMeOH)	Available CO_2 (ktpa)
Route 5	1000	154
Route 6	957	623
Route 2	956	646
Route 4	956	658
Route 9	953	735
Route 1	952	778
Route 7	947	1012
Route 8	945	1110
Route 10	940	1551
Route 3	936	2023
Average	**954**	**929**

In this case, to help the examination of the LCO eMeOH Production plant figures, Table 19 presents the different scenarios in ascending order of available CO_2 capacity, showing decreasing levelized costs. Given that the "0.6 rule" is applied for modelling the CAPEX of the eMeOH production plant in Section 4.3.5, scenarios with the highest CO_2 availability yield lower LCOeM production costs. This is evident when comparing the industrial emitter with the highest CO_2 capacity, emitter 3, with emitter 5, which has the lowest CO_2 capacity. Scenario 3 yields the lowest value of €936/ton of eMeOH, while scenario 5 yields a value of €1,000/ton of eMeOH. All other scenarios with intermediate CO_2 capacities follow the same principle, showing higher LCOeM production costs as their capacity decreases.

5.1.2 Levelized cost of carbon dioxide analysis

When excluding the eMeOH production stage from all the stages in the CCU value chain model, the metric of $LCOCO_2$ can be analysed in CO_2 units. This includes the CCU value chain stages of CC, liquefaction, loading intermediate storage, transport, and unloading intermediate storage, as presented in Figure 10.

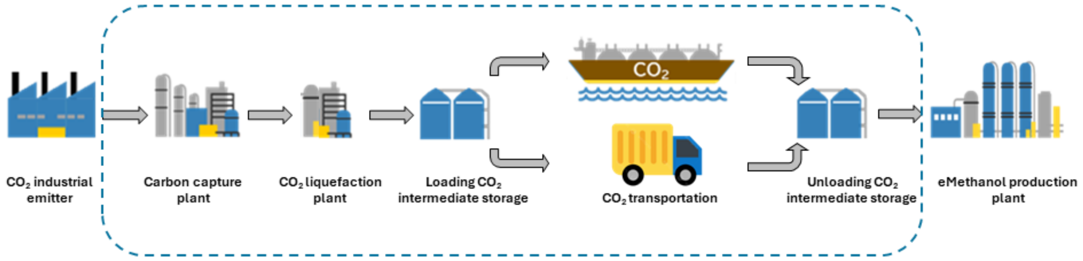

Figure 10: CCU value chain stages which are necessary to handle the CO_2 from the emitter to the eMeOH plant

Regarding the $LCOCO_2$ results considering maritime transport, Figure 11 shows how each of the CCU value chain stages presented in Figure 10 contributes to the overall $LCOCO_2$ for each scenario.

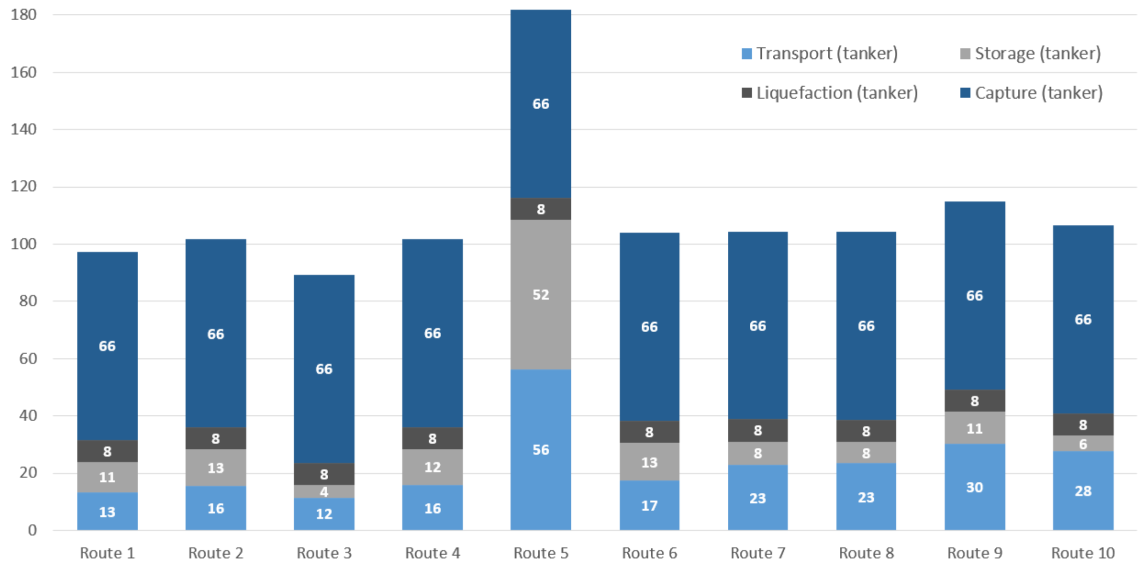

Figure 11: $LCOCO_2$ discretized per CCU value chain stage (excluding eMeOH) for the different tanker scenarios

For a CCU value chain connected by tanker, route 5 presents a very elevated total $LCOCO_2$, standing out from the others. In this low CO_2 capacity case, the economies of scale that characterize tanker transport make it impractical to connect this industrial emitter by tanker. Moreover, routes 6, 7, 8, 9, and 10, which connect to Spanish emitters, show higher values compared to the Portuguese routes due to the greater distance. The differences in the $LCOCO_2$ Transport values are influenced not only by economies of scale and distance but also by the substantial increase in CAPEX and OPEX when an additional tanker is added to the fleet. This is highlighted in the following Table 20, which shows the number of tankers needed for each scenario.

Table 20: Number of tankers required for each scenario, loop time, loops per year and time that a tanker of the fleet is stopped for each loop

	Tankers number	Loop time (hours) *(1)*	Loops per tanker/year *(1)*	Hours per loop the tanker is stopped
Route 1 - PT	1	31	91	59
Route 2 - PT	1	31	76	77
Route 3 - PT	2	37	119	16
Route 4 - PT	1	54	119	52
Route 5 - PT	1	60	119	398
Route 6 - SP	1	72	119	41
Route 7 - SP	2	91	119	24
Route 8 - SP	2	115	119	6
Route 9 - SP	2	121	119	35
Route 10 - SP	3	122	182	4

(1) Loop is understood as the time that takes to load the tanker, travel to the eMeOH plant, unload it and travel back to the emitter

This table helps to understand how the model sizes the tanker fleet based on distance and CO_2 capacity. Among the Portuguese emitters, scenario 3 requires two tankers, whereas scenarios 1, 2, 4, and 5 each require only one. Although this emitter is the third closest to the eMeOH plant, its high CO_2 availability necessitates an additional tanker. Its substantial CO_2 capacity results in a lower marginal cost for adding another tanker compared to other Portuguese cases, making its $LCOCO_2$ for transport the lowest of all at €12/ton of CO_2. This is further supported by the fact that its tankers have the least idle time among the Portuguese cases. This metric indicates how much time is lost because the fleet's capacity exceeds the emitter's CO_2 production. The higher the idle time, the less justified the additional tanker.

The same principle applies when comparing scenarios 2 and 4. It is evident that despite both emitters producing similar amounts of CO_2, emitter 2, being 290 km closer to Sines, results in more idle time for its tanker. Interestingly, the $LCOCO_2$ for transport in scenario 4 is not cheaper than in scenario 2. The longer distance of scenario 4 increases OPEX due to higher fuel costs and harbour fees, leading to a transport cost of €16/ton of CO_2 compared to €15.6/ton for scenario 2.

In the Spanish scenarios on the bottom of Table 20, emitter 6, with the shortest distance to the eMeOH plant, requires only one tanker, while others need two or three. This is justified by their CO_2 capacities handled, as shown previously in Table 17. Despite being further from the eMeOH plant than the Portuguese emitters, emitter 6's relatively low CO_2 capacity allows for the use of only one tanker. In contrast, scenarios 7 and 8 require two tankers each, reflecting their CO_2 capacities, which are nearly double that of emitter 6. Scenario 10, with the second-highest CO_2 capacity and the longest distance to Sines, necessitates a third tanker to meet the eMeOH plant's CO_2 demands. The long distance and the need for a third tanker increase both CAPEX and OPEX, primarily influenced by fuel costs and harbour fees. This scenario yields €28/ton of CO_2, making it the second most expensive among the Spanish scenarios for $LCOCO_2$ transport, with scenario 9 being the most expensive at €30/ton of CO_2.

Interestingly, calculations reveal that harbour fees exceed fuel costs in annual OPEX for scenarios where the emitter is within 600 km of Sines port by maritime transport. This applies to Portuguese emitters and scenario 6. Among these, scenario 3 incurs the highest harbour fees due to its significant CO_2 capacity, which dilutes the harbour fee expenditure. This is because its highest CO_2 capacity across all scenarios ultimately dilutes the harbour fee expenditure.

Additionally, the intermediate storage stage analysis indicates that scenario 5 presents the highest levelized cost. This is influenced not only by its scale but also by the fixed intermediate storage capacity of 9,150 m^3, regardless of the actual annual capacity handled. This assumption also affects emitters 1, 2, 4, 6, and 9, each having less than 1,000 ktpa of CO_2 availability, resulting in $LCOCO_2$ storage costs exceeding €10/ton of CO_2. Emitters with over 1,000 ktpa of CO_2 incur storage costs below €10/ton, with the lowest costs corresponding to those handling the most CO_2.

For the liquefaction and CC stages, all scenarios exhibit the same values: €66/ton of CO_2 for CC and €8/ton of CO_2 for liquefaction. In this Master Thesis, both the liquefaction and CC plants have been sized to adapt their scale to the quantities processed. Given the established linear increase assumption, disregarding economies of scale, the per-unit CO_2 results remain constant across all scenarios.

After this analysis, the goal is to identify which stage has the most significant impact on the $LCOCO_2$. To derive a meaningful metric, the values from all the scenarios are averaged. Scenario 5 presents significantly higher levelized cost values and is clearly an outlier among the scenarios due to its low CO_2 capacity; therefore, it is excluded from the averaging process. Calculations for the remaining scenarios yield the following values:

Table 21: Averaged values from the different stages of the $LCOCO_2$

Transport	20	19%
Storage	10	9%
Liquefaction	8	8%
Capture	66	64%
$LCOCO_2$	**103**	**€/ton CO_2**

Table 21 reveals that the CC stage represents the most significant cost in implementing a CO_2 capture and logistics value chain. This cost is notably higher compared to other stages, with maritime transportation emerging as the second most expensive component. Notably, the transportation costs are double those of both the storage and liquefaction stages.

Due to the aforementioned reasons and the assumptions considered in this work, the transport stage exhibits the greatest variability in results. This variability is notably dependent on the distance covered by the tankers, with costs increasing for longer distances. Additionally, there is a significant dependency of the $LCOCO_2$ transport costs on the mismatch between the capacity of the selected tankers and the available CO_2 capacity of the emitter. This mismatch is particularly pronounced given the large capacity of the selected tankers and the corresponding CAPEX and OPEX associated with the tanker fleet.

For CO_2 road transportation, Figure 12 illustrates how each component of the CCU value presented in Figure 10 contributes to the overall $LCOCO_2$ for each industrial emitter case.

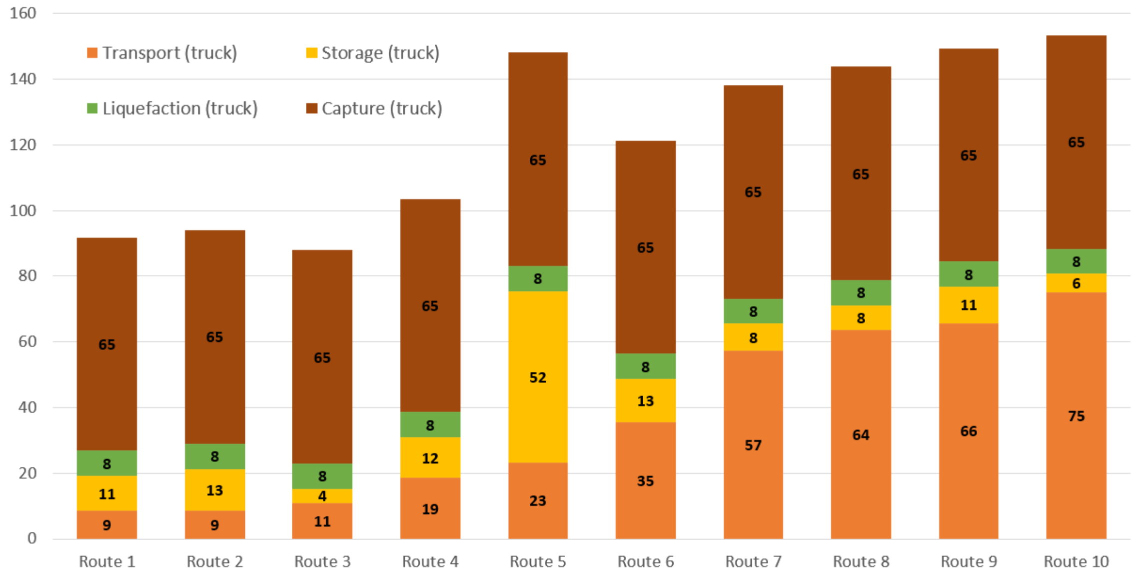

Figure 12: $LCOCO_2$ discretized per CCU value chain stage (excluding eMeOH) for the different truck scenarios

In the context of the road transportation stage, the most significant observation is the increase in cost with growing distances. Unlike maritime transport, where both distance and the mismatch between tanker size and capacity significantly impact the $LCOCO_2$ Transport, the primary factor for trucks is distance. Notably, there is a significant difference between the scenarios for Portuguese and Spanish industry emitters when trucks are used, as shown in Figure 12, compared to when tanker fleets are utilized, as seen in Figure 11.

Moreover, the capacity of trucks is significantly smaller compared to the volumes that need to be transported annually from various emitters to the eMeOH production plant. This implies that the truck fleet size for each scenario must be counted in tens or even hundreds, as detailed in Table 22.

Table 22: Distances and number of trucks for the different routes from emitters to Sines eMeOH plant

	DISTANCE (km)	NUMBER OF TRUCKS
Route 1 - PT	138	47
Route 2 - PT	139	48
Route 3 - PT	181	55
Route 4 - PT	321	78
Route 5 - PT	400	102
Route 6 - SP	623	139
Route 7 - SP	878	361
Route 8 - SP	994	381
Route 9 - SP	1029	387
Route 10 - SP	1203	416

From a technical sizing perspective, this helps to minimize mismatches between the CO_2 capacity available from each industrial emitter and the fleet size. Logistically, the truck fleet operates continuously but is constrained by driver rest times, as explained in Section 4.2.5.2. Economically, the smaller size of trucks transporting CO_2 continuously helps reduce the cost inefficiencies associated with having transport assets idle due to misaligned industrial emitter capacity and fleet size.

If the storage, liquefaction and CC of both are compared both maritime transport (Figure 11) and road transport (Figure 12) it can be observed that they share the same values. Consequently, the same conclusions applicable to CO_2 transported by tanker also apply when CO_2 is transported by truck, given that the other components remain the same. Table 23 presents a comparison of both value chains under the two transport options, highlighting the differences in the LCOCO$_2$ Transport stage due to the different transport mediums.

Table 23: Comparison of the average LCOCO$_2$ discretized per stages for option with tanker and option with truck

	WITH TANKER TRANSPORT		WITH TRUCK TRANSPORT	
Transport	20	19%	38	37%
Storage	10	9%	10	9%
Liquefaction	8	8%	8	7%
Capture	66	64%	65	63%
LCOCO$_2$	**103**	**€/ton CO$_2$**	**120**	**€/ton CO$_2$**

A notable difference, aside from the transport stage, is observed in the CC stage values. Section 4.2 explains that each stage of the CCU value chain is interconnected. And, due to assumed unavailability times, the upstream stages have been oversized to ensure the downstream demand at the eMeOH plant is met. For instance, if tankers have an assumed operational availability of 94% annually, the upstream stages such as intermediate storage, liquefaction, and CC need to be oversized to compensate for the tankers' unavailability. Conversely, with trucks having an assumed 95% operational availability annually, the required oversizing for this transport option results in a lower LCOCO$_2$ CC. Table 24 shows the LCOCO$_2$ values per stage for different routes, differentiating when tankers or trucks are used.

Table 24: LCOCO$_2$ values per stage for the different routes and transportation mediums

	TRANSPORT		STORAGE		LIQUEFACTION		CAPTURE	
	Tanker	Truck	Tanker	Truck	Tanker	Truck	Tanker	Truck
Route 1	13,36	8,58	10,58	10,58	7,77	7,69	65,63	65,00
Route 2	15,56	8,64	12,71	12,71	7,77	7,69	65,63	65,00
Route 3	11,52	10,88	4,35	4,35	7,77	7,69	65,63	65,00
Route 4	15,97	18,53	12,40	12,39	7,77	7,69	65,63	65,00
Route 5	56,39	23,31	52,11	52,11	7,77	7,69	65,63	65,00
Route 6	17,37	35,46	13,21	13,21	7,77	7,69	65,63	65,00
Route 7	22,83	57,34	8,23	8,22	7,77	7,69	65,63	65,00
Route 8	23,42	63,57	7,58	7,57	7,77	7,69	65,63	65,00
Route 9	30,28	65,64	11,16	11,16	7,77	7,69	65,63	65,00
Route 10	27,60	75,22	5,53	5,53	7,77	7,69	65,63	65,00

By examining the centesimal differences in Table 24, variations can be observed not only in the CC column but also in storage and liquefaction. These differences are due to the oversizing required to cover downstream unavailability and ensure the demand at the eMeOH plant is met.

Subsequently, to select the most suitable transport medium for each scenario, the LCO CO$_2$ Transport metric is crucial and must be isolated from the rest of the CCU value chain, as illustrated in Figure 13.

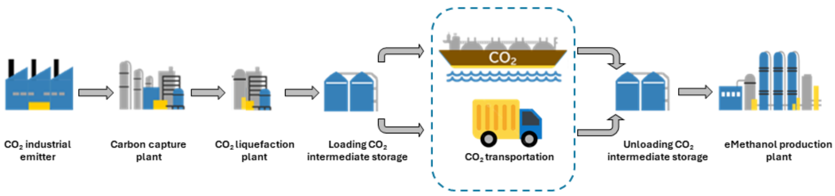

Figure 13: CCU value chain schematic isolating the CO$_2$ transport stage

The following Figure 14 presents only the LCOCO$_2$ Transport stage values for the two transportation mediums selected.

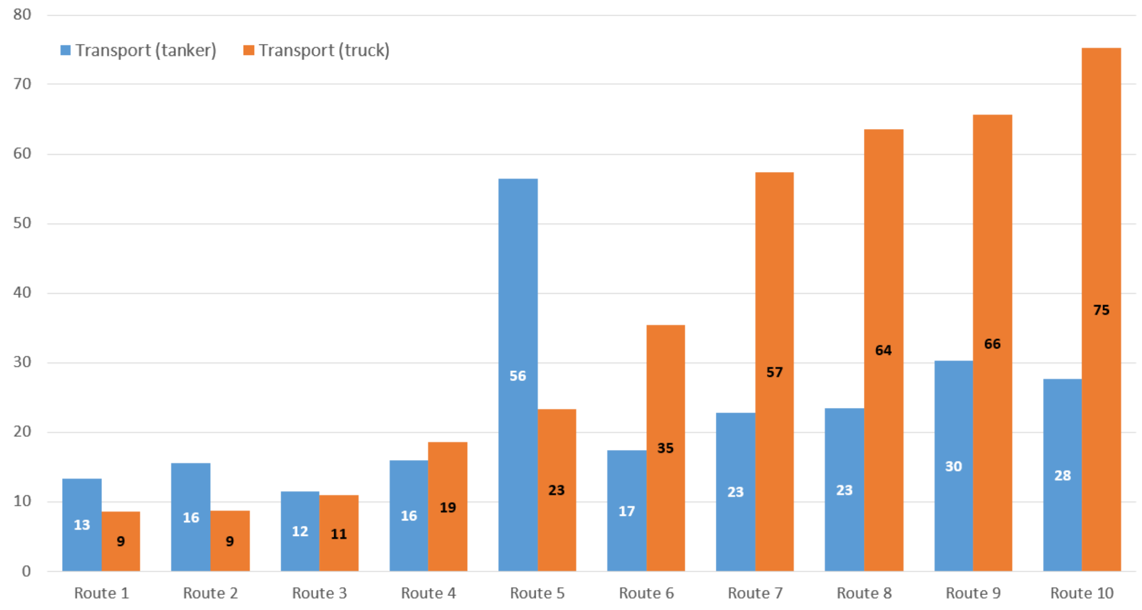

Figure 14: LCOCO$_2$ Transport for the different scenarios per tanker and truck transport options

The analysis reveals that choosing trucks is not cost-efficient for scenarios involving Spanish industrial plants. In comparison, tankers present significantly lower costs for the more distant industrial emitters, such as scenarios 7, 8, 9, and 10, where the levelized cost of trucks is double that of tankers. This disparity is primarily due to the impact of distance on both the CAPEX and OPEX of trucks. To meet the CO_2 demand at the eMeOH plant, a larger fleet of trucks is required for longer distances, as detailed in Table 22.

Also, the primary drivers of OPEX are fuel costs, followed by labour and toll costs. Increased distances to transport the same amount of CO_2 as in Portuguese cases result in higher operational costs. Additionally, longer distances necessitate more breaks for truck drivers, affecting both CAPEX and OPEX since a larger fleet and more drivers are needed. The third operational cost driver is the toll cost, which particularly affects the Portuguese part of the route, as Spain is not characterized by as many tolls as the neighbouring country. However, the reduction in toll costs while driving through Spain does not compensate for the higher fuel and labour costs associated with longer routes.

Tankers connecting Spanish emitters, on the other hand, show lower levelized costs due to their ability to carry larger quantities of CO_2 at once. Although the main operational cost driver for tankers in Spanish scenarios shifts to fuel costs, which are significantly higher than for Portuguese scenarios, the increase in levelized cost is less pronounced than for trucks

Table 25: Key metrics for the scenarios corresponding to Spanish CO_2 emitters

	Available CO_2 (ktpa)	eMeOH production capacity (ktpa)	Distance (km)	LCOCO$_2$ Transport (€/ton of CO_2)
Route 6	623	365	591	17,4
Route 7	1012	600	836	22,8
Route 8	1110	655	1149	23,4
Route 9	735	435	1225	30,3
Route 10	1551	920	1250	27,6

Table 25 illustrates the impact of annual CO_2 capacity on levelized costs for Spanish emitters. It is evident that scale significantly influences these costs. Emitters 6 and 9 in Spain, each with less than 1,000 ktpa of CO_2 available, exhibit higher levelized costs due to both distance and lower scale, as previously shown in Table 17. Hence, their levelized costs are impacted not only by distance but also by their lower scale compared to scenarios 7, 8, and 10. This is particularly pronounced in scenario 9, which has the highest levelized cost of all. Interestingly, scenario 6, despite being 591 km from Sines and handling 623 ktpa of CO_2, presents a lower levelized cost than scenario 7, which is 836 km away and has a capacity of 1,012 ktpa. For this comparison, it would be expected that, with a distance difference of an extra 5% and a capacity increase of 62%, the levelized cost of scenario 7 would be lower than that of scenario 6. This interesting phenomenon is explained in Table 20, where it can be observed that scenario 7 requires an extra tanker to meet demand, thus incurring larger CAPEX and OPEX. Similarly, if scenarios 9 and 10 are compared, the differences show an extra capacity of 211% compared to an extra distance of 2%. A significantly higher levelized cost would be expected for scenario 9, but scenario 10 requires 3 tankers. This increases its levelized cost to transport substantially more CO_2 at a similar distance to Sines than from industrial emitter 9.

Among the Spanish industrial emitter scenarios presented in Table 25, scenario 6 yields the lowest LCOCO$_2$ Transport at 17.4 €/ton of CO_2, benefiting from being the closest to Sines, but also characterized by the lowest eMeOH potential. This is followed by scenarios 7 and 8 at 22.8 and 23.4 €/ton of CO_2, with a potential of producing more than 600 ktpa of eMeOH, roughly doubling the capacity of scenario 6. Additionally, scenario 10 should not be disregarded, given that although it results in a higher levelized cost of 27.6 €/ton of CO_2, its eMeOH potential production capacity is more than 50% higher than that of scenarios 7 and 8. Only scenario 9 does not prove to be a suitable emitter because of its limited CO_2 capacity and significant distance, resulting in the highest cost among the Spanish industrial emitters.

To determine which of the Spanish scenarios yields the most cost-effective results, the analysis should focus on the overall cost of the CCU value chain in units of eMeOH.

Table 26: Key levelized cost metrics for the Spanish emitting scenarios

	Available CO_2 (ktpa)	eMeOH production (ktpa)	LCOCO$_2$ Transport (€/ton of CO_2)	LCO eMeOH Prod. (€/ton of eMeOH)	LCOeM (€/ton of eMeOH)
Route 6	623	365	17	957	1116
Route 7	1012	600	23	947	1107
Route 8	1110	655	23	945	1105
Route 9	735	435	30	953	1129
Route 10	1551	920	28	940	1102

In Table 26, it can be observed that higher eMeOH production in scenarios 8 and 10 results in LCOeM values of 945 and 940 €/ton, respectively, compared to scenario 7 at 947 € per ton of eMeOH. The last column clearly shows that although scenario 10 incurs higher costs than the other two, its elevated capacity yields the lowest LCOeM of all Spanish scenarios, at 1,102 €/ton. Thus, this industrial emitter should be targeted if the deployment of the CCU value chain is not restricted by the incurred expenditure or other relevant constraints typical to this project typology, such as securing grid connection, ensuring sufficient renewable electricity to meet project needs, environmental permits, and land availability.

Focusing on the Portuguese industrial emitters, which are significantly closer to the eMeOH plant, the values for tanker or truck transport do not show significant differences compared to the Spanish scenarios, except for scenario 5. As seen in Table 27, scenario 5 has the lowest CO_2 availability, resulting in elevated costs per unit of CO_2 transported and will be excluded from further analysis.

Table 27: Key metrics for the Portuguese emitters regarding tanker and truck transport

	Available CO_2 (ktpa)	eMeOH production (ktpa)	Distance of the route with different transport mediums (km) (1)		LCOCO$_2$ Transport (€/ton of CO_2)	
			Tanker	Truck	Tanker	Truck
Route 1	778	460	66	138	13	9
Route 2	646	380	70	139	16	9
Route 3	2023	1200	142	181	12	11
Route 4	658	390	360	321	16	19
Route 5	154	90	438	400	56	23

(1) Nautical miles from the tanker route have been converted to km to provide a comparable metric between truck and tanker transport distances.

From the remaining Portuguese cases, scenarios 1, 2, and 3 yield more economic values for truck transportation than for tanker, unlike scenario 4, which shows the opposite behaviour. This can be attributed to the significantly greater distance characterizing scenario 4. As previously justified, large distances are not cost-effective to be covered by truck, and the LCOCO$_2$ Transport for tankers is 3 €/ton of CO_2 cheaper than for trucks. For scenarios 1 and 2, the distances and capacities are very similar, yielding the same values for truck transport. Conversely, for tanker transport, scenario 2 is more expensive because its CO_2 capacity is lower. As observed in Table 20, scenario 2 will have more hours when the single tanker in its fleet is stopped. Also, scenario 1 is less significantly affected by this, but this still results in cost inefficiencies for tanker transport that truck transportation does not experience. This is because the truck fleet size better matches the available CO_2 capacities for short distances, making it more suitable for scenarios 1 and 2. Lastly, scenario 3, with the highest CO_2 capacity available, manages to significantly reduce the differences between transport options. Yet, truck transportation yields a lower LCOCO$_2$ Transport at 11 €/ton of CO_2, which is 2 € more expensive than running scenarios 1 and 2 with truck fleets.

Similar to the Spanish scenarios, attention should be paid to a broader scale when considering which scenario yields a better LCOeM. This evaluation is necessary given that the eMeOH production plant stage accounts for a major part of the costs within the stages comprising the CCU value chain.

Table 28: Key levelized cost metrics for the Portuguese emitting scenarios

	eMeOH production (ktpa)	LCOCO$_2$ Transport (€/ton of CO_2)		LCO eMeOH Prod. (€/ton of eMeOH)	LCOeM (€/ton of eMeOH)	
		Tanker	Truck		Tanker	Truck
Route 1	460	13	9	952	1101	1093
Route 2	380	16	9	956	1112	1100
Route 3	1200	12	11	936	1072	1070
Route 4	390	16	19	956	1111	1114
Route 5	90	56	23	1000	1278	1227

The effect of higher eMeOH production is particularly notable in the LCO eMeOH Production column, yielding the lowest values for scenario 3, with a reduction of 16 €/ton of eMeOH compared to the second cheapest option, which is scenario 1. This results in scenario 3 also having the most cost-effective total LCOeM. Truck transport remains the cheaper option in this scenario, with the cost difference being only 2 €/ton of eMeOH between choosing a fleet of 55 trucks or 2 tankers. In other scenarios, the differences are more significant. For example, in the second most cost-effective scenario, which corresponds to route 1, the truck option is 7 €/ton cheaper than the tanker option, despite having a CO_2 capacity one-third that of scenario 3.

After thoroughly analysing each scenario within the Iberian Peninsula, the most cost-effective scenarios can be compared to draw conclusions on the implications of each choice. If the most promising scenarios from both Portuguese and Spanish emitters are ordered from left to right in increasing eMeOH production capacity, the following Figure 15 can be derived.

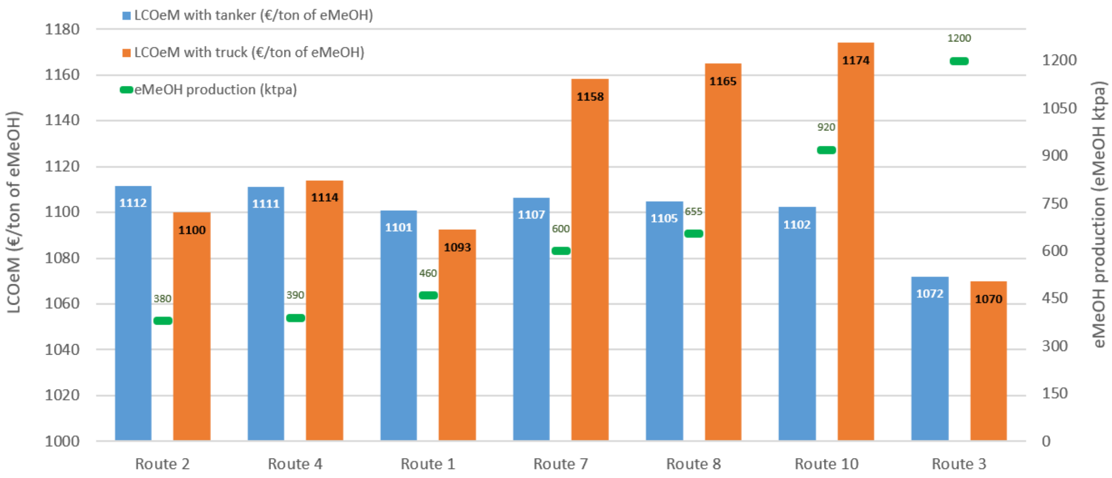

Figure 15: LCOeM with tanker and truck transport options for most suitable scenarios with corresponding eMeOH production capacity in ktpa

The predominance of Portuguese industry emitters is evident, with scenarios 1 and 3 being notably below the 1,100 €/ton of eMeOH threshold. Scenario 1 yields 1,093 €/ton with truck transport, while scenario 3 achieves the lowest LCOeM with both tanker and truck fleets, at 1,072 and 1,070 €/ton of eMeOH, respectively, due to its highest eMeOH production potential. Right at the 1,100 €/ton threshold is scenario 2, which has the lowest eMeOH potential. This is followed by the Spanish emitter scenario 10 at 1,102 €/ton, balancing elevated distance with eMeOH potential. Spanish industrial emitter scenarios 7 and 8, using tanker transport, yield 1,107 and 1,105 €/ton, respectively, closely followed by scenario 4 at 1,111 €/ton of eMeOH.

From these comparisons, it is evident that economies of scale significantly impact scenarios 3 and, to a lesser extent, 10. However, scenario 2, with half the eMeOH production potential of scenario 10 and nearly a third of emitter 3, has managed to yield more competitive values than scenario 10 with either tanker or truck CO_2 transport.

This analysis identifies two scenarios as the most competitive for eMeOH production at the Sines port location. First, if there are no restrictions on expenditure or securing sufficient grid connection capacity and renewable energy sources, industrial emitter 3 is preferred. This cement industry emitter has the largest RFNBO-compliant CO_2 capacity, allowing full utilization of economies of scale and achieving eMeOH production above one million tons per annum. Conversely, if any of the mentioned restrictions constrain the development of such large quantities of eMeOH, scenario 1 is recommended. This pulp and paper plant has sufficient available CO_2 to supply an eMeOH plant with a production capacity of 460 ktpa. Regarding the transport option, both plants are within a 150 km radius of the Sines port, resulting in differences of less than 10 €/ton of eMeOH between transport mediums, with lower values for truck transport. While this difference may not seem significant, the following table calculates the economic implications of this variance.

Table 29: Calculation in lifecycle cost of selecting tanker vs. truck as transport option in the selected scenarios

	eMeOH production (ktpa)	LCOeM (€/ton of eMeOH)		Difference between tanker and truck	Lifecycle cost of the project
		Tanker	Truck		
Route 1	460	1101	1093	3.872.204 €	504.494.960 €
Route 3	1200	1072	1070	2.501.623 €	1.285.097.944 €

The additional lifecycle cost of selecting a tanker fleet is more significant for scenario 1, despite its smaller capacity. Both extra costs, surpassing the €2 million threshold, represent less than 1% of the total lifecycle cost of deploying such projects. Consequently, this work does not define a preference in the selection of the transport option other than the one which yielded the lowest costs, which is truck CO_2 transportation. Consequently, this study does not define a preference in the selection of transport option, rather it highlights that the one which yielded the lowest costs is truck CO_2 transportation.

With this last statement the author aims to acknowledge the inaccuracies that an academic model, like the one developed in this work, may incur. The resulting model has successfully approximated the techno-economic implications of deploying a CCU value chain. Therefore, it is intended to serve as an estimate for potential users of the model who may not have the resources or time to develop these estimates.

5.2 Results validation from literature

In this section the results LCOeM and $LCOCO_2$ are compared with the available literature. It is important to note that not all the values presented in Table 14 and Table 15 are typical metrics available for verification in the literature. For instance, the values in Table 14 such as $LCOCO_2$ Transport, $LCOCO_2$ Intermediate storage, $LCOCO_2$ Liquefaction, and $LCOCO_2$ Capture, are generally expressed in CO_2 feedstock units as shown in Table 15 rather than in eMeOH production units. The purpose of Table 14 is to illustrate how different components impact the total LCOeM, and therefore, they will not be compared with literature values.

The values that need validation with literature are:

- LCOeM in eMeOH units
- $LCOCO_2$ Transport in CO_2 units
- $LCOCO_2$ Intermediate storage in CO_2 units
- $LCOCO_2$ Liquefaction in CO_2 units
- $LCOCO_2$ Capture in CO_2 units

This work reports LCOeM values ranging from 1,000 to 1,350 €/ton of eMeOH for production capacities between 2,000 and 100 ktpa, respectively. Literature sources indicate that the LCOeM generally falls within 790 to 1,410 €/ton of eMeOH [26], [28], [135]. In comparison, the current European market price for fossil methanol is 535 €/ton, presenting an uncompetitive barrier for eMeOH adoption by off-takers [136]. This price difference mainly arises from the high cost associated with H_2 production, which in this thesis is assumed to have an LCOH of 4€/ton, largely influenced by renewable electricity prices due to the energy-intensive nature of electrolytic H_2 production. eMeOH is also impacted by the cost of CO_2 sourcing and electricity prices, unlike fossil methanol which depends mainly on policies and NG prices [135].

For tanker transport, intermediate storage, and liquefaction, the levelized costs per ton of CO_2 were benchmarked against the work of Fraga et al., who modelled a CCS hub operating at a pressure of 15 bar with a capacity to handle 2 million tons of CO_2 annually [39]. Selecting a route similar to route 4, which reflects the distance covered by the 6 kton liquid CO_2 tankers described by Fraga et al., yielded comparable results. The $LCOCO_2$ for maritime transport in this thesis is 11.9 €/ton, compared to Fraga et al.'s reported value of 21.9 €/ton. The lower cost in this Thesis is attributed to the selection of larger tankers with an 8.23 kton capacity, which enhances cost-efficiency. Other papers, such as the work by Seo et al., modelled CO_2 transport by tanker, intermediate storage, and liquefaction at various pressures for a scale of 1,000 ktpa [121]. Their results present values of 15.2 €/ton of CO_2, whereas this Thesis yields a higher value of 21.1 €/ton of CO_2 at the same scale. This difference can be explained by the fact that this Thesis necessitates 2 tankers with a capacity of 8,230 tons of CO_2 each to handle the 1,000 ktpa of CO_2, while Seo et al. modelled with a single tanker of 12,310 tons. The larger single tanker reduces both OPEX and CAPEX, resulting in lower levelized costs in their study.

To compare CO_2 transport by truck, the work of Alves is reviewed, as it models several transport modalities for roughly 800 ktpa of CO_2 originating from a pulp and paper plant [53]. In this thesis, for a comparable case such as the route 4 scenario, the levelized cost is 9.4 €/ton, which is significantly close to Alves' value of 5.4 €/ton. The difference is explained by Alves' lower capital and operational costs. This Master Thesis recognizes that a new fleet of trucks should be acquired every five years, while Alves considers ten years, which is unrealistic given the annual mileage. Additionally, in the OPEX area, with fuel and labour being the highest expenditures, Alves uses optimistic values for fuel price and driver wages. Alves assumes a fuel price of 1.56€/litre compared to this Thesis' 1.67 €/litre, and a wage of 14€/hour, which is too low when considering gross salary, social security, health insurance, and bonuses. This thesis accounts for approximately 25 €/hour for drivers.

Regarding $LCOCO_2$ Intermediate Storage, this Thesis calculates a value of 2.0 €/ton, while Fraga et al. report a lower value of 1.1 €/ton of CO_2. The difference can be explained by Fraga et al. using a cost ratio of 1,191 €/m^3 of CO_2 capacity for vertical tanks, whereas this thesis uses 2,506 €/m^3 [39]. Additionally, this Master Theis includes loading and unloading systems as part of the intermediate storage site, contributing to the higher $LCOCO_2$ Storage cost. In comparison, Seo et al. present values of 2.71 €/ton, while this thesis presents 7.6 €/ton [121]. This more significant difference is majorly reflected in the fact that this Thesis did not optimize the size of the intermediate storage for different capacities and fixed the value at 9,500 m^3 of CO_2, regardless of the capacities to be handled. Additionally, the difference is aggravated, as in the case of Fraga et al. due to a higher CAPEX ratio per vertical tank as well as the inclusion of loading and unloading systems in the intermediate storage stage in this Thesis, which increases the overall storage cost.

For liquefaction, the levelized costs per ton of CO_2 show similar results between both studies: Fraga et al. report 8.5 €/ton, while this Thesis reports 7.8 €/ton of CO_2 [39]. Upon revising the liquefaction cost assumptions for both cases, it is recognized that the Master Thesis mirrors Fraga et al.'s work and used the same levelized cost calculation methodology, which should result in the same value. However, the observed difference in results is attributed to Fraga et al.'s higher real discount rate, despite their consideration of a 10-year longer lifetime compared to this Master Thesis. A higher discount rate means that future cash flows are discounted more heavily to their present value. This typically increases the present value of costs over the project's lifetime, potentially resulting in higher annualized levelized costs. Conversely, a longer project lifetime spreads initial capital and operational costs over more years, which can reduce annualized costs and lower the levelized cost compared to a shorter-lifetime project. Since both Fraga et al. and this Thesis employ same cost assumptions and calculation methodologies, it is understood that the higher discount rate in Fraga et al.'s study outweighs the impact of the longer lifetime, resulting in higher levelized costs for their work.

In regard to the metric of $LCOCO_2$ Capture, this work presents values of 65 to 66 €/ton of CO_2. Literature sources indicate a range of 42 to 94 €/ton for other technoeconomic analyses of cement and pulp and paper plants using amine post-combustion technology [30], [86], [94], [132]. The values obtained in this Master Thesis align closer to the lower bound, possibly due to the consideration of only CAPEX and OPEX in the technoeconomic analysis.

Finally, when comparing $LCOCO_2$ for transport, intermediate storage, and liquefaction, this thesis generally presents higher values for the transport stage. In line with the results shared by Fraga et al., at pressures of 15 bar, tankers imply an elevated CAPEX, placing the transport stage with the largest share, followed by liquefaction and intermediate storage [39].

5.3 Limitations and future work

This Master Thesis has several limitations that provide opportunities for future research. The current model is restricted to scenarios where a single CO_2 emitter supplies the eMeOH plant. It does not explore the potential of sourcing CO_2 from multiple emitters, which could enhance the flexibility and efficiency of the system. Additionally, only specific transportation modes were considered in this work, such as tanker and truck transport.

Pipeline and rail transportation, which could be highly relevant for certain scenarios, were not included. These modes should be investigated to determine the most suitable transportation method for each industrial emitter, depending on their distance to the CO_2 consuming point.

Further work could improve the model by integrating various modalities connecting the emitting point with the eMeOH plant. Enhancing the model to include multiple emitting points and various transportation modes could identify the optimal transport mode for each emitter.

Moreover, the flexible positioning of the eMeOH plant based on the availability of CO_2 should be considered. While this Master Thesis selected Sines as the location for the eMeOH plant for specific reasons outlined in Section 4.2.2., other locations closer to the emitting points might reduce the overall levelized cost of CO_2 and, consequently, the cost of eMeOH.

If relocating the eMeOH plant is considered, it is recommended to extend the model to include eMeOH logistics from the production plant to the consumption points. Such an extension would be crucial to validate whether relocating the eMeOH production plant is justified both upstream and downstream.

Furthermore, the tankers selected have a capacity of 7,500 m^3 of liquid CO_2 or 8,230 tons of liquid CO_2 capacity. This has been considered given the reasons explained in Section 4.3.3.1. However, considering tankers with less capacity or a mix of different capacity tankers will reduce the mismatching between the available CO_2 capacity of the emitter and the size of the fleet. This misalignment has been observed to incur cost inefficiencies while tankers are stopped due to this mismatch. Further work is suggested if the aim is to drive cost optimization in this model, which was out of the scope of this Master Thesis.

Also, given that the intermediate storages are sized at a fixed 9,150 m^3 CO_2 capacity, regardless of whether the transport option is tanker or truck, and without considering different volumes handled throughout the day, cost optimization will be suggested in this part to enhance the model. As it is for now, the goal of the model is not to optimize the costs, hence not presenting an accurate metric when the intermediate storage sites are modelled. Additionally, it is recommended that both CC and liquefaction plants are modelled under the assumptions of economies of scale. This could include employing the "0.6 rule" or a similar approach. With this methodology, the levelized costs for different capacities will vary, contrary to the current model where all the levelized costs for CC and liquefaction yield the same results for all capacities due to the assumed linear increase in techno-economic adaptations

Additionally, if the aim is to reduce the environmental footprint of transportation, it is suggested that the fuel for the transport modalities be changed. For tankers, eMeOH could be a viable option, while for trucks, biofuels might be the most suitable solution.

In conclusion, coupling different modalities, considering multiple emitting points, and exploring various transportation modes can provide a more comprehensive and efficient model. These enhancements could lead to more accurate and economically viable solutions for the production and transportation of eMeOH, while also reducing the environmental footprint of the transportation processes.

5.4 Sustainability aspect

This study on CCU for eMeOH production presents significant sustainability implications that could contribute to the transition toward a low-carbon economy. By transforming industrial CO_2 emissions into valuable chemical products, this research highlights a pathway to not only reduce GHG emissions but also create a circular economy model where emissions are converted into a resource.

One of the primary outcomes of this work is the potential reduction of CO_2 emissions from high-emission industries such as cement and pulp and paper, which are traditionally challenging to decarbonize and are among the largest contributors to global GHG emissions.

The study delves into the logistics of CO_2, highlighting the variability in costs depending on scenario characteristics. It emphasizes the importance of strategically selecting CO_2 sources to ensure adequate capacity for eMeOH production, thereby minimizing expenditure.

The findings indicate that the careful selection of transport options, logistics infrastructure technologies, and CO_2 sources not only reduces costs but also limits the emissions associated with CCU project deployment, keeping the environmental footprint to a minimum.

By leveraging economies of scale, the cost of eMeOH production can be reduced, enhancing its competitiveness against fossil-based alternatives. This economic feasibility is crucial for the widespread adoption of eMeOH as a sustainable fuel and chemical feedstock, potentially leading to broader market penetration and increased demand.

In conclusion, this work underscores a future where industrial CO_2 emissions are not just reduced but repurposed into valuable products, supporting a more sustainable and resilient industrial landscape. The insights gained provide a foundation for developing more cost-effective CCU solutions, which are essential for achieving long-term environmental sustainability and climate goals.

6 Conclusions

In this work, a comprehensive techno-economic analysis was conducted to model a CCU value chain, with a particular focus on the production of eMeOH from industrial CO_2 emissions in the Iberian Peninsula. The study explored the various components of the CCU chain, including CO_2 capture, liquefaction, storage, and transportation, ultimately connecting CO_2 emitters to an eMeOH production plant in Sines, Portugal. The primary objective was to evaluate the LCOeM and the $LCOCO_2$ under different scenarios, thereby providing insights into the cost drivers for each stage of the CCU value chain and shedding light on which would be the most cost-effective CCU scenario when coupling an industrial emitter with the eMeOH plant.

The analysis revealed that the eMeOH production stage is the dominant factor influencing the overall cost of the CCU value chain, accounting for over 80% of the PLC cost. This is followed by the CC stage, which represents approximately 9% of the total project cost throughout its operational lifetime. Subsequent cost factors, in descending order, include the transportation, storage, and liquefaction of CO_2.

The production capacity of eMeOH, constrained by CO_2 availability, emerged as a key driver in reducing both the LCOeM and the $LCOCO_2$ through economies of scale. This effect was particularly evident in scenarios involving the Portuguese cement factory CIMPOR in Alhandra, which yielded the lowest LCOeM among the modelled scenarios. These findings suggest that strategic selection of CO_2 sources and optimization of plant capacity are crucial for enhancing the economic viability of eMeOH production in a CCU value chain.

In evaluating the transportation options for connecting CO_2 emitters with the eMeOH production facility, the study found transport costs to be highly variable. Significant differences were observed between truck and tanker transportation methods. Maritime transport, particularly for routes connecting Spanish emitters, was identified as a more cost-effective option compared to truck transport, which resulted in substantially higher costs per ton of CO_2 transported. These findings underscore the importance of selecting appropriate transportation methods based on the specific logistical and geographical context of the CO_2 emitters and the eMeOH production site.

The research contributes to the growing body of knowledge on CCU value chains by offering detailed techno-economic assessments and identifying key factors that influence cost and feasibility. By shifting focus from the commonly studied H_2 and electricity inputs to the CO_2 feedstock, this work provides a novel perspective on the various stages of CC and CO_2 logistics necessary to meet the CO_2 feedstock requirements for eMeOH production processes.

Finally, the study acknowledges its limitations, highlighting opportunities for future research to explore additional variables and advancements in CCU technology. These developments could further reduce costs and enhance the sustainability of eMeOH production. Overall, this work lays the groundwork for future investigations into the integration of CCU value chains and the role of eMeOH in the transition to a low-carbon economy.

7 Bibliography

[1] T. F. Stocker, D. Qin, G.-K. Plattner, and M. Tignor, “Climate Change 2013: The Physical Science Basis. Contribution of Working Group I to the Fifth Assessment Report of the Intergovernmental Panel on Climate Change,” Cambridge, 2013. Accessed: Feb. 07, 2024. [Online]. Available: https://www.ipcc.ch/site/assets/uploads/2018/02/WG1AR5_all_final.pdf

[2] IRENA, *Decarbonising hard-to-abate sectors with renewables: Perspectives for the G7*. 2024. [Online]. Available: www.irena.org

[3] J. Podder, B. R. Patra, F. Pattnaik, S. Nanda, and A. K. Dalai, “A Review of Carbon Capture and Valorization Technologies,” *Energies (Basel)*, vol. 16, no. 6, p. 2589, Mar. 2023, doi: 10.3390/en16062589.

[4] Y. L. Dorokhov, E. V. Sheshukova, and T. V. Komarova, “Methanol in plant life,” *Front Plant Sci*, vol. 871, 2018, doi: 10.3389/FPLS.2018.01623/FULL.

[5] S. Kang, F. Boshell, A. Goeppert, S. G. Prakash, and I. landälv, *Innovation Outlook : Renewable Methanol*. Abu Dhabi: International Renewable Energy Agency and Methanol Institute, 2021. Accessed: Feb. 06, 2024. [Online]. Available: https://www.methanol.org/wp-content/uploads/2020/04/IRENA_Innovation_Renewable_Methanol_2021.pdf

[6] European Parliament, “DIRECTIVE (EU) 2018/2001 OF THE EUROPEAN PARLIAMENT AND OF THE COUNCIL,” Dec. 2018. Accessed: Feb. 06, 2024. [Online]. Available: https://eur-lex.europa.eu/legal-content/EN/TXT/PDF/?uri=OJ:L:2018:328:FULL

[7] *Commission Delegated Regulation (EU) 2023/1185 of 10 February 2023*. 2023. Accessed: Apr. 05, 2024. [Online]. Available: https://eur-lex.europa.eu/legal-content/EN/TXT/?uri=CELEX%3A32023R1185

[8] *DIRECTIVE 2003/87/EC*. European Parliament, 2003.

[9] H. Lee, K. Calvin, and D. Dasgupta, “Synthesis Report of the IPCC Sixth Assessment Report (AR6),” *Diriba Korecha Dadi*, 2023.

[10] “Solving green fuel ‘chicken and egg’ – Robert Maersk Uggla.” Accessed: Apr. 19, 2024. [Online]. Available: https://www.seatrade-maritime.com/sustainability-green-technology/committed-solving-green-fuel-chicken-and-egg-robert-maersk-uggla

[11] “Maersk names second vessel of its large methanol-enabled fleet ‘Astrid Mærsk’ in Yokohama, Japan | Press Release.” Accessed: Apr. 19, 2024. [Online]. Available: https://www.maersk.com/news/articles/2024/04/04/maersk-names-second-vessel-of-its-large-methanol-enabled-fleet-as-astrid-maersk-in-yokohama

[12] “CMES pens contract for world’s 1st methanol-fuelled VLCC - Offshore Energy.” Accessed: Apr. 19, 2024. [Online]. Available: https://www.offshore-energy.biz/cmes-pens-contract-for-worlds-1st-methanol-fuelled-vlcc/

[13] “Maersk Commits to Large, Green Methanol Offtake Deal with China’s Goldwind.” Accessed: Apr. 17, 2024. [Online]. Available: https://maritime-

executive.com/article/maersk-commits-to-large-green-methanol-offtake-deal-with-china-s-goldwind

[14] "Cepsa and C2X set up joint project for green methanol plant | Tank Storage." Accessed: Apr. 17, 2024. [Online]. Available: https://tankstorage.com/all-news/terminal-news/cepsa-and-c2x-set-up-joint-project-for-green-methanol-plant/

[15] "European Energy partners with Novo Nordisk & the LEGO Group - About Us - LEGO.com." Accessed: Apr. 19, 2024. [Online]. Available: https://www.lego.com/en-us/aboutus/news/2023/april/european-energy-partners-with-novo-nordisk-and-the-lego-group?locale=en-us

[16] "Mabanaft - Mabanaft and HIF close MOU to distribute E-Fuels in Germany." Accessed: Apr. 19, 2024. [Online]. Available: https://www.mabanaft.com/en/news-info/current-news-and-press-releases/news-detail/mabanaft-and-hif-close-mou-to-distribute-e-fuels-in-germany/

[17] "Methanex Egypt and Suez Methanol Derivatives Company Sign a New Methanol Pipeline Construction and Maintenance Agreement - Methanex | Methanex." Accessed: Apr. 19, 2024. [Online]. Available: https://www.methanex.com/news/update/methanex-egypt-and-suez-methanol-derivatives-company-sign-a-new-methanol-pipeline-construction-and-maintenance-agreement/

[18] Joana. Serpa, Joris. Morbee, and Evangelos. Tzimas, *Technical and economic characteristics of a CO2 transmission pipeline infrastructure.* Institute for Energy (European Commission) Publications Office, 2011.

[19] "The Atmosphere | National Oceanic and Atmospheric Administration." Accessed: Apr. 23, 2024. [Online]. Available: https://www.noaa.gov/jetstream/atmosphere

[20] T. Stein, "No sign of greenhouse gases increases slowing in 2023 - NOAA Research." Accessed: Apr. 23, 2024. [Online]. Available: https://research.noaa.gov/2024/04/05/no-sign-of-greenhouse-gases-increases-slowing-in-2023/

[21] R. K. Pachauri and L. A. Meyer, "Climate Change 2014: Synthesis Report. Contribution of Working Groups I, II and III to the Fifth Assessment Report of the Intergovernmental Panel on Climate Change," Geneva, 2014. Accessed: Feb. 06, 2024. [Online]. Available: https://www.ipcc.ch/site/assets/uploads/2018/02/SYR_AR5_FINAL_full.pdf

[22] "What is the EU ETS? - European Commission." Accessed: Jul. 31, 2024. [Online]. Available: https://climate.ec.europa.eu/eu-action/eu-emissions-trading-system-eu-ets/what-eu-ets_en

[23] "Carbon Border Adjustment Mechanism - European Commission." Accessed: Jul. 31, 2024. [Online]. Available: https://taxation-customs.ec.europa.eu/carbon-border-adjustment-mechanism_en

[24] "Europe's Definition of Green Hydrogen (RFNBO) Adopted into EU Law - King & Spalding." Accessed: Jul. 23, 2024. [Online]. Available: https://www.kslaw.com/news-and-insights/europes-definition-of-green-hydrogen-rfnbo-adopted-into-eu-law

[25] M. Pérez-Fortes, J. C. Schöneberger, A. Boulamanti, and E. Tzimas, "Methanol synthesis using captured CO2 as raw material: Techno-economic and environmental assessment," *Appl Energy*, vol. 161, pp. 718–732, Jan. 2016, doi: 10.1016/j.apenergy.2015.07.067.

[26] S. Sollai, A. Porcu, V. Tola, F. Ferrara, and A. Pettinau, "Renewable methanol production from green hydrogen and captured CO2: A techno-economic assessment," *Journal of CO2 Utilization*, vol. 68, p. 102345, Feb. 2023, doi: 10.1016/j.jcou.2022.102345.

[27] Y. Gu, D. Wang, Q. Chen, and Z. Tang, "Techno-economic analysis of green methanol plant with optimal design of renewable hydrogen production: A case study in China," *Int J Hydrogen Energy*, vol. 47, no. 8, pp. 5085–5100, Jan. 2022, doi: 10.1016/j.ijhydene.2021.11.148.

[28] J. Nyári, "Techno-economic feasibility study of a methanol plant using carbon dioxide and hydrogen," 2018.

[29] S. M. Nazmul, "Techno-Economic Study of CO 2 Capture Process for Cement Plants," 2005. Accessed: Jul. 10, 2024. [Online]. Available: https://uwspace.uwaterloo.ca/handle/10012/925

[30] A. N. Antzaras, T. Papalas, E. Heracleous, and C. Kouris, "Techno–economic and environmental assessment of CO2 capture technologies in the cement industry," *J Clean Prod*, vol. 428, p. 139330, Nov. 2023, doi: 10.1016/j.jclepro.2023.139330.

[31] C.-C. Cormos, "Decarbonization options for cement production process: A techno-economic and environmental evaluation," *Fuel*, vol. 320, p. 123907, Jul. 2022, doi: 10.1016/j.fuel.2022.123907.

[32] R. K. Pachauri *et al.*, "Ottmar Edenhofer (Germany), Ismail Elgizouli (Sudan), Christopher B. Field (USA), Piers), Mark Howden (Australia)," Gian-Kasper Plattner, 2014. Accessed: Jul. 07, 2024. [Online]. Available: http://www.ipcc.ch.

[33] A. Dubey and A. Arora, "Advancements in carbon capture technologies: A review," *J Clean Prod*, vol. 373, p. 133932, Nov. 2022, doi: 10.1016/j.jclepro.2022.133932.

[34] C. Wu *et al.*, "A comprehensive review of carbon capture science and technologies," *Carbon Capture Science & Technology*, vol. 11, p. 100178, Jun. 2024, doi: 10.1016/j.ccst.2023.100178.

[35] G. Realmonte *et al.*, "An inter-model assessment of the role of direct air capture in deep mitigation pathways," *Nat Commun*, vol. 10, no. 1, p. 3277, Jul. 2019, doi: 10.1038/s41467-019-10842-5.

[36] "A technical introduction to carbon capture and storage," 2014.

[37] J. Gervasi, L. Dubois, and D. Thomas, "Simulation of the Post-combustion CO2 Capture with Aspen HysysTM Software: Study of Different Configurations of an Absorption-regeneration Process for the Application to Cement Flue Gases," *Energy Procedia*, vol. 63, pp. 1018–1028, 2014, doi: 10.1016/j.egypro.2014.11.109.

[38] A. Singh and K. Stéphenne, "Shell Cansolv CO2 capture technology: Achievement from First Commercial Plant," *Energy Procedia*, vol. 63, pp. 1678–1685, 2014, doi: 10.1016/j.egypro.2014.11.177.

[39] D. M. Fraga *et al.*, "Design of a multi-user CO2 intermediate storage facility in the Grenland region of Norway," *International Journal of Greenhouse Gas Control*, vol. 112, p. 103514, Dec. 2021, doi: 10.1016/J.IJGGC.2021.103514.

[40] S. Solomon and T. Bellona Foundation, "Criteria for Intermediate Storage of Carbon Dioxide in Geological Formations," 2006.

[41] P. A. Brownsort, "Briefing on carbon dioxide specifications for transport 1st Report of the Thematic Working Group on: CO 2 transport, storage and networks Release Status: FINAL," 2019, Accessed: Apr. 23, 2024. [Online]. Available: http://www.ccusnetwork.eu/

[42] D. Coleman, J. Davison, C. Hendriks, O. Kaarstad, and M. Ozaki, "Transport of CO2: IPCC Special Report on Carbon dioxide Capture and Storage." Accessed: Apr. 22, 2024. [Online]. Available: https://www.ipcc.ch/site/assets/uploads/2018/03/srccs_chapter4-1.pdf

[43] H. Wang, J. Chen, and Q. Li, "A Review of Pipeline Transportation Technology of Carbon Dioxide," *IOP Conf Ser Earth Environ Sci*, vol. 310, no. 3, p. 032033, Aug. 2019, doi: 10.1088/1755-1315/310/3/032033.

[44] D. Asger Cáceres Larsen and J. Ask Hansen, "Maritime Transport of CO2," 2022, Accessed: Apr. 22, 2024. [Online]. Available: https://maerskbroker.com/wp-content/uploads/2022/11/Maritime-Transportation-of-CO2-ENG.pdf

[45] "First CO2 Carriers Launched in China for Northern Lights Project." Accessed: Apr. 22, 2024. [Online]. Available: https://maritime-executive.com/article/video-first-co2-carriers-launched-in-china-for-northern-lights-project

[46] "Riviera - News Content Hub - Capital Maritime orders world's largest LCO2 carriers." Accessed: Apr. 22, 2024. [Online]. Available: https://www.rivieramm.com/news-content-hub/news-content-hub/capital-maritime-orders-worlds-largest-lco2-carriers-77037

[47] J. Ovcina Mandra, "Bernhard Schulte orders LNG dual-fuel CO2 carrier backed by Northern Lights' long-term charter - Offshore Energy." Accessed: Apr. 22, 2024. [Online]. Available: https://www.offshore-energy.biz/bernhard-schulte-orders-lng-dual-fuel-co2-carrier-backed-by-northern-lights-long-term-charter/

[48] "CO2 in bulk," ACP. Accessed: May 28, 2024. [Online]. Available: https://www.acpco2.com/en/co2-bulk

[49] "40 ft ISO tank containers for lease, rental and hire," Bofort. Accessed: May 28, 2024. [Online]. Available: https://www.bofort.com/40-ft-iso-tank-containers-for-lease-rental-and-hire/

[50] "Liquid CO2 21.2 ISO Container," TOMCO2 Systems. Accessed: May 28, 2024. [Online]. Available: https://acrobat.adobe.com/id/urn:aaid:sc:US:8788db46-4766-41b3-ab0a-73d47e53e36f

[51] J. K. Stolaroff *et al.*, "Transport Cost for Carbon Removal Projects With Biomass and CO2 Storage," *Front Energy Res*, vol. 9, May 2021, doi: 10.3389/fenrg.2021.639943.

[52] E. Johansson and V. Pétursdóttir, "Evaluation of onshore transportation methods for captured CO between facility and 2 harbour in Stockholm," 2021.

[53] M. I. G. H. Alves, “Comparative cost analysis of different CO2 Capturing, Storage and Transport modes in Portugal,” NOVA University Lisbon, 2023. Accessed: Jun. 03, 2024. [Online]. Available: https://run.unl.pt/bitstream/10362/161322/1/Alves_2023.pdf

[54] “A Report of the National Petroleum Council DUAL CHALLENGE A Roadmap to At-Scale Deployment of CARBON CAPTURE, USE, AND STORAGE CHAPTER SIX-CO 2 TRANSPORT,” 2019.

[55] “CO2 Storage ASCO Transportable CO2 Tanks / ASCO CO2 Semi-Trailers,” ASCO.

[56] “CO2 Shipping Study Final Report for BEIS,” 2018. Accessed: May 09, 2024. [Online]. Available: https://assets.publishing.service.gov.uk/media/5c07a24f40f0b67052a55bf9/BEIS_Shipping_CO2.pdf

[57] “Northern Lights Project Concept report,” 2019. Accessed: Apr. 22, 2024. [Online]. Available: www.equinor.com

[58] C. Su, H. Wei, Z. Wang, H. Ayed, A. Mouldi, and A. A. Shayesteh, “Economic accounting and high-tech strategy for sustainable production: A case study of methanol production from CO2 hydrogenation,” *Int J Hydrogen Energy*, vol. 47, no. 62, pp. 25929–25944, Jul. 2022, doi: 10.1016/j.ijhydene.2022.01.124.

[59] P. Borisut and A. Nuchitprasittichai, “Methanol Production via CO2 Hydrogenation: Sensitivity Analysis and Simulation—Based Optimization,” *Front Energy Res*, vol. 7, Sep. 2019, doi: 10.3389/fenrg.2019.00081.

[60] B. Lacerda de Oliveira Campos *et al.*, “A Detailed Process and Techno-Economic Analysis of Methanol Synthesis from H2 and CO2 with Intermediate Condensation Steps,” *Processes*, vol. 10, no. 8, p. 1535, Aug. 2022, doi: 10.3390/pr10081535.

[61] É. S. Van-Dal and C. Bouallou, “Design and simulation of a methanol production plant from CO2 hydrogenation,” *J Clean Prod*, vol. 57, pp. 38–45, Oct. 2013, doi: 10.1016/j.jclepro.2013.06.008.

[62] J. Leipold, C. Seidel, D. Nikolic, A. Seidel-Morgenstern, and A. Kienle, “Optimization of methanol synthesis under forced periodic operation in isothermal fixed-bed reactors,” *Comput Chem Eng*, vol. 175, p. 108285, Jul. 2023, doi: 10.1016/j.compchemeng.2023.108285.

[63] A. M. Eltamaly and M. A. Mohamed, “Optimal Sizing and Designing of Hybrid Renewable Energy Systems in Smart Grid Applications,” in *Advances in Renewable Energies and Power Technologies*, Elsevier, 2018, pp. 231–313. doi: 10.1016/B978-0-12-813185-5.00011-5.

[64] J. Aldersey-Williams and T. Rubert, “Levelised cost of energy – A theoretical justification and critical assessment,” *Energy Policy*, vol. 124, pp. 169–179, Jan. 2019, doi: 10.1016/j.enpol.2018.10.004.

[65] “Electricity generation costs 2023,” 2023. Accessed: May 25, 2024. [Online]. Available: https://assets.publishing.service.gov.uk/media/6556027d046ed400148b99fe/electricity-generation-costs-2023.pdf

[66] P. Dogliani, A. N. Ruas Rego Canha, A. M. Elberry, and J. Thakur, "Multi-option analytical modeling of levelized costs across various hydrogen supply chain nodes," *Int J Hydrogen Energy*, vol. 70, pp. 737–755, Jun. 2024, doi: 10.1016/j.ijhydene.2024.05.142.

[67] "Value of money converter | Statistics Finland." Accessed: Jul. 16, 2024. [Online]. Available: https://stat.fi/tup/laskurit/rahanarvonmuunnin_en.html

[68] "Why energy production is also discounted for the LCOE calculation.," ResearchGate. Accessed: Jul. 03, 2024. [Online]. Available: https://www.researchgate.net/post/Why_energy_production_is_also_discounted_for_the_LCOE_calculation

[69] F. Yang, J. C. Meerman, and A. P. C. Faaij, "Carbon capture and biomass in industry: A techno-economic analysis and comparison of negative emission options," *Renewable and Sustainable Energy Reviews*, vol. 144, p. 111028, Jul. 2021, doi: 10.1016/j.rser.2021.111028.

[70] CaptureMap, "THE BIOGENIC CO2 BREAKDOWN: WHICH 6 SECTORS HAVE THE MOST EMISSIONS?," CaptureMap.

[71] A. Lorin, D. Héleine, J. McGreer, and J.-B. Arminjon, "Biogenic CO2 from the biogas industry," Suez, 2023.

[72] K. Kuparinen, E. Vakkilainen, and T. Tynjälä, "Biomass-based carbon capture and utilization in kraft pulp mills," *Mitig Adapt Strateg Glob Chang*, vol. 24, no. 7, pp. 1213–1230, Oct. 2019, doi: 10.1007/s11027-018-9833-9.

[73] K. Onarheim, S. Santos, P. Kangas, and V. Hankalin, "Performance and costs of CCS in the pulp and paper industry part 1: Performance of amine-based post-combustion CO 2 capture," *International Journal of Greenhouse Gas Control*, vol. 59, pp. 58–73, Apr. 2017, doi: 10.1016/j.ijggc.2017.02.008.

[74] R. McKaskle, K. Fisher, P. Selz, and L. Yongqi, "Evaluation of Carbon Dioxide Capture Options from Ethanol Plants," Illinois, 2018.

[75] S. S. Cordova, M. Gustafsson, M. Eklund, and N. Svensson, "Potential for the valorization of carbon dioxide from biogas production in Sweden," *J Clean Prod*, vol. 378, p. 134392, Dec. 2022, doi: 10.1016/j.jclepro.2022.134392.

[76] O. Linjala, "Review on post-combustion carbon capture technologies and capture of biogenic CO_2 using pilot-scale equipment," Lappeenranta-Lahti University of Technology LUT, 2021.

[77] "The business of sustainability Assessment of European biogenic CO2 balance for SAF production," 2022. [Online]. Available: www.erm.com

[78] "Cement - IEA." Accessed: Jul. 01, 2024. [Online]. Available: https://www.iea.org/energy-system/industry/cement

[79] S. Dietz, W. Irwin, B. Rauis, V. Jahn, and J. Noels, "Carbon Performance Assessment of Paper Producers: Note on Methodology," 2019, Accessed: Jul. 01, 2024. [Online]. Available: http://www.lse.ac.uk/GranthamInstitute/tpi/about/how-investors-can-use-

[80] "Thyssenkrupp to modernize SECIL cement plant in Portugal." Accessed: Jul. 01, 2024. [Online]. Available: https://insights.thyssenkrupp-polysius.com/news/thyssenkrupp-to-modernize-secil-cement-plant-in-portugal/

[81] "The Navigator Company, our activity." Accessed: Jul. 01, 2024. [Online]. Available: https://en.thenavigatorcompany.com/Institutional/Our-activity

[82] "Alhandra - Cimpor." Accessed: Jul. 01, 2024. [Online]. Available: https://www.cimpor.com/en/alhandra

[83] "Votorantim Cimentos Spain acquires Heidelberg Materials' Southern Spanish businesses - Cement industry news from Global Cement." Accessed: Jul. 01, 2024. [Online]. Available: https://www.globalcement.com/news/item/14859-votorantim-cimentos-spain-acquires-heidelberg-materials-southern-spanish-businesses

[84] "Alcanar | Oficemen." Accessed: Jul. 01, 2024. [Online]. Available: https://www.oficemen.com/en/alcanar/

[85] O. E. Ige, D. V. Von Kallon, and D. Desai, "Carbon emissions mitigation methods for cement industry using a systems dynamics model," *Clean Technol Environ Policy*, vol. 26, no. 3, pp. 579–597, Mar. 2024, doi: 10.1007/s10098-023-02683-0.

[86] M. Yugo and A. Soler, "Technology Scouting-Carbon Capture: From Today's to Novel Technologies," Brussels, 2020.

[87] H. Barlow, S. S. M. Shahi, and M. Loughrey, "STATE OF THE ART: CCS TECHNOLOGIES 2023," 2023.

[88] "Bosch Electric steam boiler ELSB: Sustainably generated steam with green electricity," *Bosch Industriekessel GmbH*, Accessed: Mar. 26, 2024. [Online]. Available: www.bosch-industrial.com

[89] "Electric steam boiler, electric hot water boiler, industrial electric boiler," Yuanda Boiler. Accessed: Mar. 26, 2024. [Online]. Available: https://www.yd-boiler.com/products/electric-boiler/electric-boiler.html?campaignid=21060338604&device=c&keyword=electrical%20steam%20boiler&gad_source=1&gclid=CjwKCAjw5ImwBhBtEiwAFHDZx8_YVD8iMDhuCrT5OkFjOkIsyN541v9uk2P8s_5kaW2OvMAmTxfUoBoCPkwQAvD_BwE

[90] "e-Pack - Babcock Wanson," Babcock Wanson. Accessed: Mar. 26, 2024. [Online]. Available: https://www.babcock-wanson.com/products/industrial-electric-boilers/e-pack/

[91] C. Schoeneberger, J. Zhang, C. McMillan, J. B. Dunn, and E. Masanet, "Electrification potential of U.S. industrial boilers and assessment of the GHG emissions impact," *Advances in Applied Energy*, vol. 5, p. 100089, Feb. 2022, doi: 10.1016/j.adapen.2022.100089.

[92] "Interview with industry expert," 2024, *Lisbon*.

[93] H. Gerbelová, M. van der Spek, and W. Schakel, "Feasibility Assessment of CO2 Capture Retrofitted to an Existing Cement Plant: Post-combustion vs. Oxy-fuel Combustion Technology," *Energy Procedia*, vol. 114, pp. 6141–6149, Jul. 2017, doi: 10.1016/j.egypro.2017.03.1751.

[94] A. Parkhi, S. Cremaschi, and Z. Jiang, “Techno-Economic Analysis of CO2 Capture from Pulp and Paper Mill Limekiln,” *IFAC-PapersOnLine*, vol. 55, no. 7, pp. 284–291, 2022, doi: 10.1016/j.ifacol.2022.07.458.

[95] “Carbon capture, storage and utilisation,” 2019. Accessed: Jun. 14, 2024. [Online]. Available: https://www.linde-engineering.com/en/images/Carbon-capture-storage-utilisation-Linde-BASF_tcm19-462558.pdf

[96] “How to store CO2 with Northern Lights - Northern Lights,” 2024. Accessed: May 06, 2024. [Online]. Available: https://norlights.com/how-to-store-co2-with-northern-lights/

[97] G. Helen Askvik, “Northern Lights Annual Report 2023,” 2023.

[98] M. Lindgren, “Northern Lights shows the way to seaborne CCS solutions,” DNV. Accessed: May 30, 2024. [Online]. Available: https://www.dnv.com/expert-story/maritime-impact/Northern-Lights-shows-the-way-to-seaborne-CCS-solutions/

[99] “CO2 Cargo Quality Specifications,” 2024. Accessed: Jun. 10, 2024. [Online]. Available: https://norlights.com/wp-content/uploads/2024/02/Northern-Lights-GS-co2-Spec2024.pdf

[100] “Northern Lights FEED Report,” 2020.

[101] “The Basics of the Tanker Shipping Market,” 2017. Accessed: Aug. 13, 2024. [Online]. Available: https://www.scribd.com/document/413635360/CP-special-report-2017-eng-pdf

[102] O. Dinu and A. M. Ilie, “Maritime vessel obsolescence, life cycle cost and design service life,” *IOP Conf Ser Mater Sci Eng*, vol. 95, p. 012067, Nov. 2015, doi: 10.1088/1757-899X/95/1/012067.

[103] “Tiempos de conducción y descanso - Conducción,” Gobierno de España - Ministerio de Transportes y Movilidad Sostenible. Accessed: Jun. 04, 2024. [Online]. Available: https://www.transportes.gob.es/transporte-terrestre/inspeccion-y-seguridad-en-el-transporte/tiempos-de-conduccion-y-descanso/conduccion/tiempos-de-conduccion

[104] “Average Truck Speeds,” Office of Energy Efficiency & Renewable Energy. Accessed: May 30, 2024. [Online]. Available: https://www.energy.gov/eere/vehicles/fact-671-april-18-2011-average-truck-speeds

[105] L. Tze, L. K., and K. V., “How many hours of business downtime does a business with a fleet of vehicles face because of refueling, washing and maintenance each?,” Wonder. Accessed: Jun. 03, 2024. [Online]. Available: https://askwonder.com/research/hours-business-downtime-does-fleet-vehicles-face-refueling-washing-maintenance-3wdyaqyc7

[106] “Carbon dioxide | Gas Encyclopedia Air Liquide.” Accessed: May 15, 2024. [Online]. Available: https://encyclopedia.airliquide.com/carbon-dioxide#properties

[107] S. Overå, “EL001 Northern Lights-Receiving and permanent storage of CO 2 Plan for development, installation and operation Part II-Impact Assessment,” 2019. Accessed: Apr. 23, 2024. [Online]. Available: https://northernlightsccs.eu/

[108] D. Menmuir, S. Florence, and K. Taylor, "Next Generation Carbon Capture Technology Technoeconomic Analysis Work Package 6 Department for Business, Energy and Industrial Strategy," 2022.

[109] K. Onarheim, P. Kangas, S. Kaijaluoto, V. Hankalin, and S. Santos, "TECHNO-ECONOMIC EVALUATION OF RETROFITTING CCS IN A MARKET PULP MILL AND AN INTEGRATED PULP AND BOARD MILL," 2016. [Online]. Available: www.ieaghg.org

[110] K. Onarheim, "Tackling CO2 emissions in the pulp and paper industry with innovative technology," Aker Carbon Capture.

[111] C.-C. Cormos, "Oxy-combustion of coal, lignite and biomass: A techno-economic analysis for a large scale Carbon Capture and Storage (CCS) project in Romania," *Fuel*, vol. 169, pp. 50–57, Apr. 2016, doi: 10.1016/j.fuel.2015.12.005.

[112] Y. Xing, T. A. D. Santoso, and Y. Ma, "Technical–Economic Feasibility Analysis of Subsea Shuttle Tanker," *J Mar Sci Eng*, vol. 10, no. 1, p. 20, Dec. 2021, doi: 10.3390/jmse10010020.

[113] "Rotterdam Bunker Prices - Ship & Bunker." Accessed: May 09, 2024. [Online]. Available: https://shipandbunker.com/prices/emea/nwe/nl-rtm-rotterdam#LNG

[114] "Bunker Ports News Worldwide." Accessed: May 09, 2024. [Online]. Available: https://www.bunkerportsnews.com/PortDetails.aspx?ElementID=57d9e30f-88b9-4589-8888-95f3aeb06a43

[115] C. Ekström, K. Kerssemakers, S. Liljemark, H. Pershad, and S. Vall de, "The Costs of CO 2 Transport Post-demonstration CCS in the EU 2," 2011.

[116] "Europe Fuel Prices: Stats & Averages." Accessed: Jun. 03, 2024. [Online]. Available: https://www.rhinocarhire.com/World-Fuel-Prices/Europe.aspx

[117] "Autopistas de peaje actuales | Ministerio de Transportes y Movilidad Sostenible," Gobierno de España - Ministerio de Transportes y Movilidad Sostenible. Accessed: Jun. 03, 2024. [Online]. Available: https://www.transportes.gob.es/carreteras/peajes-actuales

[118] "Calculador de Portagens," Via Verde. Accessed: Jun. 03, 2024. [Online]. Available: https://www.viaverde.pt/particulares/ferramentas/calculador-de-portagens

[119] K. Lauri, R. Jouko, N. Nicklas, and T. Sebastian, "Scenarios and new technologies for a North-European CO2 transport infrastructure in 2050," *Energy Procedia*, vol. 63, pp. 2738–2756, 2014, doi: 10.1016/j.egypro.2014.11.297.

[120] R. Svensson, M. Odenberger, F. Johnsson, and L. Strömberg, "Transportation systems for CO2––application to carbon capture and storage," *Energy Convers Manag*, vol. 45, no. 15–16, pp. 2343–2353, Sep. 2004, doi: 10.1016/j.enconman.2003.11.022.

[121] Y. Seo, C. Huh, S. Lee, and D. Chang, "Comparison of CO 2 liquefaction pressures for ship-based carbon capture and storage (CCS) chain," *International Journal of Greenhouse Gas Control*, vol. 52, pp. 1–12, Sep. 2016, doi: 10.1016/j.ijggc.2016.06.011.

[122] M. A. Tribe and R. L. W. Alpine, “Scale economies and the ‘0.6 rule,’” *Engineering Costs and Production Economics*, vol. 10, no. 4, pp. 271–278, Dec. 1986, doi: 10.1016/S0167-188X(86)80025-8.

[123] R. P. Borges, F. Franco, F. N. Serralha, and I. Cabrita, “Green Hydrogen Production at the Gigawatt Scale in Portugal: A Technical and Economic Evaluation,” *Energies (Basel)*, vol. 17, no. 7, p. 1638, Mar. 2024, doi: 10.3390/en17071638.

[124] F. Eckl, L. Eltrop, A. Moita, and R. Costa Neto, “Techno-economic evaluation of two hydrogen supply options to southern Germany: On-site production and import from Portugal,” *Int J Hydrogen Energy*, vol. 47, no. 60, pp. 25214–25228, Jul. 2022, doi: 10.1016/j.ijhydene.2022.05.266.

[125] “IRENA LCOH Scenario Viewer.” Accessed: Jul. 16, 2024. [Online]. Available: https://lcoh.irena.org/

[126] L. M. Rodrigues, T. Soares, I. Rezende, J. P. Fontoura, and V. Miranda, “Economic Analysis of a Hydrogen Power Plant in the Portuguese Electricity Market,” *Energies (Basel)*, vol. 16, no. 3, p. 1506, Feb. 2023, doi: 10.3390/en16031506.

[127] “EU-ETS price 2022-2024 | Statista.” Accessed: Jul. 14, 2024. [Online]. Available: https://www.statista.com/statistics/1322214/carbon-prices-european-union-emission-trading-scheme/

[128] “EU Carbon Permits - Price - Chart - Historical Data - News.” Accessed: Jul. 14, 2024. [Online]. Available: https://tradingeconomics.com/commodity/carbon

[129] “Carbon Price Viewer - Sandbag Climate Campaign.” Accessed: Jul. 14, 2024. [Online]. Available: https://sandbag.be/carbon-price-viewer/

[130] S. Twidale, “Analysts cut EU carbon price forecasts on weak industry, power sector demand | Reuters.” Accessed: Jul. 14, 2024. [Online]. Available: https://www.reuters.com/business/energy/analysts-cut-eu-carbon-price-forecasts-weak-industry-power-sector-demand-2024-01-23/

[131] “Global Carbon Market Outlook 2024 | BloombergNEF.” Accessed: Jul. 14, 2024. [Online]. Available: https://about.bnef.com/blog/global-carbon-market-outlook-2024/

[132] D. Kearns, H. Liu, and C. Consoli, “Technology readiness and costs of CCS,” 2021.

[133] *Delegated regulation - 2023/1184 - EN - EUR-Lex*. 2023. Accessed: Jul. 17, 2024. [Online]. Available: https://eur-lex.europa.eu/eli/reg_del/2023/1184/oj

[134] D. Khatiwada, R. A. Vasudevan, and B. H. Santos, “Decarbonization of natural gas systems in the EU – Costs, barriers, and constraints of hydrogen production with a case study in Portugal,” *Renewable and Sustainable Energy Reviews*, vol. 168, p. 112775, Oct. 2022, doi: 10.1016/j.rser.2022.112775.

[135] G. Zomer, S. Finner, J. Harmsen, L. Vredeveldt, and P. van Lieshout, “Green Maritime Methanol: Operation aspects and the fuel supply chain ,” Sep. 2020.

[136] “Pricing - Methanex | Methanex.” Accessed: Jul. 17, 2024. [Online]. Available: https://www.methanex.com/about-methanol/pricing/